BRUNO DO NASCIMENTO SILVA

PHOTORESPIRATORY CHANGES AND INDUCED RESISTANCE ON TOMATO AGAINST SEPTORIA LEAF SPOT BY A PHOSPHITE COMBINED WITH FREE AMINO ACIDS

Thesis submitted to the Plant Physiology Graduate Program of the Universidade Federal de Viçosa in partial fulfillment of the requirements for the degree of *Doctor Scientiae*.

Adviser: Fabrício Ávila Rodrigues

VIÇOSA - MINAS GERAIS
2022

Ficha catalográfica elaborada pela Biblioteca Central da Universidade Federal de Viçosa - Campus Viçosa

T

S586p
2022

Silva, Bruno do Nascimento, 1989-
Photorespiratory changes and induced resistance on tomato against septoria leaf spot by a phosphite combined with free amino acids / Bruno do Nascimento Silva. - Viçosa, MG, 2022.
1 tese eletrônica (90 f.): il.

Texto em inglês.
Orientador: Fabrício de Ávila Rodrigues.
Tese (doutorado) - Universidade Federal de Viçosa, Departamento de Fitopatologia, 2022.
Inclui bibliografia.
DOI: https://doi.org/10.47328/ufvbbt.2022.623
Modo de acesso: World Wide Web.

1. Tomate - Resistência a doenças e pragas. 2. Fotossíntese. 3. Resistência induzida. 4. *Septoria lycopersici*. I. Rodrigues, Fabrício de Ávila, 1974-. II. Universidade Federal de Viçosa. Departamento de Fitopatologia. Programa de Pós-Graduação em Fisiologia Vegetal. III. Título.

CDD 22. ed. 635.64294

Bibliotecário(a) responsável: Alice Regina Pinto Pires CRB-6/2523

BRUNO DO NASCIMENTO SILVA

PHOTORESPIRATORY CHANGES AND INDUCED RESISTANCE ON TOMATO AGAINST SEPTORIA LEAF SPOT BY A PHOSPHITE COMBINED WITH FREE AMINO ACIDS

Thesis submitted to the Plant Physiology Graduate Program of the Universidade Federal de Viçosa in partial fulfillment of the requirements for the degree of *Doctor Scientiae*.

APPROVED: October 05, 2022.

Assent:

Bruno do Nascimento Silva
Author

Fabrício Ávila Rodrigues
Adviser

ACKNOWLEDGMENTS

I thank God first for all the blessings and opportunities.

Thanks are due to the Universidade Federal de Viçosa (UFV), Department of Plant Biology, Department of Plant Pathology, the Plant-Pathogen Interaction Laboratory and the Postgraduate Program in Plant Physiology for providing conditions for this work.

This study was financed in part by the Coordenação de Aperfeiçoamento de Pessoal de Nível Superior - Brasil (CAPES) - Finance Code 001.

I thank Professor Fabricio Ávila Rodrigues for his guidance, attention, competence, advice and for supporting my professional skills.

Professor Samuel Cordeiro Vitor Martins for their help and excellent contributions to the work.

To the teachers of the Graduate Program in Plant Physiology.

Colleagues at the Laboratory of Host-Pathogen Interaction for all their learning and help Bárbara, Lilian and Andersom for their friendship and help while conducting the experiments.

To our roommates Daniel, Bruno and Moab for sharing smiles, dreams and concerns.

Graduate students for their help and companionship during the courses.

My family Monalisa, Fernanda, Antonio and wife Aline for all their support in the most difficult times.

UFV employees Bruno, Daniel, Delfim and Luciene.

Thanks to all colleagues who contributed, directly or indirectly, to this work.

BIOGRAPHY

BRUNO DO NASCIMENTO SILVA was born on October 23, 1989 in the state of Brasília.

In 2017, he obtained the title of Agricultural Engineer from the Federal University of Ceará. At the same institution, she was a scholarship holder of the Programa de Educação Tutorial (PET) developing research on water relations under the guidance of Prof. Rosilene Oliveira Mesquita.

In March 2018, started the Master's degree program in the Postgraduate Program in Plant Physiology of the Department of Plant Biology of the Federal University Viçosa under the guidance of Professor. Fabrício Ávila Rodrigues defending his dissertation on July 25, 2019. In August 2019, he started the doctoral degree in the Plant Pathology Program at UFV under the guidance of Professor Fabrício Ávila Rodrigues defending his thesis on October 05, 2022.

ABSTRACT

SILVA, Bruno do Nascimento, D.Sc., Universidade Federal de Viçosa, October 2022. **Photorespiratory changes and induced resistance on tomato against septoria leaf spot by a phosphite combined with free amino acids.** Advisor: Fabrício Ávila Rodrigues.

Septoria leaf spot (SLS), caused by *Septoria lycopersici*, is a destructive disease in tomato. Infection of plants by pathogens causes changes in photosynthesis, photorespiration and respiration that will affect defense responses. The first study investigated the impacts caused on photorespiration in tomato leaves by *S. lycopersici* infection. Infection reduced photosynthesis and pigment concentration and increased respiration and the photorespiration/crude photosynthesis ratio increased in infected leaves. *S. lycopersici* infection caused great oxidative damage as demonstrated by increased concentrations of malonaldehyde, superoxide anion and hydrogen peroxide. We evaluated the expression of genes involved in the photorespiratory pathway (*GOX1*, *GOX2*, *SHMT2*, *SMHT3* and *GLYK*), nitrogen metabolism (*Fd-GOGAT*) and stress acclimatization (*mMDH1*, *mMDH2* and *CAT*) and observed an up-regulation during the process of *S. lycopersici* infection. A better understanding of the physiological changes that occur in the leaves of tomato plants infected by *S. lycopersici* at the level of photorespiration may contribute to the development of cultivars more efficiently to cope with the fungal infection. In the second study, we investigated the use of potassium phosphite combined with free L-α-amino acids (called stimulus induced resistance (IR)) to increase tomato defense responses against *S. lycopersici* infection. Plants that received the RI stimulus showed a reduction in the severity of SLS and less colonization of leaf tissue by S. lycopersici (lower expression of *TEF-1*α). Plants sprayed with IR stimulus showed lower concentrations of malonaldehyde, hydrogen peroxide and superoxide anion radical, while sucrose, fructose and starch concentrations and high ascorbate peroxidase, catalase, glutathione reductase and superoxide dismutase activities increased when compared to plants sprayed with IR stimulus. water in response to *S. lycopersici* infection. The photosynthetic apparatus was less compromised, which resulted in higher concentrations of chlorophyll *a*+*b* and carotenoids in plants sprayed with RI stimulus. We observed that genes involved in host defense reactions (*CHI3*, *CHI9*, *GLU*, *PAL3*, *POX3*, *PPOB* and *PPOF*) and those related to acquired systemic resistance (*PAL3* and *ICS*) or induced systemic resistance ((ethylene production - *ACO2*, *ACO3*, *ACO5* and *ACO4*) and the jasmonic acid signaling pathway (*LOX1.1*, *LOXB*, *LOXC* and

PDF1.2)) and we observed an up-regulation for plants infected and sprayed with RI stimulus. These findings highlight the potential of using this IR stimulus for the management of SLS.

Keywords**:** Antioxidative metabolism. Foliar disease. Host defense responses. Induced resistance. Necrotrophic pathogen.

RESUMO

SILVA, Bruno do Nascimento, D.Sc., Universidade Federal de Viçosa, outubro de 2022. **Alterações fotorrespiratórias e resistência induzida em tomateiro à mancha foliar de septoria por um fosfito combinado com aminoácidos livres.** Orientador: Fabrício Ávila Rodrigues.

A mancha foliar de Septoria (SLS), causada por *Septoria lycopersici*, é uma doença destrutiva em tomateiro. A infecção de plantas por patógenos causa alterações na fotossíntese, fotorrespiração e respiração que afetarão as respostas de defesa. O primeiro estudo investigou os impactos causados na fotorrespiração em folhas de tomate pela infecção por *S. lycopersici*. A infecção reduziu a fotossíntese e a concentração de pigmentos e aumentou a respiração e a razão fotorrespiração/fotossíntese bruta aumentaram nas folhas infectadas. A infecção por *S. lycopersici* causou grande dano oxidativo como demonstrado pelo aumento das concentrações de malonaldeído, ânion superóxido e peróxido de hidrogênio. Nós avaliamos a expressão de genes envolvidos na via fotorrespiratória (*GOX1*, *GOX2*, *SHMT2*, *SMHT3* e *GLYK*), metabolismo do nitrogênio (*Fd-GOGAT*) e aclimatação ao estresse (*mMDH1*, *mMDH2* e *CAT*) e observamos uma regulação positivamente durante o processo de infecção por *S. lycopersici*. Uma melhor compreensão das alterações fisiológicas que ocorrem nas folhas de tomateiros infectados por *S. lycopersici* ao nível da fotorrespiração pode contribuir para o desenvolvimento de cultivares de forma mais eficiente para o enfrentamento da infecção fúngica. No segundo estudo, nós investigamos o uso de fosfito de potássio combinados com de L-α-aminoácidos livres (estímulo chamado resistência induzida (RI)), para aumentar as respostas de defesa do tomateiro contra a infecção por *S. lycopersici*. Plantas que receberam o estímulo RI apresentaram redução na severidade de SLS e menor colonização do tecido foliar por *S. lycopersici* (menor expressão de *TEF-1*α). As plantas pulverizadas com estímulo IR mostraram menores concentrações de malonaldeído, peróxido de hidrogênio e radical ânion superóxido, enquanto as concentrações de sacarose, frutose e amido e grandes atividades de ascorbato peroxidase, catalase, glutationa redutase e superóxido dismutase aumentaram quando comparada com plantas pulverizadas com água em resposta à infecção por *S. lycopersici*. O Aparato fotossintético foi menos comprometido o que resultou em maiores concentrações dee clorofila *a*+*b* e carotenoides em plantas pulverizadas com estímulo RI. Nós observamos que os genes envolvidos em reações de defesa do hospedeiro (*CHI3*, *CHI9*, *GLU*, *PAL3*, *POX3*, *PPOB* e *PPOF*) e aqueles relacionados à resistência sistêmica adquirida (*PAL3* e *ICS*) ou resistência

sistêmica induzida ((produção de etileno - *ACO2*, *ACO3*, *ACO5* e *ACO4*) e a via de sinalização do ácido jasmônico (*LOX1.1*, *LOXB*, *LOXC* e *PDF1.2*)) e observamos uma regulação positivamente para plantas infectadas e pulverizadas com estímulo RI. Esses achados destacam o potencial do uso desse estímulo de RI para o manejo de SLS.

Palavras-chave: Metabolismo antioxidante. Doença foliar. Respostas de defesa do hospedeiro. Resistência induzida. Patógeno necrotrófico.

SUMMARY

Chapter 1

Infection of tomato leaves by *Septoria lycopersici* impairs the photorespiratory pathway

ABSTRACT

Septoria leaf spot (SLS), caused by *Septoria lycopersici*, is a destructive disease in tomato. Infection of plants by pathogens causes changes in photosynthesis, photorespiration and respiration that will affect defense responses. The first study investigated the impacts caused on photorespiration in tomato leaves by *S. lycopersici* infection. Infection reduced photosynthesis and pigment concentration and increased respiration and the photorespiration/crude photosynthesis ratio increased in infected leaves. *S. lycopersici* infection caused great oxidative damage as demonstrated by increased concentrations of malonaldehyde, superoxide anion and hydrogen peroxide. We evaluated the expression of genes involved in the photorespiratory pathway (*GOX1*, *GOX2*, *SHMT2*, *SMHT3* and *GLYK*), nitrogen metabolism (*Fd-GOGAT*) and stress acclimatization (*mMDH1*, *mMDH2* and *CAT*) and observed an up-regulation during the process of *S. lycopersici* infection. A better understanding of the physiological changes that occur in the leaves of tomato plants infected by *S. lycopersici* at the level of photorespiration may contribute to the development of cultivars more efficiently to cope with the fungal infection.

Keywords: *Solanum lycopersicum.* Fungal foliar disease. Photosynthesis.

RESUMO

A mancha foliar de Septoria (SLS), causada por *Septoria lycopersici*, é uma doença destrutiva em tomateiro. A infecção de plantas por patógenos causa alterações na fotossíntese, fotorrespiração e respiração que afetarão as respostas de defesa. O primeiro estudo investigou os impactos causados na fotorrespiração em folhas de tomate pela infecção por *S. lycopersici*. A infecção reduziu a fotossíntese e a concentração de pigmentos e aumentou a respiração e a razão fotorrespiração/fotossíntese bruta aumentaram nas folhas infectadas. A infecção por *S. lycopersici* causou grande dano oxidativo como demonstrado pelo aumento das concentrações de malonaldeído, ânion superóxido e peróxido de hidrogênio. Nós avaliamos a expressão de genes envolvidos na via fotorrespiratória (*GOX1*, *GOX2*, *SHMT2*, *SMHT3* e *GLYK*), metabolismo do nitrogênio (*Fd-GOGAT*) e aclimatação ao estresse (*mMDH1*, *mMDH2* e *CAT*) e observamos uma regulação positivamente durante o processo de infecção por *S. lycopersici*. Uma melhor compreensão das alterações fisiológicas que ocorrem nas folhas de tomateiros infectados por *S. lycopersici* ao nível da fotorrespiração pode contribuir para o desenvolvimento de cultivares de forma mais eficiente para o enfrentamento da infecção fúngica.

Palavras-chave: *Solanum lycopersicum.* Doença fúngica foliar. Fotossíntese.

1. Introduction

Tomato production is seriously affected by the occurrence of septoria leaf spot (SLS) (Stevenson, 2014). Epidemics of SLS, caused by the fungus *Septoria lycopersici* Speg., are more severe on tomato plants grown in regions with temperatures ranging from 20 to 25ºC and high relative humidity (Ávila et al., 2020). Tomato plants are susceptible to *S. lycopersici* infection at all growth stages (Stevenson, 2014). Circular to elliptical necrotic lesions with tan to gray centers surrounded by dark brown margins and containing several black pycnidia are often noticed on basal leaves of plants (Stevenson, 2014). Reduced photosynthetically active leaf area due to higher SLS severity linked to intense defoliation and reduced plant growth is responsible for yield losses and lower fruit quality (Ávila et al., 2020).

At the physiological level, drastic changes in CO_2 fixation, respiration, and photorespiration occur in plant tissues infected by pathogens (Berger et al., 2007). Indeed, reactive oxygen species (ROS) are profusely produced especially in chloroplasts, peroxisomes, and mitochondria causing irreversible damage to DNA, RNA, proteins, and membrane of cell walls and organelles (Sørhagen et al., 2013). A prompt and efficient photorespiratory pathway help plants against the harmful oxidative damage caused by the ROS originating from different types of stress by lowering their levels in the tissues (Lima Neto et al., 2017). During photorespiration, hydrogen peroxide (H_2O_2) is produced in high concentrations in the peroxisome and catalase plays a pivotal role as the main antioxidant enzyme for its decomposition into water and oxygen in the plant cells (Voss et al., 2013).

The photorespiration pathway is a consequence of the oxygenation of ribulose-1,5-bisphosphate which is catalyzed by ribulose-1,5-bisphosphate carboxylase/oxygenase (RuBisCO) to produce 2-phosphoglycolate (Dong et al., 2016). The photorespiratory pathway converts 2-phosphoglycolate into 3-phosphoglycerate to recover almost 75% of the carbon that would be lost in this biochemical process (Peterhansel and Maurino, 2020). Photorespiration represents a net loss of fixed carbon that reduces biomass production (Sørhagen et al., 2013). This high-flow metabolic pathway associated with photosynthesis takes place in the cytosol and also in the chloroplasts, peroxisomes, and mitochondria (Lima Neto et al., 2017) and functions as a safety valve to prevent an excess of energy, especially in stressed plants (Peterhansel and Maurino, 2020; Zivcak et al., 2014). Photorespiratory reactions can directly dissipate the excess of energy (ATP, NAD(P)H, and reduced ferredoxin) or indirectly via the alternative oxidase (AOX) pathway (Voss et al., 2013). Furthermore, photorespiration plays a crucial role to

maintain the functionality of the Calvin-Benson cycle by preventing the accumulation of enzyme-inhibiting metabolites (Norman and Colman, 1991).

Plants infected by pathogens of different lifestyles need to balance energy demands between primary metabolism and the activation of cell defense reactions (Berger et al., 2007). In this scenario, photorespiration, the electron transport chain, and the alternative oxidase pathway are of pivotal importance in protecting and optimizing the photosynthetic apparatus (Sørhagen et al., 2013; Takahashi and Badger, 2011). Therefore, down-regulation of the photosynthetic electron transport has been the initial reaction in plant tissues infected by pathogens (Aldea et al., 2006). Photorespiration plays an important role during host defense reactions against pathogen infection as noticed by an increase in glycolate oxidase (GOX) activity together with a rise in H_2O_2 formation that acts as an important secondary messenger for a prompt activation of these reactions (Peterhansel and Maurino, 2020). During the photorespiratory cycle, the glycine migrates to the mitochondria where it is partially decomposed into CO_2 and ammonia by glycine decarboxylase (Aldea et al., 2006). Inhibition of glycine decarboxylase by the toxin victorin was detrimental for *Cochliobolus victoriae* infection in the leaves of oat plants (Navarre and Wolpert, 1995). According to Chen et al. (2013) higher serine:glyoxylate aminotransferase (SGT) and alanine:glyoxylate aminotransferase (AGT) activities in melon plants increased their resistance against *Pseudoperonospora cubensis* infection. In contrast, rice plants with reduced *GOX* expression become more resistant against *Xanthomonas oryzae* pv. *oryzae* infection (Ahammed et al., 2018). Tomato plants infected with *Pseudomonas syringae* pv. tomato showed a higher photorespiration rate and higher expression of genes encoding for *GOX*, *SGT*, and serine hydroxylmethyltransferase (*SHMT*) (Taler et al., 2004). Furthermore, C_1 metabolism provides precursors to lignin production that help to reduce the colonization of plant tissues by the pathogen (Bush, 2020). Moreover, photorespiration is an important process to maintain adequate nitrogen homeostasis which is closely related to its metabolism. The enzyme glutamate:glyoxylate aminotransferase (GGT) links photorespiration to the metabolism of amino acids and organic acids by transferring the amino group from glutamate to glyoxylate to produce glycine and 2-oxoglutarate (2-OG) (Dellero et al., 2015). The 2-OG is converted back to glutamate in the chloroplasts by glutamine synthetase (GS) and glutamate synthase (GOGAT) (Lima Neto et al., 2017). Cucumber plants receiving nitrate became more resistant to infection by *Fusarium oxysporum* f. sp. *cucumerinum* due to an increase in their photorespiratory rate (Sun et al., 2021).

In this current study, it was hypothesized that the infection of *S. lycopersici* on tomato leaves could deeply perturb the photorespiratory pathway that ultimately would compromise the basal level of host defense. An in-depth analysis of the photosynthesis and the pool of related pigments, some metabolites (*e.g.*, malondialdehyde, hydrogen peroxide, and superoxide anion radical) involved in cellular reactions, and the expression of genes involved in both photorespiratory pathway and host defense were performed to validate this hypothesis and to advance our knowledge on this important subject in tomato-*S. lycopersici* interaction.

2. Material and methods

2.1. Plant growth

Tomato seedlings (cultivar Santa Cruz Kada (Isla Sementes, São Paulo, Brazil) were grown according to Silva et al. (2021) in a greenhouse (temperature of 25 ± 5°C, relative humidity of 70 ± 5%, and natural photosynthetically active radiation (PAR) of 900 ± 15 μmol photons m^{-2} s^{-1} measured at midday until being inoculated with *S. lycopersici*.

2.2. Obtaining inoculum of *S. lycopersici* and inoculation of plants

The inoculum of *S. lycopersici* isolate UFV-DFP *Sl*-12 to be used to inoculate the plants was obtained following the methodology of Silva et al. (2022). A conidial suspension (5×10^4 conidia/mL, 15 mL per plant) of *S. lycopersici* was used to inoculated three leaves, from top to basis, of each plant with the aim of a VL Airbrush atomizer. The inoculated plants were placed inside of a mist growth chamber (25°C and relative humidity of 90 ± 5%) while the not inoculated ones were kept in a separate growth chamber with the same temperature and relative humidity. After this period, not inoculated and inoculated plants were transferred to a greenhouse (28 ± 2°C, relative humidity of 80 ± 5%, and natural PAR of 875 ± 15 μmol photons m^{-2} s^{-1} measured at midday) until the end of the experiments.

2.3. Measurements of leaf gas exchange and chlorophyll (Chl) a fluorescence

An open-flow infrared gas exchange analyzer system equipped with an integrated fluorescence chamber (IRGA, Li-color Inc. LI-6400XT, NE) was used to obtain simultaneously the leaf gas exchange and Chl *a* fluorescence parameters at the central leaflet of the third leaf, from top to basis, of each plant per replication of each treatment (four replications (four plants and four leaflets)) per sampling time at 4 5, 6, 7, and 8 dai. Leaflets from not inoculated plants

were used to obtain the leaf gas exchange and Chl *a* fluorescence parameters at the same above-mentioned evaluation time. The net carbon assimilation rate (A), stomatal conductance to water vapor (g_s), internal CO_2 concentration (C_i), and transpiration rate (E) were measured during the day (from 08:00 to 12:00 h) with the following conditions: leaf chamber at 25ºC, constant CO_2 concentration (400 ppm), PAR of 1000 μmol photons m^{-2} s^{-1}, and amount of blue light set with 10% of PAR to optimize stomatal aperture (Marçal et al., 2021). A time series of CO_2 concentrations (400, 300, 200, 100, 50, 400, 400, 600, 800, 1000, 1200, and 1600 ppm) inside the chamber of the LI-6400XT instrument was used to obtain the A/C_i curves. The A-C_i curves were converted into A-C_c curves using the g_m values. From these curves, the maximum rate of carboxylation (V_{cmax}) and the maximum rate of carboxylation limited by electron transport (J_{max}), both on a C_c basis, were calculated by fitting the mechanistic model of CO_2 assimilation as proposed by Farquhar et al. (1980) using the C_c-based temperature dependence of the kinetic parameters of RuBisCO (Bernacchi et al., 2002). The values of V_{cmax}, J_{max}, and g_m were normalized to 25°C using the temperature response equations previously described Harley and Sharkey (1991). The R_d (daytime respiration rate) was estimated according to Lloyd et al. (1995). The photorespiratory rate of RuBisCO (R_P) was calculated as $R_P = 1/12[ETR - 4(A + R_d)]$ according to Valentini et al. (1995). Corrections for the leakage of CO_2 into and out of the chamber were applied for all measurements according to Rodeghiero et al. (2007). Finally, the photorespiration-to-gross photosynthesis ratio (R_P/A_G) was calculated by computing the values of R_P, A, and R_d as described by DaMatta et al. (2016). Plants were acclimatized in the dark for 30 min before the Chl *a* fluorescence parameters (variable-to-maximum Chl *a* fluorescence ratio was calculated (F_v/F_m), effective PSII quantum yield (Y(II)), quantum yield of regulated energy dissipation (Y(NPQ)), quantum yield of non-regulated energy dissipation (Y(NO)), and apparent electron transport rate (ETR)) were obtained following the procedures described by Aucique-Perez et al. (2014).

2.4. Imaging of Chl a fluorescence parameters

The Imaging-PAM fluorometer (MAXI version) associated with the Imaging Win software (Heinz Walz GmbH, Effeltrich, Germany) was used to obtain the images of Chl *a* fluorescence parameters following the procedures described by (Chaves et al., 2021). The central leaflet of the third leaf, from top to basis, of each plant per replication of each treatment (four replications (four plants and four leaflets) per sampling time for either not inoculated or inoculated with *S. lycopersici*) were collected at 4, 5, 6, 7, and 8 dai. The circular option (area

of 1 cm^2) on the Imaging Win software was selected for the quantification of Chl *a* fluorescence parameters on the images obtained from the central leaflet of not inoculated and inoculated.

2.5. Determining photosynthetic pigments concentration

The chlorophyll (Chl) *a*, Chl *b*, and carotenoids were quantified in the same leaflets used for Chl *a* fluorescence parameters assessment. Briefly, leaf tissue (50 mg) was ground in liquid nitrogen using a vibration ball mill (Retsch, Haan, Germany) and the fine powder was homogenized in 1 mL methanol to determine the concentrations of Chl *a*, Chl *b*, and carotenoids according to (Silva et al., 2022).

2.6. Biochemical and molecular assays

The fourth leaf, from top to basis, of each plant per replication of each treatment (four replications per evaluation time totalizing 8 plants and 8 leaves that were either not inoculated or inoculated with *S. lycopersici*) was collected at 4, 5, 6, 7, and 8 dai. Leaf samples were collected from plants and rapidly kept in liquid nitrogen and stored at -80°C until further analysis.

2.7. Determining malondialdehyde (MDA) concentration

Leaf tissue (50 mg) was ground as described above and the fine powder was used to determine MDA concentration according to (Dias et al., 2020).

2.8. Determining hydrogen peroxide (H_2O_2) and superoxide anion radical ($O_2^{\bullet-}$) concentrations

Leaf tissue (100 mg) was ground as described above and the fine powder was used to determine H_2O_2 concentration according to (Dias et al., 2020). Leaf tissue (50 mg) was ground as described above and the fine powder was used to quantify $O_2^{\bullet-}$ following the procedures of (Chaves et al., 2021).

2.9. Genes expression using reverse transcription quantitative real-time PCR (RT-PCR)

Leaf tissue (75 mg) was ground as described above and the fine powder was used to extract RNA using TRIzol (Invitrogen). The procedures described by Silva et al. (2022) were carefully followed to remove DNA contamination, quantify RNA, determine RNA quality and integrity, and synthesize single-stranded cDNAs. Expression analysis of genes coding for

glycolate oxidase (*GOX1* and *GOX2*), glutamate:glyoxylate aminotransferase (*GGT*), serine:glyoxylate aminotransferase (*SGT*), alanine:glyoxylate aminotransferase (*AGT1* and *AGT2*), glycine decarboxylase H subunit (*GDC-H*), serine hydroxymethyl transferase (*SHMT1*, *SHMT2*, and *SHMT3*), formyltetrahydrofolate synthetase (*FTHFS*), hydroxypyruvate reductase (*HPR2*), glycerate kinase (*GLYK*), glutamine synthetase (*GS*), ferredoxin-dependent glutamate synthetase (*Fd-GOGAT*), chloroplast malate dehydrogenase (*chMDH*), peroxisomal malate dehydrogenase (*pMDH*), mitochondrial malate dehydrogenase (*mMDH1* and *mMDH2*), catalase (*CAT*), alternative oxidase (*AOX1a*, *AXO1b*, and *AOX1c*), host defense (non-expressor of pathogenesis-related genes 1 (*NPR1*) and pathogenesis-related protein 1 (*PR1b1*)) were determined by RT-qPCR on a Bio-Rad CFX Real-Time Thermal Cycler using SYBR Green PCR Master Mix according to the manufacturer's recommendations. The genes studied were amplified using specific primer sequences (Table 1). All reactions were performed in triplicate and the relative expression values for each gene studied were calculated using the $2^{-\Delta\Delta Ct}$ method Livak and Schmittgen (2001). The expression of the translation elongation factor 1α of *S. lycopersici* (*TEF-1α*) was also quantified to confirm its presence in leaflet tissues. The Actin (*ACT*) gene of tomato was used as a reference for normalization Ahammed et al. (2018).

2.10. Data analysis

Two experiments (Experiments 1 and 2) were arranged in a completely randomized design with two treatments (plants non-inoculated (NI) or inoculated (I) with *S. lycopersici*) and four replications per each evaluation or sampling time. Plants from these experiments were used to evaluate leaf gas exchange and Chl *a* fluorescence parameters and also to determine the concentration of photosynthetic pigments. Two other experiments (Experiments 3 and 4) were arranged in a completely randomized design with two treatments (plants not inoculated or inoculated with *S. lycopersici*) and four replications per each sampling time to obtain leaflet samples for biochemical assays and to determine genes expression. Each experimental unit consisted of one plastic pot containing one plant. Data from variables and parameters evaluated in each experiment were analyzed to determine if data from variables and parameters of Experiments 1 and 2 and Experiments 3 and 4 could be combined (Moore and Dixon, 2014). Data from variables and parameters were checked for normality and homogeneity of variance and subjected to analysis of variance. Principal components analysis (PCA) was performed using data from all variables and parameters evaluated from inoculated and not inoculated

plants at 8 dai. Treatment means were compared by the *F* test ($P \leq 0.05$) using the Minitab software (version 18, Minitab Corporation).

3. Results

3.1. Analysis of variance

The factor PC was significant for A, C_i, V_{cmax}, J_{max}, R_p/A_G, F_v/F_m, Y(II), Y(NPQ), Y(NO), Chl *a+b,* Car, MDA, H_2O_2, *GOX1*, *AGT1*, *GDC-H*, *SHMT2*, *SHMT3*, *Fd-GOGAT*, and *TEF-1α* (Table 2).

3.2. Leaf gas exchange parameters

There were significant decreases for A (26, 40, and 66% at 6, 7, and 8 dai, respectively), g_s (40% at 8 dai), J_{max} (11, 46, and 67% at 6, 7, and 8 dai, respectively), and V_{cmax} (23 and 35% at 7 and 8 dai, respectively) and significant increases for C_i (15, 10, and 17% at 6, 7, and 8 dai, respectively), R_d (35, 28, 20, and 30% at 5, 6, 7, and 8 dai, respectively), and R_p/A_G (37, 33, 47, and 68% at 5, 6, 7, and 8 dai, respectively) for inoculated plants in comparison to not inoculated ones (Figs. 1 a-c and 2 a-d).

3.3. Imaging and quantification of Chl a fluorescence parameters and concentrations of photosynthetic pigments

The inoculated plants showed remarkable damage to their photosynthetic apparatus (dark areas noticed in the images for F_v/F_m, Y(II), Y(NPQ), and Y(NO) compared to not inoculated ones from 6 to 8 dai (Fig. 3). Significant decreases for F_v/F_m (11, 62, and 76% at 6, 7, and 8 dai, respectively) and Y(II) (33, 56, and 80% at 6, 7, and 8 dai, respectively) and significant increases for Y(NPQ) (8, 10, and 31% at 6, 7, and 8 dai, respectively) and Y(NO) (25, 42, and 43% at 6, 7, and 8 dai, respectively) were obtained for inoculated plants in comparison to not inoculated ones (Fig. 4 a-d). The concentrations of Chl *a+b* (41, 38, and 64% at 6, 7, and 8 dai, respectively) and carotenoids (61, 45, and 73% at 6, 7 and 8 dai, respectively) significantly decreased for inoculated plants in comparison to not inoculated ones (Fig. 5 a-b).

3.4. Concentrations of MDA, H_2O_2, and $O_2^{\bullet-}$

The concentrations of MDA (61 and 121% at 7 and 8 dai, respectively), H_2O_2 (18, 19, and 21% at 6, 7, and 8 dai, respectively), and $O_2^{\bullet-}$ (39, 31, and 37% at 6, 7, and 8 dai,

respectively) significantly decreased for inoculated plants in comparison to not inoculated ones (Fig. 6 a-c).

3.5. Genes expression

The *GGT2* (at 7 dai), *SGT* (at 8 dai), *GDC-H* (at 6, 7, and 8 dai), and *mMDH2* (at 7 days) were significantly up-regulated for not inoculated plants in comparison to inoculated ones (Fig. 7a). The *GOX1* and *SHMT2* (at 5 and 6 dai), *GOX2* (at 7 dai), *SHMT3*, *GLYK*, and *NPR1* (at 6 dai), *mMDH1* (at 7 and 8 dai), *mMDH2* (at 6 and 8 dai), *CAT* (at 4 dai), and *AOX1B* (at 6 and 7 dai) were significantly up-regulated for inoculated plants in comparison to not inoculated ones (Fig. 7b).

3.6. PCA analysis

According to the cluster analysis with complete linkage and Pearson distance, NI and I plants were separated into two clusters (Fig. 8a). One principal component (PC) explained most of the data variation (53 and 28% for PC1 and PC2, respectively) (Fig. 8a-b). The first PC was characterized by negative scores for C_i, *E*, Y(II), Y(NO), Car, MDA, $O_2^{\bullet-}$, *SGT*, *SHMT1*, and *pMDH*. Positive scores were obtained for *A*, g_s, Y(NPQ), Chl *a*+*b*, *E*, R_d, V_{cmax}, J_{max}, H_2O_2, *GOX1*, *GOX2, GGT*, *SGT*, *AGT1, AGT2*, *GDC-H*, *SHMT2*, *SHMT3*, *FTHFS*, *HPR2*, *GLYK*, *GS*, *Fd-GOGAT*, *chMDH*, *mMDH1*, *mMDH*, *CAT*, *AOX1a*, *AXO1b*, *AOX1c*, *NPR1*, and *PR1b1* (Fig. 8a-b).

4. Discussion

Investigating the impact caused by the infection of pathogens on the photosynthetic apparatus of their host is of utmost importance when considering that their level of basal resistance can be seriously compromised. In this regard, the present study aimed to fill out this gap by demonstrating the profound impact caused by *S. lycopersici* infection on photorespiration and correlated changes in photosynthesis, nitrogen metabolism, acclimation to reduced CO_2 availability, and host defense.

Photosynthesis is a key physiological process perturbed in plants infected by pathogens and has been deeply investigated in different host-pathogen interactions (Aucique-Pérez et al., 2014; Fagundes-Nacarath et al., 2019; Rios et al., 2017; Dias et al., 2020). Infection of leaves from blueberry plants by *Septoria albopunctata* affected photosynthesis due to stomatal limitations (Roloff et al., 2004). On the other hand, reduction in photosynthesis was associated

with stomatal and biochemical limitations as reported for wheat plants infected by *Pyricularia oryzae* (Aucique-Perez et al., 2014). In the present study, low values of g_s explained the reductions in A only at 8 dai, while C_i increased sharply from 6 to 8 dai for infected leaflets.

Plants infected by pathogens besides having their photosynthetic capacity greatly impaired also show an increase in respiration, photorespiration, and invertase activity in order to maximize their defense responses against pathogen infection (Lopes and Berger, 2001; Bassanezi et al., 2002; Major et al., 2010; Debona et al., 2012). Infection of tomato leaves by *S. lycopercisi* caused a sharp increase in R_d from 5 to 8 dai possibly as a strategy mounted by the plants to defend themselves against fungal infection. The V_{cmax} and J_{max} are closely linked to the photosynthetic capacity of leaves (Fan et al., 2011). Similarly, to infection caused by other pathogens (Nogués and Baker, 2000; Hajji et al., 2009; Zhou et al., 2014; Ghosh et al., 2016), reductions in A at 6 dai were accompanied by expressive reductions in both J_{max} (at 6 to 8 dai) and V_{cmax} (at 7 and 8 dai) suggesting that impairment in the photosynthetic apparatus was due to lower efficiency of ETR and RuBisCO activity. In addition, the R_P/A_G ratio increased from 5 to 8 dai indicating the role played by the photorespiratory metabolism as a sink of excess energy produced during the infection process of *S. lycopersici*.

In the present study, lower F_v/F_m and Y(II) values were closely linked to increases in Y(NPQ) and Y(NO) during the infection process of *S. lycopersici*. Therefore, it is plausible to suggest that damage to photosynthesis on tomato leaves caused by *S. lycopersici* infection may also be associated with photochemical restrictions. Reduced values of Y(II) indicated loss of efficiency in directing light energy to photochemistry probably due to a direct effect caused by *S. lycopersici* infection. On top of that, the progressive increases in Y(NPQ) and Y(NO) values showed that photoprotection mechanisms became quite ineffective on infected tomato leaves. Decreases in the quantum yield of electron transfer at PSII (ϕPSII) in wheat leaves infected by *Zymoseptoria tritici* were linked to higher Y(NPQ) values demonstrating that heat dissipation was used to prevent photoinhibition and damage to PSII (Mihailova et al., 2019). As the SLS lesions expanded and the photodamage in the photosynthetic apparatus became more expressive, along with less efficient use of light to optimize carbon fixation, the pool of foliar photosynthetic pigments dramatically decreased. Many reports highlighted the decrease in the concentrations of Chl *a*, Chl *b*, and carotenoids in leaves infected by pathogens of different lifestyles (Aucique-Pérez et al., 2014; Rios et al., 2017; Dias et al., 2020; Fagundes-Nacarath et al., 2019).

Regarding the changes in the expression of genes involved in the photorespiratory pathway, the enzyme GOX, which catalyzes the conversion of glycolate to glyoxylate and H_2O_2, plays an important role in increasing the pool of ROS in foliar green tissues (Lima Neto et al., 2017). Indeed, melon plants displaying higher GOX activity were more resistant against *P. cubensis* infection (Dong et al., 2016). In the present study, the up-regulation of *GOX1* and *GOX2* in the infected leaves might have contributed, at least in part, to generate H_2O_2. However, according to Foyer et al. (2009), higher SGT and AGT activities increase glyoxylate consumption and accelerate GOX activity upstream for H_2O_2 generation. The down-regulation of *GGT2* and *SGT* in the infected leaves possibly contributed to raising the pool of glyoxylate which would decrease H_2O_2 production. Thus, it is plausible to postulate that H_2O_2 generation at advanced stages of *S. lycopersici* infection could be linked not only to the photorespiratory pathway but to closed-related biochemical pathways.

Higher photorespiratory rate and higher expressions of *GOX*, *SGT*, and *SHMT* proved to be crucial for tomato plants to cope successfully with *Pseudomonas syringae* pv. *tomato* infection (Ahammed et al., 2018). In the present study, *SHMT2* and *SHMT3* (which are involved in the conversion of glycine to serine) were also up-regulated. However, even with *NPR1* upregulation, which is highlighted to be important in the increased resistance of plants to pathogen infection (Chen et al., 2016), the absence of *PR1B1* expression indicated that tomato defense response against *S. lycopersici* infection was barely affected and any attempt of tomato leaves to respond against its infection was not necessary.

In the present study, *GDC-H* and *Fd-GOGAT* were down-regulated in infected leaves and likely impacted R_p/A_G and nitrogen metabolism. The GDC is placed at a point of convergence with diverse metabolic processes in plant tissues such as C_1 metabolism, nitrogen assimilation, respiration, and the tricarboxylic acid cycle (Bauwer et al., 2010). During GDC activity, CO_2, tetrahydrofolate (THF), and NH_3 are produced while ATP and reducing equivalents are consumed (Moreno et al., 2005). Considering that ammonia (NH_3) is harmful to plant cells, it must be rapidly reassimilated in chloroplasts through the GS/Fd-GOGAT reactions (Backer et al., 2019). Indeed, rice resistance against *R. solani* infection was linked to an abundance of the proteins Fd-GOGAT and GDC-H (Zhou et al., 2004).

Photorespiration is part of the plant stress response to avoid ROS accumulation by using the excess of NADPH and ATP formed during the photochemical step (Palmieri et al., 2010). Increases in the activities of catalase, alternative oxidase, and malate dehydrogenase are also important to help to dissipate excess energy (Wingler et al., 2000). The MDHs do not directly

prevent ROS accumulation, but play an important role in transporting reducing equivalents between chloroplasts, peroxisomes, and mitochondria via malate-aspartate/oxaloacetate transport during photorespiration (Farahani and Taghavi, 2015). In this scenario, restrictions on photosynthetic electron flow are avoided and the electron flow is redirected to be used in any other metabolic processes (Sunil et al., 2019). In the present study, *mMDH1* (7 and 8 dai) and *mMDH2* (6 and 8 dai) were up-regulated in infected leaves. In line with the fact that MDH expression is closely associated with the resistance of plants against pathogen infection (Timm and Hagemann, 2020), it can be postulated that up-regulation of *mMDH* may be involved in the stress acclimatization of tomato plants during the infection process of *S. lycopersici* as well with their better metabolic readjustment and defense.

In plant tissues, electrons produced during the respiratory oxidation of NADPH can flow through the usual respiratory cytochrome pathway or the AOX in mitochondria (Ma et al., 2020). The AOX helps to maintain the redox balance and metabolic homeostasis and its modulation confers plant tolerance to different types of abiotic and biotic stresses (Zhang et al., 2017). The AOX acts as a photoprotective mechanism of PSII in C_3 plants and contributed to maintaining photorespiration to detoxify glycolate and export reducing equivalents (Maurino and Peterhansel, 2010). Some reports have shown that infected tomato plants showed an increase in *AOX* expression (Gao et al., 2020) and *AOX1b* was up-regulated at 6 and 7 dai in the leaves infected by *S. lycopersici* at the present study. Furthermore, a connection between photorespiratory glycine decarboxylation and AOX activity seems to be a protective mechanism that occurs in plant tissues (Dong et al., 2016). Oxidative damage caused by ROS accumulation inhibited GDC activity (Taylor et al., 2002). In the present study, infection by *S. lycopersici* resulted in down-regulation of *GDC-H* and up-regulation of *AOX1b* as indicated by ROS accumulation that could have directly impacted the photorespiratory cycle.

The *CAT* was up-regulated only at 4 dai in infected leaves and great H_2O_2 concentration may have reflected a redox imbalance caused by *S. lycopersici* infection rather than any perturbation in the photorespiratory pathway. Catalase plays a key role during photorespiration by preventing the accumulation of H_2O_2 from the oxidation of glycolate by GOX (Bao et al., 2021). Peroxisomal CAT activity was involved as an electron sink or perhaps as a signal for the photorespiratory pathway of H_2O_2 production in melon plants supplied with ammonia and infected by *F. oxysporum* f. sp. *cucumerinum* (Ding et al., 2021). In Arabidopsis plants, *CAT2* was down-regulated during *P. syringae* pv. tomato infection and up-regulated in response to *Pseudomonas syringae* pv. *maculicola* (Sørhagen et al., 2013).

Taken together, the effect of *S. lycopersici* infection on the photorespiratory pathway of tomato plants was highlighted by a robust set of physiological, biochemical, and molecular evidences. In this regard, fungal infection dramatically reduced carbon fixation, increased respiration, and modify the photorespiration pathway. Interestingly, the perturbation imposed by *S. lycopersici* infection on the photorespiration of tomato plants barely affected their basal capacity for defense. Taking into consideration the PCA analysis, the separation of the clusters not inoculated plants from inoculated plants highlights notorious changes occurring in both photorespiratory pathway and protective system as the infection process of *S. lycopersici* took place. On top of that, finding a way to enhance the photorespiration of tomato plants coping against *S. lycopersici* infection may be translated into reduced yield losses on tomato production.

5. References

Ahammed GJ, Li X, Zhang G, Zhang H, Shi J, Pan C, Yu J, Shi K (2018) Tomato photorespiratory glycolate-oxidase-derived H_2O_2 production contributes to basal defence against *Pseudomonas syringae*. Plant, Cell & Environment 4:1126-1138.

Aldea M, Hamilton JG, Resti JP, Zangerl JP, Berenbaum R, Frank RM, Delucia EHL (2006) Comparison of photosynthetic damage from arthropod herbivory and pathogen infection in understory hardwood saplings. Oecologia 149:221-232.

Aucique-Pérez CEA, Rodrigues FA, Moreira WR, DaMatta FM (2014) Leaf gas exchange and chlorophyll *a* fluorescence in wheat plants supplied with silicon and infected with *Pyricularia oryzae*. Phytopathology 104:143-149.

Ávila MCR, Lourenco Junior V, Quezado-Duval AM, Becker WF, Abreu-Tarazi MF, Borges LC, Nascimento A (2020) Field validation of TOMCAST modified to manage Septoria leaf spot on tomato in the central-west region of Brazil. Crop Protection 138:105333.

Backer R, Naidoo S, Van den Berg N (2019) The NONEXPRESSOR OF PATHOGENESIS-RELATED GENES 1 (*NPR1*) and related family: mechanistic insights in plant disease resistance. Frontier in Plant Science 10:102.

Bao H, Morency M, Rianti W, Saeheng S, Roje S, Weber APM, Walker BJ (2021) Catalase protects against nonenzymatic decarboxylations during photorespiration in *Arabidopsis thaliana*. Plant Direct 5:e366.

Bassanezi RB, Amorim L, Bergamin Filho A, Berger RD (2002) Gas exchange and emission of chlorophyll fluorescence during the monocycle of rust, angular leaf spot and anthracnose on bean leaves as a function of their trophic characteristics. Journal of Phytopathology 150:37-47.

Bauwe H, Hagemann M, Fernie AR (2010) Photorespiration: players, partners and origin. Trends in Plant Science 15:330-336.

Berger S, Sinha AK, Roitsch T (2007) Plant physiology meets phytopathology: plant primary metabolism and plant-pathogen interactions. Journal of Experimental Botany 58:4019-4026.

Bernacchi CJ, Portis AR, Nakano H, Von Caemmerer S, Long SP (2002) Temperature response of mesophyll conductance. Implications for the determination of Rubisco enzyme kinetics and for limitations to photosynthesis in vivo. Plant Physiology 130:1992-1998.

Busch FA (2020) Photorespiration in the context of Rubisco biochemistry, CO_2 diffusion and metabolism. Plant Journal 101:919-939.

Chaves JAA, Oliveira LM, Silva LC, Silva BN, Dias CS, Rios JA, Rodrigues FA (2021) Physiological and biochemical responses of tomato plants to white mold affected by manganese phosphite. Journal of Phytopathology 169:149-167.

Chen H, Li C, Liu L, Zhao J, Cheng X, Jiang G, Zhai W (2016) The Fd-GOGAT1 mutant gene *lc7* confers resistance to *Xanthomonas oryzae* pv. *oryzae* in rice. Scientific Reports 6:1-13.

Chern M, Bai W, Chen X, Canlas PE, Ronald PC (2013) Reduced expression of glycolate oxidase leads to enhanced disease resistance in rice. PeerJ, 1:e28.

DaMatta FM, Godoy AG, Menezes-Silva PE, Martins SC, Sanglard LM, Morais LE, Torre-Neto A, Ghini R (2016) Sustained enhancement of photosynthesis in coffee trees grown under free-air CO_2 enrichment conditions: disentangling the contributions of stomatal, mesophyll, and biochemical limitations. Journal of Experimental Botany 67:341-352.

Debona D, Rodrigues FA, Rios JA, Nascimento KJT (2012) Biochemical changes in the leaves of wheat plants infected by *Pyricularia oryzae*. Phytopathology 102:1121-1130.

Dellero Y, Lamothe-Sibold M, Jossier M, Hodges, M (2015) *Arabidopsis thaliana ggt1* photorespiratory mutants maintain leaf carbon/nitrogen balance by reducing RuBisCO content and plant growth. Plant Journal 83:1005-1018.

Dias CS, Rios JA, Einhardt AM, Chaves JA, Rodrigues FA (2020) Effect of glutamate on *Pyricularia oryzae* infection of rice monitored by changes in photosynthetic parameters and antioxidant metabolism. Physiologia Plantarum 169:179-193.

Ding S, Shao X, Li J, Ahammed GJ, Yao Y, Ding J, Hu Z, Yu J, Shi K (2021) Nitrogen forms and metabolism affect plant defence to foliar and root pathogens in tomato. Plant, Cell & Environment 44:1596-1610.

Dong X, Wang M, Ling N, Shen Q, Guo S (2016) Potential role of photosynthesis-related factors in banana metabolism and defense against *Fusarium oxysporum* f. sp. *cubense*. Environmental and Experimental Botany 129:4-12.

Fagundes-Nacarath IR, Debona D, Rodrigues FA (2018) Oxalic acid-mediated biochemical and physiological changes in the common bean-*Sclerotinia sclerotiorum* interaction. Plant Physiology and Biochemistry 129:109-121.

Fan Y, Zhong Z, Zhang X (2011) Determination of photosynthetic parameters V_{cmax} and J_{max} for a C_3 plant (spring hulless barley) at two altitudes on the Tibetan Plateau. Agricultural and Forest Meteorology 151:1481-1487.

Farahani AS, Taghavi SM (2015) Expression profiling of malate dehydrogenase, superoxide dismutase and polygalacturonase-inhibiting protein in common bean in response to host and non-host pathogens. Journal of Plant Pathology 97.

Farquhar G, von Caemmerer SV, Berry JA (1980) A biochemical model of photosynthetic CO_2 assimilation in leaves of C_3 species. Planta 149:78-90.

Foyer CH, Bloom AJ, Queval G, Noctor G (2009) Photorespiratory metabolism: genes, mutants, energetics, and redox signaling. Annual review of plant biology 60:455-484.

Gao C, Xu H, Huang J, Sun B, Zhang F, Savage Z, Yan DT, Wu C, Wang Y, Vleeshouwers VGAA, Kamoun S, Bozkurt TO, Dong S (2020) Pathogen manipulation of chloroplast function triggers a light-dependent immune recognition. Proceedings of the National Academy of Sciences 117:9613-9620.

Ghosh P, Sen S, Chakraborty J, Das S (2016) Monitoring the efficacy of mutated *Allium sativum* leaf lectin in transgenic rice against *Rhizoctonia solani*. BMC Biotechnology 16:1-10.

Hajji M, Dreyer E, Marçais B (2009) Impact of *Erysiphe alphitoides* on transpiration and photosynthesis in *Quercus robur* leaves. European Journal of Plant Pathology 125:63-72.

Harley PC, Sharkey TD (1991) An improved model of C_3 photosynthesis at high CO_2: reversed O_2 sensitivity explained by lack of glycerate re-entry into the chloroplast. Photosynthesis Research 27:169-178.

Lima Neto MC, Cerqueira JVA, Cunha JR, Ribeiro RV, Silveira JAG (2017) Cyclic electron flow, NPQ and photorespiration are crucial for the establishment of young plants of *Ricinus communis* and *Jatropha curcas* exposed to drought. Plant Biology 19:650-659.

Livak KJ, Schmittgen TD (2001) Analysis of relative gene expression data using real-time quantitative PCR and the $2^{-\Delta\Delta CT}$ method. Methods 25:402-408.

Lopes DB, Berger RD (2001) The effects of rust and anthracnose on the photosynthetic competence of diseased bean leaves. Phytopathology 91:212-220.

Ma Q, Liu Y, Fang H, Wang P, Ahammed GJ, Zai W, Shi K (2020) An essential role of mitochondrial α-ketoglutarate dehydrogenase E2 in the basal immune response against bacterial pathogens in tomato. Frontier in Plant Science 11:30.

Major IT, Nicole MCC, Duplessis S, Séguin A (2010) Photosynthetic and respiratory changes in leaves of poplar elicited by rust infection. Photosynthesis Research 104:41-48.

Marçal DM, Avila RT, Quiroga-Rojas LF, Souza RP, Junior CCG, Ponte LR, DaMatta FM (2021) Elevated [CO_2] benefits coffee growth and photosynthetic performance regardless of light availability. Plant Physiology and Biochemistry158:524-535.

Maurino VG, Peterhansel C (2010) Photorespiration: current status and approaches for metabolic engineering. Current Opinion in Plant Biology 13:248-255.

Mihailova G, Stoyanova Z, Rodeva R, Bankina B, Bimšteine G, Georgieva K (2019) Physiological changes in winter wheat genotypes in response to the *Zymoseptoria tritici* infection. Photosynthetica 57:428-437.

Moore KJ, Dixon PM (2015) Analysis of combined experiments revisited. Agronomy Journal 107:763-771.

Moreno JI, Martín R, Castresana C (2005) Arabidopsis *SHMT1*, a serine hydroxymethyltransferase that functions in the photorespiratory pathway influences resistance to biotic and abiotic stress. Plant Journal 41:451-463.

Navarre DA, Wolpert TJ (1995) Inhibition of the glycine decarboxylase multienzyme complex by the host-selective toxin victorin. Plant Cell 7:463-471.

Nogués S, Baker NR (2000) Effects of drought on photosynthesis in Mediterranean plants grown under enhanced UV-B radiation. Journal of Experimental Botany 51:1309-1317.

Norman EG, Colman B (1991) Purification and characterization of phosphoglycolate phosphatase from the cyanobacterium *Coccochloris peniocystis*. Plant Physiology 95:693-698.

Palmieri MC, Lindermayr C, Bauwe H, Steinhauser C, Durner J (2010) Regulation of plant glycine decarboxylase by S-nitrosylation and glutathionylation. Plant Physiology 152:1514-1528.

Peterhansel C, Maurino VG (2020) Photorespiration redesigned. Plant Physiology 155:49-55.

Rios JA, Rios VS, Aucique-Pérez CE, Cruz MFA, Morais LE, DaMatta FM, Rodrigues FA (2017) Alteration of photosynthetic performance and source-sink relationships in wheat plants infected by *Pyricularia oryzae*. Plant Pathology 66:1496-1507.

Rodeghiero M, Niinemets U, Cescatti A (2007) Major diffusion leaks of clamp-on leaf cuvettes still unaccounted: how erroneous are the estimates of Farquhar et al. model parameters? Plant, Cell & Environment 30:1006-1022.

Roloff I, Scherm H, Van Iersel MW (2004) Photosynthesis of blueberry leaves as affected by Septoria leaf spot and abiotic leaf damage. Plant Disease 88:397-401.

Silva BN, Picanço BBM, Hawerroth C, Silva LC, Rodrigues FA (2022) Physiological and biochemical insights into induced resistance on tomato against septoria leaf spot by a phosphite combined with free amino acids. Physiological and Molecular Plant Pathology 120:101854.

Sørhagen K, Laxa M, Peterhänsel C, Reumann S (2013) The emerging role of photorespiration and non-photorespiratory peroxisomal metabolism in pathogen defence. Plant Biology 15:723-736.

Stevenson WR (2014) Septoria leaf spot. In: Jones JB, Zitter TA, Momol TM, Miller SA, (Eds.), Compendium of Tomato Diseases and Pests. The APS Press, St. Paul, pp. 42-43.

Sun Y, Li Y, Li Y, Wang M, Mur LAJ, Shen Q, Guo S (2021) Nitrate mediated resistance against *Fusarium* infection in cucumber plants acts via photorespiration. Plant, Cell & Environment 44:3412-3431.

Sunil B, Saini D, Bapatla RB, Aswani V, Raghavendra AS (2019) Photorespiration is complemented by cyclic electron flow and the alternative oxidase pathway to optimize photosynthesis and protect against abiotic stress. Photosynthesis Research 139:67-79.

Takahashi S, Badger MR (2011) Photoprotection in plants: a new light on photosystem II damage. Trends in Plant Science 16:53-60.

Taler D, Galperin M, Benjamin I, Cohen Y, Kenigsbuch D (2004) Plant eR genes that encode photorespiratory enzymes confer resistance against disease. Plant Cell 16:172-184.

Taylor NL, Day DA, Millar AH (2002) Environmental stress causes oxidative damage to plant mitochondria leading to inhibition of glycine decarboxylase. Journal of Biological Chemistry 277:42663-42668.

Timm S, Hagemann M (2020) Photorespiration-how is it regulated and how does it regulate overall plant metabolism?. Journal of Experimental Botany 71:3955-3965.

Valentini R, Epron D, Angelis P, Matteucci G, Dreyer E (1995) *In situ* estimation of net CO_2 assimilation, photosynthetic electron flow and photorespiration in Turkey oak (*Q. cerris* L.) leaves: diurnal cycles under different levels of water supply. Plant, Cell & Environment 18:631-640.

Voss I, Sunil B, Scheibe R, Raghavendra AS (2013) Emerging concept for the role of photorespiration as an important part of abiotic stress response. Plant Biology 15:713-722.

Wingler A, Lea PJ, Quick WP, Leegood RC (2000) Photorespiration: metabolic pathways and their role in stress protection. Philosophical Transactions of the Royal Society of London. Series B: Biological Sciences 355:1517-1529.

Zhang ZS, Liu MJ, Scheibe R, Selinski J, Zhang LT, Yang C, Meng XL, Gao HY (2017) Contribution of the alternative respiratory pathway to PSII photoprotection in C_3 and C_4 plants. Molecular Plant 10:31-142.

Zhou YH, Peng YH, Lei JL, Zou LY, Zheng JH, Yu JQ (2004) Effects of potato virus YNTN infection on gas exchange and photosystem 2 function in leaves of *Solanum tuberosum* L. Photosynthetica 42:417-423.

Zivcak M, Kalaji HM, Shao HB, Olsovska K, Brestic M (2014) Photosynthetic proton and electron transport in wheat leaves under prolonged moderate drought stress. Journal of Photochemistry and Photobiology B:Biology. 137:107-115.

List of Tables and Figures

Table 1. Sequences of primers for the genes encoding glycolate oxidase (*GOX1* and *GOX2*), glutamate:glyoxylate aminotransferase (*GGT*), serine:glyoxylate aminotransferase (*SGT*), alanine:glyoxylate aminotransferase (*AGT1* and *AGT2*), glycine decarboxylase H subunit (*GDC-H*), serine hydroxymethyl transferase (*SHMT1*, *SHMT2*, and *SHMT3*), formyltetrahydrofolate synthetase (*FTHFS*), hydroxypyruvate reductase (*HPR2*), glycerate kinase (*GLYK*), glutamine synthetase (*GS*), ferredoxin-dependent glutamate synthetase (*Fd-GOGAT*), chloroplast malate dehydrogenase (*chMDH*), peroxisomal malate dehydrogenase (*pMDH*), mitochondrial malate dehydrogenase (*mMDH1* and *mMDH2*), catalase (*CAT*), alternative oxidase (*AOX1a*, *AXO1b*, and *AOX1c*), non-expressor of pathogenesis-related genes 1 (*NPR1*) and pathogenesis-related protein 1 (*PR1b1*)), actin (*ACT*), and translation elongation factor 1-α (*TEF-1α*) analyzed by quantitative reverse transcription PCR using leaflets of tomato plants non-inoculated or inoculated with *Septoria lycopersici*.

Genes	GenBank Identifications	Primer sense 5'-3'	Primer antisense 5'-3'
GOX1	544106	TGAAGGAGAAGCTGGAGTGA	GACAGCCACTCAATGCCATA
GOX2	100134875	ATGCTGGTTCTTTCCTCTTATCT	CTCCCAAGCAATGAAGAGTG
GGT2	101265236	TTCGGTCAAAAGGAAGGGTG	TAGGTGAGAGTCAGCGGAAA
SGT	101244469	CTCATACCATCAAGGCGGTT	CAGGATGCTGGTAGTGATCG
AGT1	101265236	ACTTGACTGCTGGTCTCTCT	TGCTCCAATAATGAGGGCAC
AGT2	101268729	CGATTGGGCTAACTGCTCTT	TTCTCTAGATCCCTCAGCCG
GLDH	101260070	AGATGCATGGACAAAGCCAT	GTTTGGCTGAACACCTCTAAA
SHMT1	101264818	GACGTTGAGGACTATGCCAA	CGCGCACTCAACACTAGAT
SHMT2	101254439	AGGCCACTACTCCAGAAT	CCTCTAAAGCCTGGGCAAAT
SHMT3	101263138	TTTTTCCTGGTTTGCAGGGT	AGGTGATTTGGCATGCTTCA
FTHFS	101265950	ACCCGCTGGATATAGGTATCA	AGTGCAGCAATAGGTATGAGC
HPR	101251910	GAAGAGAGGTGAGATTGGCG	ACAACATCCTGTGGATTCTTTC
GLYK	101244755	GAACATTCACTGCCTGCACA	GTTAAAATGCTGCCCTGCCA
GS2	543998	GTGAACATGGCTCAGATCCT	AAGGGACTAGCATCGGTTGA
FD-GOGAT	101246028	TCACACTCACTCTGCGATTC	GAGTAACTGCGGAACGTTTG
chLMDH	778287	ACTGGTGCACTGGAACAATA	TCACCCCTTACTACTTGTGTT
pMDH	778286	CCACCTTTTGCTCTGCAATTT	TGTTGTTTTTCGCTATACTCGT
mMDH	543805	CAGTCTGTGTGGTGCTGTTA	GTTCGTACCCGAGCAAATCT

mMDH2	101258530	AGCCTTCCCTAGCTGTTCTT	ACGACCTCAGTGTCTGATCT
CAT1	543990	TGGAAGCCAACTTGTGGTGT	ACTGGGATCAACGGCAAGAG
AOX1a	543824	AATCCATCGGAGAAAGTGGC	TGATCCATCCACCACTCTGT
AOX1b	543825	GAGACAATTACGGGGCGAAT	ATCCGTTCGTTCTCTGCTTC
AOX1c	101247941	CAGAAGAGGTACGGTTGTCG	ATTCCTCCTACCATACCGGG
NPR1	AY640378	GGAGCACTTGAATCGGCTTA	TTGGTGTAAGATGTAGCTGAAGA
PR1b1*	-	TGATTCATTCTGGTGCTGGG	TTATAGCTTGGCCTCTCGGA
TEF-1α	KF253411.1	CTCCAATTTCTGGTGGGGTG	ACTTTGGAGTCTCGAACTTCC
ACT	957571262	TGGTCGGAATGGGACAGAAG	CTCAGTCAGGAGAACAGGGT

* Primer sequences for *PR1b1* were obtained from Ahammed et al. (2018).

Table 2. Analysis of variance for the effects of plant condition (PC) on parameters related to photosynthesis ((leaf gas exchange - net carbon assimilation rate (*A*), stomatal conductance to water vapor (g_s), internal CO_2 concentration (C_i), and transpiration rate (*E*)), photorespiration rate (R_P), maximum rate of RuBisCo carboxylase activity (V_{cmax}), maximum rate of photosynthetic electron transport (J_{max}), photorespiration-to-gross photosynthesis ratio (R_p/A_G), and chlorophyll *a* (maximum PSII quantum efficiency (F_v/F_m), photochemical yield (Y(II)), yield for dissipation by down-regulation (Y(NPQ)), and yield for non-regulated dissipation (Y(NO)), concentrations of chlorophyll *a*+*b* (Chl *a*+*b*), carotenoids (Car), carbohydrates (glucose, fructose, sucrose, and starch), malondialdehyde (MDA), hydrogen peroxide (H_2O_2), and superoxide anion radical ($O_2^{\bullet-}$), and genes expression (glycolate oxidase (*GOX1* and *GOX2*), glutamate:glyoxylate aminotransferase (*GGT*), serine:glyoxylate aminotransferase (*SGT*), alanine:glyoxylate aminotransferase (*AGT1* and *AGT2*), glycine decarboxylase H subunit (*GDC-H*), serine hydroxymethyl transferase (*SHMT1*, *SHMT2*, and *SHMT3*), formyltetrahydrofolate synthetase (*FTHFS*), hydroxypyruvate reductase (*HPR2*), glycerate kinase (*GLYK*), glutamine synthetase (*GS*), ferredoxin-dependent glutamate synthetase (*Fd-GOGAT*), chloroplast malate dehydrogenase (*chMDH*), peroxisomal malate dehydrogenase (*pMDH*), mitochondrial malate dehydrogenase (*mMDH1* and *mMDH2*), catalase (*CAT*), alternative oxidase (*AOX1a*, *AXO1b*, and *AOX1c*), non-expressor of pathogenesis-related genes 1 (*NPR1*) and pathogenesis-related protein 1 (*PR1b1*)), and translation elongation factor 1-α (*TEF-1α*)).

Variables/Parameters	PI
A	**<0.001**
g_s	0.077
C_i	**0.001**
E	0.084
R_P	0.960
V_{cmax}	**0.003**
J_{max}	**0.012**
R_p/A_G	**0.013**
F_v/F_m	**<0.001**
Y(II)	**<0.001**
Y(NPQ)	**0.003**
Y(NO)	**0.001**
Chl *a*+*b*	**<0.001**
Car	**0.001**
MDA	**0.016**

H_2O_2	**0.008**
$O_2^{\bullet-}$	0.058
GOX1	**0.028**
GOX2	0.577
GGT2	0.423
SGT	0.080
AGT1	**0.049**
AGT2	0.171
GDC-H	**<0.001**
SHMT1	0.286
SHMT2	**0.006**
SHMT3	**0.026**
THF	0.073
HPR2	0.260
GLYK	0.056
GS2	0.193
Fd-GOGAT	**0.078**
chMDH	0.184
mMDH	0.068
mMDH2	0.064
gMDH	0.759
CAT	0.458
AOX1B	0.565
AOX2B	0.226
AOX1C	0.150
PR1	0.058
NPR1	0.354

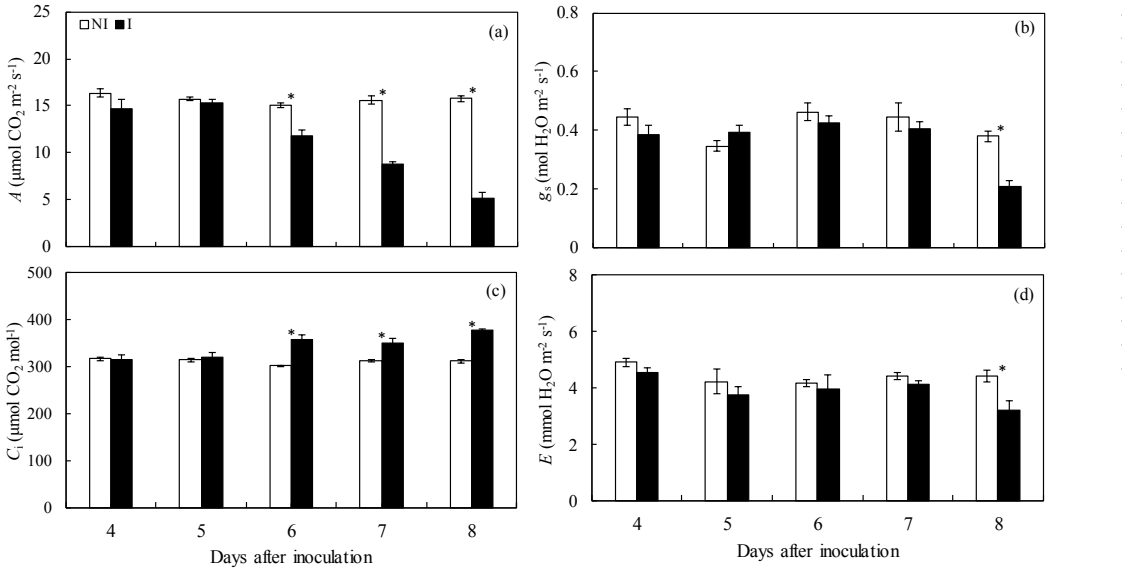

Figure 1. Leaf gas exchange parameters net carbon assimilation rate (*A*) (a), stomatal conductance to water vapor (g_s) (b), internal CO_2 concentration (C_i) (c), and transpiration rate (*E*) (d) determined on the leaflets of tomato plants non-inoculated (NI) or inoculated (I) with *Septoria lycopersici*. Means from NI and I plants, at each evaluation time, followed by an asterisk (*) are significantly different according to the *F* test ($P \leq 0.05$). Bars represent the standard deviation of the means.

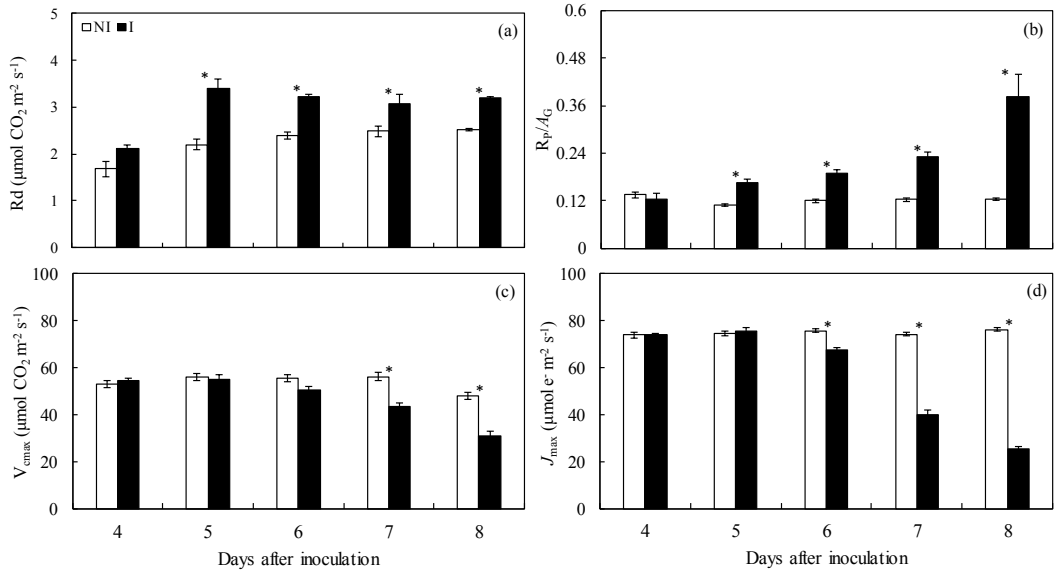

Figure 2. Respiration rate (R_P) (a), photorespiration-to-gross photosynthetic rate ratio (R_p/A_G) (b), maximum apparent carboxylation capacity (V_{cmax}) (c), and maximum rate of carboxylation limited by electron transport (J_{max}) (d) determined on the leaflets of tomato plants non-inoculated (NI) or inoculated (I) with *Septoria lycopersici*. Means from NI and I plants, at each evaluation time, followed by an asterisk (*) are significantly different according to the *F* test ($P \leq 0.05$). Bars represent the standard deviation of the means.

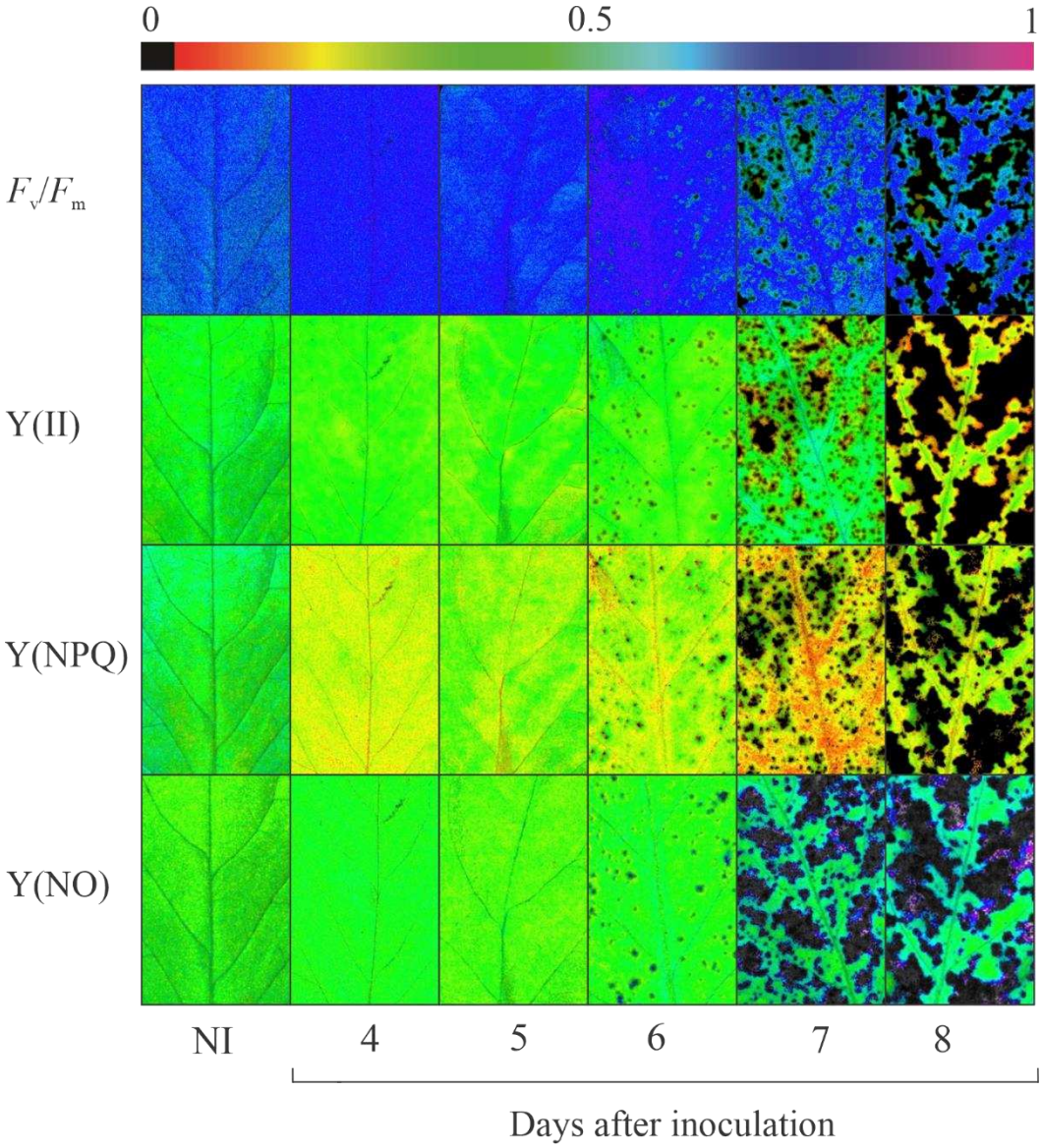

Figure 3. Images of chlorophyll *a* fluorescence parameters maximum PSII quantum efficiency (F_v/F_m), photochemical yield (Y(II)), yield for dissipation by down-regulation (Y(NPQ)), and yield for non-regulated dissipation (Y(NO)) determined on the leaflets of tomato plants non-inoculated (NI) or at different times after inoculation with *Septoria lycopersici*.

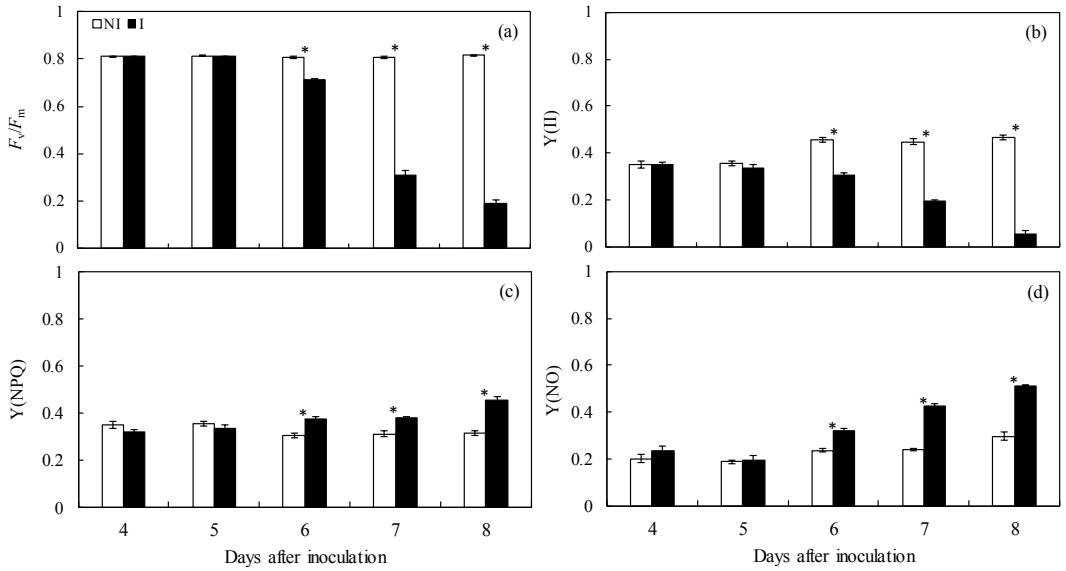

Figure 4. Chlorophyll *a* parameters maximum PSII quantum efficiency (F_v/F_m) (a), photochemical yield (Y(II)) (b), yield for dissipation by down-regulation (Y(NPQ)) (c), and yield for other non-photochemical (non-regulated) losses (Y(NO)) (d) determined on the leaflets of tomato plants non-inoculated (NI) or inoculated (I) with *Septoria lycopersici*. Means from NI and I plants, at each evaluation time, followed by an asterisk (*) are significantly different according to the *F* test ($P \leq 0.05$). Bars represent the standard deviation of the means.

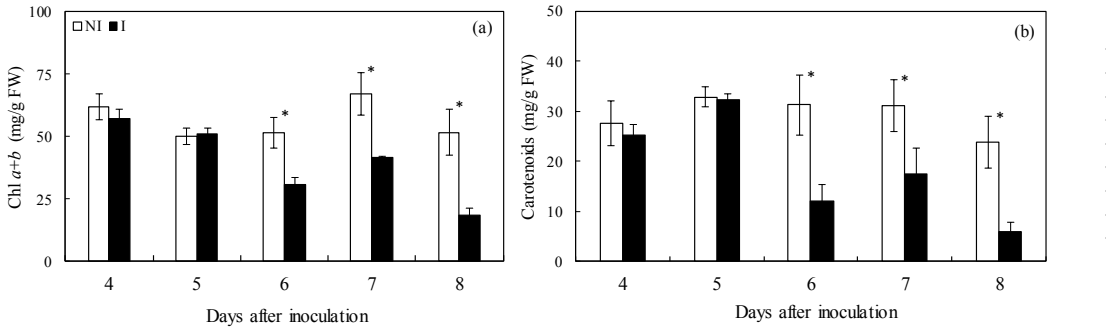

Figure 5. Concentrations of chlorophyll a+b (Chl a+b) (a) and carotenoids (b) determined on the leaflets of tomato plants non-inoculated (NI) or inoculated (I) with *Septoria lycopersici*. Means from NI and I plants, at each evaluation time, followed by an asterisk (*) are significantly different according to the F test ($P \leq 0.05$). Bars represent the standard deviation of the means. FW = fresh weight.

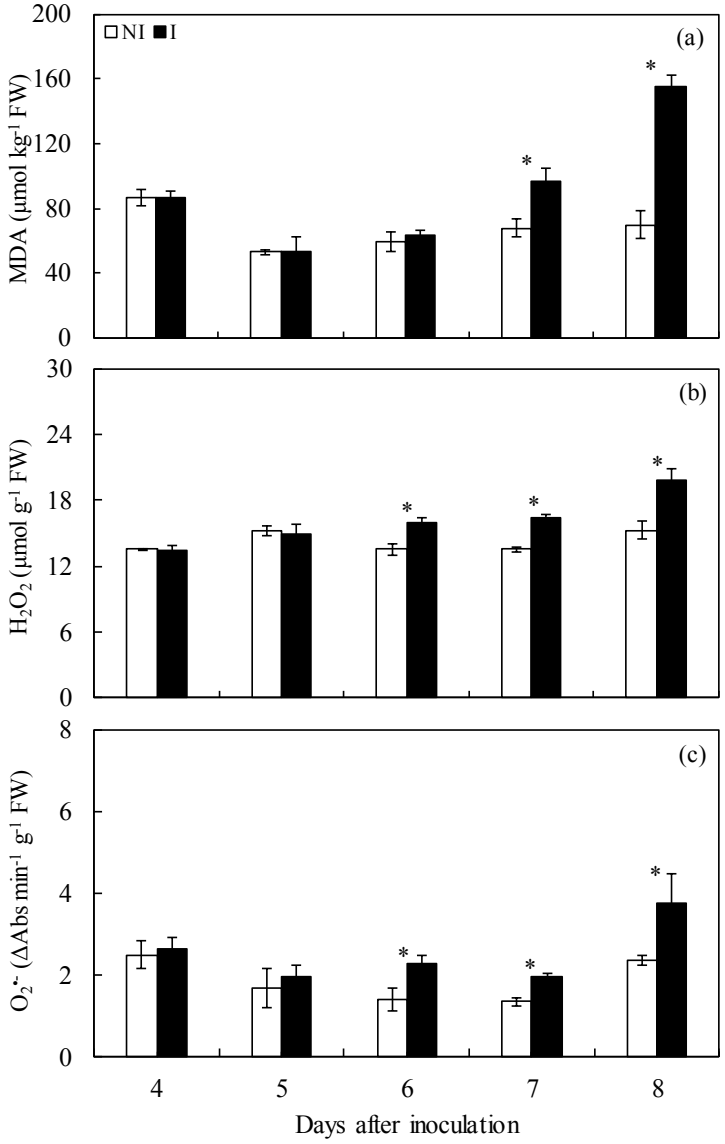

Figure 6. Concentrations of malondialdehyde (MDA) (a), hydrogen peroxide (H_2O_2) (b), and superoxide anion radical ($O_2^{\bullet-}$) (c) determined on the leaflets of tomato plants non-inoculated (NI) or inoculated (I) with *Septoria lycopersici*. Means from NI and I plants, at each evaluation time, followed by an asterisk (*) are significantly different according to the *F* test ($P \leq 0.05$). Bars represent the standard deviation of the means. FW = fresh weight.

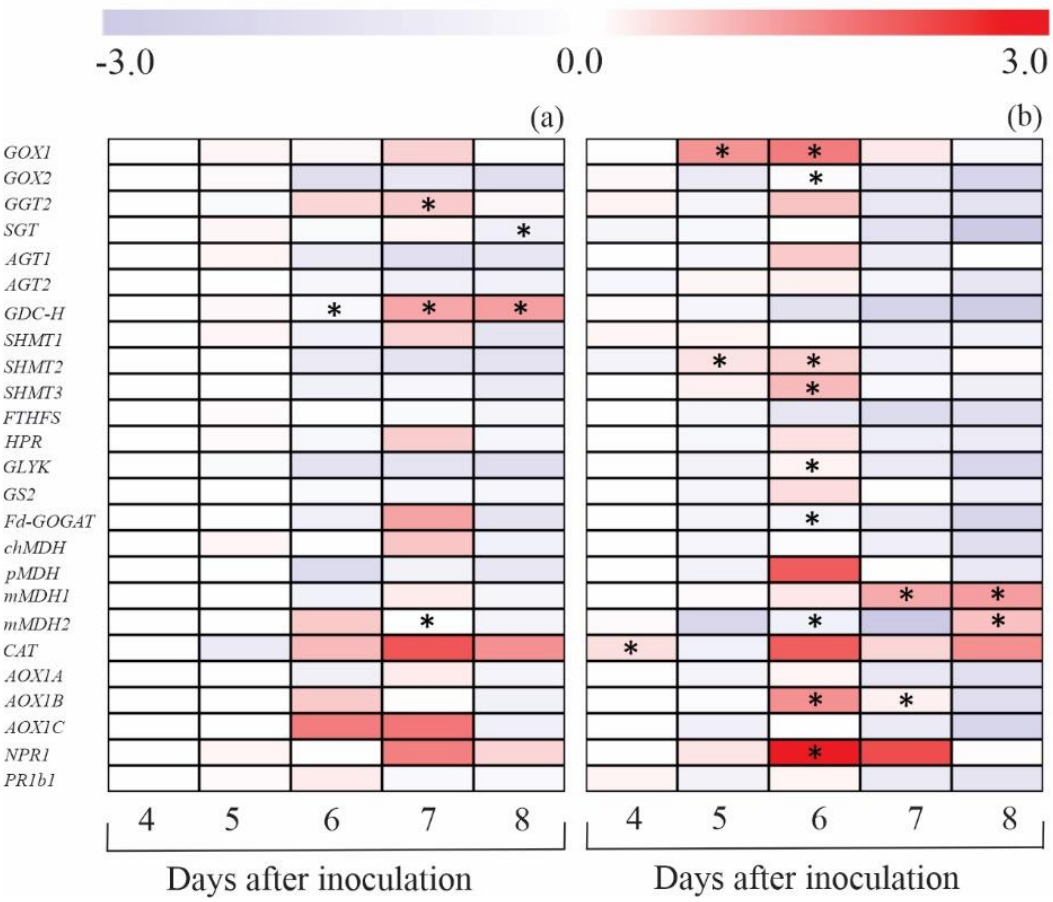

Figure 7. Expression profile of genes determined on the leaflets of tomato plants non-inoculated (NI) (a) or inoculated (I) (b) with *Septoria lycopersici*. Color cells represent the relative transcript levels ranging from blue (-3.0) to red (3.0). Amplification of actin gene (*ACT*) from tomato plants was used as an internal control for data normalization. Fold changes for each gene expression, except for *TEF-1α*, were calculated based on the transcript level obtained for leaflets samples obtained from NI plants of the control treatment at 4 days after inoculation (dai). For *TEF-1α*, transcript level obtained for leaflets samples from I plants of the control treatment at 4 dai was used in the calculation. For each leaflet sample, four biological replications were used with their respective three technical replicates. Means from NI and I plants followed by an asterisk (*), at each evaluation time, are significantly different according to the *F* test ($P \leq 0.05$).

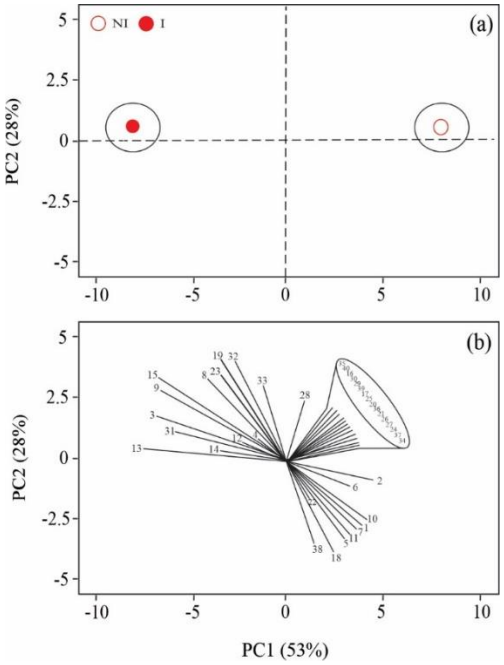

Figure 8. Score (a) and loading (b) plots of principal component analysis (PCA) comparing different physiological parameters and variables, biochemical variables, and expression of genes determined on the leaflets of tomato plants non-inoculated (NI) or inoculated (I) with *Septoria lycopersici*. Numbers in the loading plot (b) are as follow: parameters of leaf gas exchange (1, 2, 3, 4, 5, 6, and 7, respectively, to A, g_s, C_i, E, R_d, V_{cmax}, and J_{max}) and chlorophyll *a* fluorescence (8, 9, and 10, respectively, to Y(II), Y(NPQ), and Y(NO)), concentrations of photosynthetic pigments (11 and 12, respectively, to Chl *a*+*b* and Car) and metabolites involved in cellular damage (13, 14, and 15, respectively, to MDA, H_2O_2, and $O_2^{\bullet-}$), and genes expression (16, 17, 18, 19, 20, 21, 22, 23, 24, 25, 26, 27, 28, 29, 30, 31, 32, 33, 34, 35, 36, 37, 38, 39, and 40, respectively, to *GOX1*, *GOX2, GGT*, *SGT*, *AGT1, AGT2*, *GDC-H*, *SHMT1*, *SHMT2*, *SHMT3*, *FTHFS*, *HPR2*, *GLYK*, *GS*, *Fd-GOGAT*, *chMDH*, *pMDH*, *mMDH1*, *mMDH*, *CAT*, *AOX1a*, *AXO1b*, *AOX1c*, *NPR1*, and *PR1b1*). Groups were generated from cluster analysis with complete linkage and Pearson distance. Data from parameters and variables used in the PCA analysis were obtained for NI and I plants at 8 days after inoculation

Chapter II

Physiological and biochemical insights into induced resistance on tomato against septoria leaf spot by a phosphite combined with free amino acids

RESUMO

A mancha foliar de Septoria (SLS), causada por *Septoria lycopersici*, é uma doença destrutiva em tomateiro. nós investigamos o uso de fosfito de potássio combinados com de L-α-aminoácidos livres (estímulo chamado resistência induzida (RI)), para aumentar as respostas de defesa do tomateiro contra a infecção por *S. lycopersici*. Plantas que receberam o estímulo RI apresentaram redução na severidade de SLS e menor colonização do tecido foliar por *S. lycopersici* (menor expressão de *TEF-1*α). As plantas pulverizadas com estímulo IR mostraram menores concentrações de malonaldeído, peróxido de hidrogênio e radical ânion superóxido, enquanto as concentrações de sacarose, frutose e amido e grandes atividades de ascorbato peroxidase, catalase, glutationa redutase e superóxido dismutase aumentaram quando comparada com plantas pulverizadas com água em resposta à infecção por *S. lycopersici*. O Aparato fotossintético foi menos comprometido o que resultou em maiores concentrações dee clorofila *a*+*b* e carotenoides em plantas pulverizadas com estímulo RI. Nós observamos que os genes envolvidos em reações de defesa do hospedeiro (*CHI3*, *CHI9*, *GLU*, *PAL3*, *POX3*, *PPOB* e *PPOF*) e aqueles relacionados à resistência sistêmica adquirida (*PAL3* e *ICS*) ou resistência sistêmica induzida ((produção de etileno - *ACO2*, *ACO3*, *ACO5* e *ACO4*) e a via de sinalização do ácido jasmônico (*LOX1.1*, *LOXB*, *LOXC* e *PDF1.2*)) e observamos uma regulação positivamente para plantas infectadas e pulverizadas com estímulo RI. Esses achados destacam o potencial do uso desse estímulo de RI para o manejo de SLS.

Palavras-chave: Metabolismo antioxidante. Respostas de defesa do hospedeiro. Resistência sistêmica induzida. Fotossíntese. Espécies reativas de oxigênio.

ABSTRACT

Septoria leaf spot (SLS), caused by *Septoria lycopersici*, is a destructive disease in tomato. This study we investigated the use of potassium phosphite combined with free L-α-amino acids (called stimulus induced resistance (IR)) to increase tomato defense responses against *S. lycopersici* infection. Plants that received the RI stimulus showed a reduction in the severity of SLS and less colonization of leaf tissue by S. lycopersici (lower expression of *TEF-1*α). Plants sprayed with IR stimulus showed lower concentrations of malonaldehyde, hydrogen peroxide and superoxide anion radical, while sucrose, fructose and starch concentrations and high ascorbate peroxidase, catalase, glutathione reductase and superoxide dismutase activities increased when compared to plants sprayed with IR stimulus. water in response to *S. lycopersici* infection. The photosynthetic apparatus was less compromised, which resulted in higher concentrations of chlorophyll *a*+*b* and carotenoids in plants sprayed with RI stimulus. We observed that genes involved in host defense reactions (*CHI3*, *CHI9*, *GLU*, *PAL3*, *POX3*, *PPOB* and *PPOF*) and those related to acquired systemic resistance (*PAL3* and *ICS*) or induced systemic resistance ((ethylene production - *ACO2*, *ACO3*, *ACO5* and *ACO4*) and the jasmonic acid signaling pathway (*LOX1.1*, *LOXB*, *LOXC* and *PDF1.2*)) and we observed an up-regulation for plants infected and sprayed with RI stimulus. These findings highlight the potential of using this IR stimulus for the management of SLS.

Keywords: Antioxidative metabolism. Host defense responses. Induced systemic resistance. Photosynthesis. reactive oxygen species.

1. Introduction

Septoria leaf spot (SLS), caused by *Septoria lycopersici* Speg., is one of the major foliar fungal diseases affecting tomato production worldwide (Nayyer et al., 2022, Stevenson, 2014). The SLS symptoms start on basal leaves of tomato plants as circular to elliptical necrotic lesions with tan to gray centers containing several black pycnidia and surrounded by dark brown margins (Blancard, 2012; Stevenson, 2014). Yield losses caused by SLS are associated with reduced photosynthetically active leaf area linked to intense defoliation, reduced plant growth, and fruits of lower quality (*e.g.*, smaller and often burned by sunlight) (Blancard, 2012). Management of SLS has relied on using cultural practices such as adequate plant density; crop rotation, destruction of crop debris, drip irrigation, and weed control (Blancard, 2012; Nayyer et al., 2022; Stevenson, 2014). The spray of fungicides (twice or more times weekly after flowering) stands out as the most effective method for SLS control in tomato fields located in regions with environmental conditions (*e.g.*, temperatures ranging from 20 to 25^{o}C and high relative humidity) favorable for the occurrence of epidemics (Nayyer et al., 2022). Frequent fungicide sprays implicate the selection of resistant *S. lycopersici* population (Aktar et al., 2009). Therefore, searching for more environmentally friendly control strategies for SLS management needs to be prioritized for food security and an alternative to reduce the dependence of growers on using fungicides and their negative impacts on both environment and human health.

Crop plants are capable of coping with the infection by pathogens of different lifestyles through inducible defense responses (Zeier 2021). Interestingly, a localized infection by a pathogen linked to either pathogen-associated molecular pattern triggered immunity or pathogen-effector triggered immunity enables plants to trigger defense responses in distant healthy leaves through a phenomenon known as systemic acquired resistance (SAR) (Kesel et al., 2021; Vlot et al., 2021, Zeier 2021). Under SAR, plants heightened their innate immune system (rapid, more substantial, and long-lasting action of multiple defense mechanisms) that successfully counteracts further pathogen infection (Kesel et al., 2021). Salicylic acid (SA) is known as a plant hormone associated with SAR, but other compounds have been also recognized as signals for SAR (Kesel et al., 2021). Furthermore, plants after being exposed to nonpathogenic microorganisms or some induced resistance stimuli can develop induced systemic resistance (ISR) signaled by jasmonic acid (JA) and ethylene (ET) (Pieterse et al., 2012). Notably, some amino acids (*e.g.*, glutamate, phenylalanine, proline, lysine, *β*-aminobutyric acid (BABA), and γ-aminobutyric acid (GABA)) participate either directly or

indirectly in boosting the defense of plants against pathogen infection (Cohen et al., 2016, Jakab et al., 2001; Monchiero et al., 2015; Odintsova et al., 2012; Tarkowski et al., 2020; Ting et al., 2020). On top of that, phosphite-based compounds are also recognized as efficient inducers of resistance mainly for controlling diseases caused by fungi and oomycetes (Fagundes-Nacarath et al., 2019; Mohammadi et al., 2021; Novaes et al., 2019; Vinas et al., 2020).

Considering SLS as a destructive disease and the fact that tomato defense responses to cope with *S. lycopersisi* infection remain poorly understood, especially in the scenario of induced resistance, this study hypothesized that the level of basal resistance of plants from a susceptible cultivar to SLS could be increased by spraying them with Optimus®, a phosphite combined with free amino acids available to growers in the market. In this scenario, tomato defense responses could be boosted rapidly and efficiently against *S. lycopersisi* infection with fine biochemical and physiological adjustments.

2. Materials and methods

2.1 *In vitro* assays

The sensitivity of *S. lycopersici* to Optimus® (phosphorus (P_2O_5) soluble in water (30% w/w, 426 g/L) and potassium soluble in water (K_2O) (20% w/w, 284 g/L) combined with L-α-free amino acids (4% w/w, 56.8 g/L), pH 5.0; Bioiberica, Palafolls, Spain) at the concentrations of 1.5, 3, 6, 9, and 12 mL/L was evaluated *in vitro*. Melted V8 medium was amended with each solution of Optimus® (referred to as induced resistance (IR) stimulus thereafter) and poured into Petri dishes (15 mL per dish). Melted V8 medium not amended with IR stimulus served as the control treatment. One plug of V8 medium (5 mm in diameter) containing fungal mycelia obtained from the edge of a 15-day-old colony of *S. lycopersici* was placed in the center of each Petri dish. Dishes were kept in a growth chamber (25°C and photoperiod of 12 h of light and 12 h of dark). After 7 days, fungal colony in each Petri dish was measured in two orthogonal directions using a digital caliper to obtain its diameter. The surface area of the plug was subtracted from the total surface area measured on each Petri dish. Conidia obtained from 15-day-old *S. lycopersici* colonies in Petri dishes containing V8 medium were removed using a camel hair brush to obtain a conidial suspension of 5×10^4 conidia/mL. The effect of IR stimulus on conidia germination was tested by mixing different volumes of IR stimulus solution with 100 μL of conidial suspension to obtain the final concentrations of 1.5, 3, 6, 9, and 12 mL/L. Conidial suspension prepared only with water served as the control treatment. The

conidial suspension was homogeneously distributed over the agar medium surface in each dish using a Drigalski glass handle. Dishes were transferred to a growth chamber (25°C and photoperiod of 12 h of light and 12 h of dark) and after 24 h, 5 µL of lactophenol was added to each dish to stop conidia germination. One hundred conidia were randomly examined at each Petri dish under a light microscope (Carl Zeiss AxioImager A1) at 40 × magnification. A conidium was considered germinated when its germ tube was larger than its half-length. The percentage of conidia germination was calculated for each treatment.

2.2. Plant growth

Seeds from tomato cultivar Santa Cruz Kada (Isla Sementes, São Paulo, Brazil) were sown in polystyrene trays containing Tropstrato® (mixture of pine bark, peat, and expanded vermiculite; Vida Verde, São Paulo, Brazil) substrate. Seedlings (15 days after emergence) were transplanted to plastic pots containing 2 kg of the same substrate amended with 3.26 g of calcium phosphate. Each plant per pot received nutrient solution (50 mL per pot) according to Chaves et al. (2021) after being transplanted and then weekly. Plants were grown in the greenhouse (temperature of 25 ± 5°C, relative humidity of 70 ± 5%, and natural photosynthetically active radiation (PAR) of 900 ± 15 µmol photons m^{-2} s^{-1} measured at midday) and watered as needed.

2.3. Application of IR stimulus

A solution of IR stimulus at the concentration of 6 mL/L (20 mL of solution per each plant) was sprayed as a fine mist to the leaves of each plant (growth stage of five leaves, 45 days after transplanting) per pot by using a VL Airbrush atomizer (Paasche Airbrush Co., Chicago, IL, USA) at 48 h before inoculation with *S. lycopersici*. Plants sprayed with water served as the control treatment.

2.4. Inoculum production and plant inoculation

The isolate UFV-DFP *Sl*-12 of *S. lycopersici* from our fungal collection was used to inoculate the plants. The fungus was grown in Petri dishes containing V8 medium and incubated for 15 days in a growth chamber (25°C and photoperiod of 12 h of light and 12 h of dark). Conidia produced in each dish were collected in sterile water containing 0.01% Tween 20 and 0.5% gelatin (w/v). Three leaves, from top to basis, of each plant were inoculated with a conidial suspension (5×10^4 conidia/mL, 15 mL per plant) of *S. lycopersici* using a VL Airbrush

atomizer. After inoculation, plants were kept inside a mist growth chamber (25°C and relative humidity of 90 ± 5%) for 24 h. Non-inoculated plants were kept in a separate growth chamber with the same temperature and relative humidity. After this period, non-inoculated and inoculated plants were transferred to the greenhouse (28 ± 2°C, relative humidity of 80 ± 5%, and natural (PAR) of 900 ± 12 µmol photons m^{-2} s^{-1} measured at midday) until the end of the experiments.

2.5. Evaluation of septoria leaf spot (SLS) severity

The fourth leaf, from top to basis, of each plant per treatment (four replications per treatment, four plants, and 4 leaves) were collected at 8 days after inoculation (dai), scanned at 600 dpi resolution, and the obtained images were processed with the QUANT software according to obtain the values of SLS severity (Fagundes-Nacarath et al., 2019).

2.6. Photosynthetic measurements

Analyses of gas exchange and chlorophyll (Chl) *a* fluorescence were performed simultaneously using an open-flow infrared gas exchange analyzer system equipped with an integrated fluorescence chamber (IRGA, Li-color Inc. LI-6400XT; NE). The third leaf, from top to basis, of each plant per replication of each treatment (four replications (four plants and four leaves) per sampling time) was used for gas exchange analysis at 5, 6, 7, and 8 dai. Leaves from non-inoculated plants were used at this same evaluation time. Measurements of net carbon assimilation rate (A), stomatal conductance to water vapor (g_s), internal CO_2 concentration (C_i), and transpiration rate (E) were made during the day (from 08:00 to 12:00 h) with the following conditions: leaf chamber at 25ºC, constant CO_2 concentration (410 ppm), photosynthetically active radiation (PAR) of 1000 µmol photons m^{-2} s^{-1}, and amount of blue light set with 10% of PAR to optimize stomatal aperture (Marçal et al., 2021). The intrinsic water use efficiency (A/g_s) and water-use efficiency (WUE) parameters were also determined. The Chl *a* fluorescence was performed using the fluorometer coupled the to IRGA on the same third leaf used for gas exchange measurements following the procedures of Aucique-Pérez et al. (2014). The α value was estimated using the leaf transmittance according to the procedure described in Technical Note 128 of LI-COR (https://www.licor.com/documents/9bgi9ayo5yx7dwjnts8c.pdf) and used to calculate the ratio of electron transport rate-to-net carbon assimilation rate (ETR/A).

2.7. Imaging and quantification of Chl a fluorescence parameters

The Imaging-PAM fluorometer (MAXI version), associated with the Imaging Win software (Heinz Walz GmbH, Effeltrich, Germany), was used to obtain the images of Chl *a* fluorescence parameters following the procedures described by Fagundes-Nacarath et al. (2019) using the third leaf, from top to basis, of each plant per replication of each treatment (four replications (four plants and four leaves) per sampling time) were collected at 5, 6, 7, and 8 dai. The third leaf from non-inoculated plants were used at this same evaluation time. The parameters of Chl *a* fluorescence were determined by selecting the circular option on the Imaging Win software (area of 1 cm^2) for both non-inoculated and inoculated leaves.

2.8. Determining photosynthetic pigments concentration

The concentrations of Chl *a*, Chl *b*, and carotenoids were determined in the same leaves used to evaluate the Chl *a* fluorescence parameters. Briefly, leaf tissue (50 mg) was ground in liquid nitrogen using a vibration ball mill (Retsch, Haan, Germany) and the fine powder was homogenized in 1 mL methanol. The supernatant was used to quantify the concentrations of Chl *a*, Chl *b*, and carotenoids according to Fagundes-Nacarath et al. (2019).

2.9. Histochemical detection of lipid peroxidation, membrane damage, hydrogen peroxide (H_2O_2), and superoxide anion radical ($O_2^{\bullet-}$)

The fourth leaf, from basis to top, of each plant per replication of each treatment (four replications totalizing 16 plants and 16 leaves) were collected from both non-inoculated and inoculated plants at 8 dai. Lipid peroxidation and membrane damage in leaflets were visualized using Schiff and Evans' blue reagents following the procedures of Awasthi et al. (2018) and Tistama et al. (2012), respectively. Leaflets were randomly transferred to glass vials containing 50 mL of either Schiff (10% v/v prepared in deionized water) or Evans's blue (0.025% w/v prepared in 100 μM of CaCl2, pH 5.6) reagents (five leaflets per glass vial for each reagent) during 2 and 12 h, respectively. For H_2O_2 detection, leaflets were randomly placed in glass vials (five leaflets per glass vial) containing a 25 mL of 3,3'-diaminobenzidine tetrahydrochloride solution (1 mg/mL) (Sigma-Aldrich, São Paulo, Brazil) and kept in the dark at 25°C for 12 h. For O2•- detection, leaflets were randomly placed in glass vials (five leaflets per glass vial) containing 50 mL of nitro blue tetrazolium (0.1%) solution (Sigma-Aldrich, São Paulo, Brazil) prepared in potassium phosphate buffer (10 mM, pH 6.8) during 24 h. For all four histochemical tests, leaflets were cleared in boiling aqueous ethanol (80%) for 60 min until pink, blue, brown,

and blue spots were noticed that confirmed the occurrence of lipid peroxidation, membrane damage, H_2O_2, and $O_2^{\bullet-}$, respectively.

2.10. Biochemical and molecular assays

The fourth leaf, from top to basis, of each plant per replication of each treatment (four replications per evaluation time totalizing 16 plants and 16 leaves) was collected at 5, 6, 7, and 8 dai. Leaves from non-inoculated plants were sampled at this same evaluation time. Leaf samples were kept in liquid nitrogen during sampling and stored at -80°C until further analysis.

2.11. Determining sugars and starch concentrations

Leaf tissue (50 mg) was ground as described above and the fine powder was mixed with 1 mL of methanol at 70°C for 15 min to extract sugars and starch according to Medeiros et al. (2017). Sugars (glucose, fructose, and sucrose) were determined in the soluble phase of the methanolic solution and the pellet was used to quantify the starch following the procedures of Fagundes-Nacarath et al. (2019).

2.12. Determining malondialdehyde (MDA) concentration

Leaf tissue (50 mg) was ground as described above and homogenized in 2 ml of a solution of trichloroacetic acid (TCA) 0.1% (wt/vol). Homogenate was centrifuged at 12,000 × *g* for 15 min at 4°C and the MDA concentration was determined according to Chaves et al. (2021).

2.13. Determining H_2O_2 and $O_2^{\bullet-}$ concentrations

Leaf tissue (100 mg) was ground as described above and homogenized in 1 mL of solution of potassium phosphate buffer (50 mM, pH 6.5) containing hydroxylamine (1 mM). The homogenate was centrifuged at 10,000 × *g* for 15 min at 4°C. A total of 100 µL of the supernatant was used to determine H_2O_2 concentration following the procedures of Dias et al. (2020). Leaf tissue (50 mg) was ground as described above and the fine powder was homogenized in 1 mL of a solution containing sodium phosphate buffer (100 mM, pH 7.2) and sodium diethyldithiocarbamate (1 mM). The homogenate was centrifuged at 22,000 × *g* for 20 min at 4°C and 100 µL of the supernatant was used to determine $O_2^{\bullet-}$ concentration according to Chaves et al. (2021).

2.14. Determining antioxidant enzyme activities

Leaf tissue (100 mg) was ground as described above and the fine powder was homogenized with 1 mL solution containing 100 mM potassium phosphate buffer (pH 7.8), 0.1 mM EDTA, 1 mM phenylmethylsulfonyl fluoride (PMSF), and 0.5% (w/v) polyvinylpyrrolidone (PVP). The homogenate was centrifuged at 13,000 × *g* for 15 min at 4°C. The supernatant was used to determine ascorbate peroxidase (APX) (EC 1.11.1.11), catalase (CAT) (EC 1.11.1.6), glutathione reductase (GR) (EC 1.8.1.7), and superoxide dismutase (SOD) (EC 1.15.1.1) activities according to Debona et al. (2012).

2.15. Determining total soluble phenolics (TSP) and lignin-thioglycolic acid (LTGA) derivatives concentrations

Leaf tissue (100 mg) was ground as described above and the fine powder was homogenized in 1.5 mL of 80% (v/v) methanol solution. The crude extract was shaken at 300 rpm at 25°C for 12 h and the mixture was centrifuged at 13,000 × *g* for 30 min. The supernatant was used to determine TSP concentration and the pellet was washed with deionized water to determine LTGA derivatives concentration following the procedures of Rodrigues et al. (2005).

2.16. Genes expression using reverse transcription quantitative real-time PCR (RT-PCR)

Leaf tissue (75 mg) was ground as described above and the fine powder was used to extract RNA using TRIzol (Invitrogen). Contamination by DNA was removed with RQ1 RNase-free DNase (Promega). The amount of RNA was measured in a Qubit fluorometer using Qubit RNA HS Assay Kit (Invitrogen) and RNA quality and integrity were verified by 1% agarose gel electrophoresis. Single-stranded cDNAs were synthesized by reverse transcription using 3 μg of total RNA with oligo(dT) primers in a final volume of 20 μL using the SuperScript First Strand Synthesis System for RT-PCR (Invitrogen). Expression analysis of genes coding for 1-aminocyclopropane-1-carboxylate oxidase (*ACO1*, *ACO2*, *ACO3*, *ACO4*, *ACO5*, and *ACO6*), chitinase (*CHI3* and *CHI9*), glucanase (*GLU*), isochorismate synthase (*ICS*), lipoxygenase (*LOX1.1*, *LOXB*, and *LOXC*), phenylalanine ammonia-lyase (*PAL3*), plant defensin 1.2 (*PDF1*.2), peroxidase 3 (*POX3*), polyphenoloxidase (*PPOB* and *PPOF*), and pathogenesis-related protein 1 (*PR1b1*) were determined by RT-qPCR using a CFX real-time thermal cycler (Bio-Rad) and SYBR Green PCR Master Mix according to the manufacturer's recommendations. Primer sequences for amplification of the genes studied are listed in Table 1. All reactions were performed in triplicate and the relative expression values for each gene

studied were calculated using the $2^{-\Delta\Delta Ct}$ method described by Livak et al. (2001). Expression of translation elongation factor Alfa-tef1 gene (*TEF-1α*) from *S. lycopersici* was also quantified to confirm the fungal presence in leaf tissues from inoculated plants. The actin gene (*ACT*) was used as a reference for normalization according to Ahammed et al. (2018).

2.17. Data analysis

Two 2 × 2 factorial experiments (Experiments 1 and 2), consisting of water (control) or IR-stimulus sprayed plants and non-inoculated (NI) or inoculated (I) plants with *S. lycopersici*, were arranged in a completely randomized design with four replications per each evaluation or sampling time. These plants were used to evaluate SLS severity, leaf gas exchange and Chl *a* fluorescence parameters, photosynthetic pigments, and to perform the histochemical analyses. Two other 2 × 2 factorial experiments (Experiments 3 and 4, with the same factors described above) were arranged in a completely randomized design with four replications per sampling time to obtain leaf samples for biochemical and gene expression analysis. Each experimental unit consisted of one plastic pot containing one plant. Data from variables and parameters evaluated in Experiments 1 and 2 and data from variables evaluated in Experiments 3 and 4 were analyzed to determine if data from variables and parameters of these experiments could be combined (Moore and Dixon 2015). Data from variables and parameters were checked for normality and homogeneity of variance and subjected to analysis of variance (ANOVA). Principal components analysis (PCA) was performed using data from all variables and parameters evaluated from inoculated and non-inoculated plants of the four treatments at 8 dai aiming to interpret the dataset generated in this study to reduce their dimension, interpretability, and minimize information loss to better understand the parameters and variables evaluated. Treatment means were compared by F test ($P \leq 0.05$). Data were analyzed by using the Minitab software (version 18, Minitab Corporation).

3. Results

3.1. Analysis of variance

According to ANOVA, the factor IR stimulus was significant for severity, A, C_i, A/g_s, WUE, F_v/F_m, Y(II), ETR/A, Y(NO), Chl a+b, MDA, H_2O_2, $O_2^{\bullet-}$, TSP, LTGA derivatives, glucose, fructose, sucrose, starch, *ACO2*, *CHI9*, *ICS*, *PDF1.2*, *PR1b1*, and *TEF-1α*. The factor

plant inoculation (PI) and the IR stimulus × PI interaction were significant for most of the variables and parameters evaluated (Table 2).

3.2. *In vitro* assay

There was no visual difference on mycelial growth of *S. lycopersici* in the Petri dishes containing V8 medium amended with different concentrations of the IR stimulus (Supplementary Figure 1a-h) nor the effect of these concentrations on conidia germination (Fig. 1).

3.3. Symptoms of SLS and severity

Many coalesced necrotic lesions were noticed in the leaves of plants from control treatment (Fig. 2a), while the lesions that formed in the leaves of IR stimulus-sprayed plants were of reduced size and in less number (Fig. 2b). Severity of SLS was significantly reduced by 78% for IR stimulus-sprayed plants compared to plants from control treatment (Fig. 2c).

3.4. Leaf gas exchange parameters

For NI plants, A, g_s, C_i, E, A/g_s, and WUE were not affected by control and IR stimulus treatments regardless of evaluation time (Figs. 3a, c, e, and g and 3a, b, and c). For I plants from control treatment, A (41, 50, and 66% at 6, 7, and 8 dai, respectively), g_s (31% at 8 dai), A/g_s (67% at 8 dai), and WUE (53 and 90% at 7 and 8 dai, respectively) were significantly lower while C_i (8, 10, and 24% at 6, 7, and 8 dai, respectively) and E (40% at 8 hai) were significantly higher compared to inoculated IR stimulus-sprayed plants (Figs. 3b, d, f, and h and 4b, d, and f). For control treatment, A (44, 57, and 87% at 6, 7, and 8 dai, respectively), g_s (49% at 8 dai), A/g_s (72% at 8 dai), and WUE (47 and 86% at 7 and 8 dai, respectively) were significantly lower while C_i was significantly higher (7, 15, and 21% at 6, 7, and 8 dai, respectively) for I compared to NI plants (Fig. 3a-b, c-d, and e-f). The A, C_i, and were significantly lower by 8, 36, and 87%, respectively, at 8 dai for I plants from the IR stimulus treatment compared to their NI counterparts (Figs. 3a-b and c-d).

3.5. Imaging and quantification of Chl a fluorescence parameters

Remarkable damage to the photosynthetic apparatus occurred for I plants from control treatment compared to I plants sprayed with IR stimulus from 6 to 8 hai based on the darker areas in the images for F_v/F_m, Y(II), Y(NPQ), and Y(NO) parameters (Fig. 5). For NI plants,

F_v/F_m, Y(II), Y(NPQ), Y(NO), and ETR/*A* were not affected by control and IR stimulus treatments regardless of evaluation time (Fig. 6a, c, e, g, and i). For I and IR stimulus-sprayed plants, F_v/F_m (10, 14, and 28% at 6, 7, and 8 dai, respectively) and Y(II) (22, 39, and 70% at 6, 7, and 8 dai, respectively) were significantly higher while Y(NPQ) (25 and 19% at 7 and 8 dai, respectively), Y(NO) (18, 23, and, 35% at 6, 7 and 8 dai, respectively), and ETR/*A* (48, 40, and 57% at 6, 7, and 8 dai, respectively) were significantly lower compared to I plants from control treatment (Fig. 6b, d, f, h, and j). For control treatment, F_v/F_m (10, 19, and 33% at 6, 7, and 8 dai, respectively) and Y(II) (22, 41, and 85% at 6, 7, and 8 dai, respectively) were significantly lower while Y(NPQ) (18 and 31% at 7 and 8 dai, respectively), Y(NO) (23, 28, and 41% at 6, 7, and 8 dai, respectively), and ETR/*A* (41, 48, and 68% at 6, 7, and 8 dai, respectively) were significantly higher for I plants compared to NI plants (Fig. 6a-j). For IR stimulus treatment, F_v/F_m, Y(II), and Y(NPQ) were significantly lower by 10, 24, and 33%, respectively, for I plants compared to NI plants (Fig. 6a-f).

3.6. Photosynthetic pigments

Concentrations of Chl *a*+*b* and carotenoids for NI plants were not affected by control and IR stimulus treatments regardless of evaluation time (Fig. 7a and c). Concentrations of Chl *a*+*b* (23, 52, and 57% at 6, 7, and 8 dai, respectively) and carotenoids (43 and 51% at 7 and 8 dai, respectively) were significantly higher for I plants sprayed with IR stimulus compared to I plants from control treatment (Fig. 7b and d). For control treatment, concentrations of Chl *a*+*b* (23, 39, and 58% at 6, 7, and 8 dai, respectively) and carotenoids (49 and 55% at 7 and 8 dai, respectively) were significantly lower for I plants compared to NI plants (Fig. 7a-d).

3.7. Carbohydrates

For I and IR stimulus-sprayed plants, glucose (60 and 194% at 5 and 8 dai, respectively), fructose (192, 196, and 502% at 6, 7, and 8 dai, respectively), sucrose (95 and 218% at 7 and 8 dai, respectively), and starch (55, 251, 329, and 109% at 5, 6, 7, and 8 dai, respectively) concentrations were significantly higher compared to I plants from control treatment (Fig. 8b, d, f and h). For control treatment, concentrations of glucose (56 and 57% at 7 and 8 dai, respectively), fructose (44 and 50% at 7 and 8 dai, respectively), sucrose (60 and 64% at 7 and 8 dai, respectively), and starch (93, 462, and 448% at 6, 7, and 8 dai, respectively) were significantly lower for I plants compared to NI plants (Fig. 8a-h).

3.8. Histochemical localization of lipid peroxidation, membrane damage, H_2O_2, and $O_2^{\bullet-}$

The spray of IR stimulus did not cause any physiological perturbation to leaves of NI plants based on absence of staining for lipid peroxidation, membrane damage, H_2O_2, and $O_2^{\bullet-}$ compared to leaves from plants of control treatment (Fig. 9a-d). Lipid peroxidation, membrane damage, and depositions of H_2O_2 and $O_2^{\bullet-}$ (brown and blue colors, respectively) were less intense in leaves of plants sprayed with IR stimulus than leaves of plants from control treatment at 8 dai (Fig. 9a-d).

3.9. Concentrations of MDA, H_2O_2, and $O_2^{\bullet-}$

For NI plants, MDA, H_2O_2, and $O_2^{\bullet-}$ concentrations were not affected by control and IR stimulus treatments regardless of evaluation time (Fig. 10a, c, and e). For I plants, MDA (45 and 55% at 7 and 8 dai, respectively), H_2O_2 (48 and 51% at 7 and 8 dai, respectively), and $O_2^{\bullet-}$ (52 and 49% at 7 and 8 dai, respectively) were significantly lower for IR stimulus treatment compared to control treatment (Fig. 10b, d, and f). For control treatment, MDA (45 and 62% at 7 and 8 dai, respectively), H_2O_2 (55 and 61% at 7 and 8 dai, respectively), and $O_2^{\bullet-}$ (54 and 48% at 7 and 8 dai, respectively) were significantly higher for I plants compared to NI plants (Fig. 10a-f).

3.10. Antioxidant enzymes

For NI plants, SOD, APX, CAT, and GR activities were unaffected by control and IR stimulus treatments regardless of evaluation time (Fig. 11a, c, e, and g). For I plants, SOD (59 and 42% at 7 and 8 dai, respectively), APX (60% at 8 dai), CAT (33 and 36% at 7 and 8 dai, respectively), and GR (60 and 55% at 7 and 8 dai, respectively) activities were significantly higher for IR stimulus treatment compared to control treatment (Fig. 11b, d, and f). At 6 dai, CAT activity was significantly lower for I plants from IR stimulus treatment compared to I plants from control treatment (Fig. 11f). The CAT activity (48% at 6 dai) for control treatment and SOD, APX, and CAT activities (42, 58, and 53% at 8 dai, respectively) for IR stimulus treatment were significantly higher for I plants compared to NI plants (Fig. 11a-f).

3.11. Concentrations of TSP and LTGA derivatives

For NI plants, TSP concentration was not affected by control and IR stimulus treatments regardless of evaluation time (Fig. 12a). By contrast, LTGA derivatives concentration significantly increased by 48, 50, 53, and 40% at 5, 6, 7, and 8 dai, respectively, for NI plants

of IR stimulus treatment compared to NI plants from control treatment (Fig. 12c). For I plants, TSP concentration was significantly lower by 23 and 24% at 7 and 8 dai, respectively, while LTGA derivatives concentration was significantly higher (42, 43, 48, and 61% at 5, 6, 7, and 8 dai, respectively) for IR stimulus treatment compared to control treatment (Fig. 12b and d). At 8 dai, TSP concentration for control treatment and LTGA derivatives concentration for IR stimulus treatment significantly increased by 27 and 45%, respectively, for I plants compared to NI plants (Fig. 12a-d).

3.12. Genes expression

3.12.1. Comparing NI vs. I plants for control and IR stimulus treatments

Control treatment

Expressions of *ACO3* and *LOX1.1* at 7 dai and *ACO2*, *ACO3*, *CHI3*, and *ICS* at 8 dai were significantly up-regulated for NI plants compared to I plants for control treatment. Expressions of *ACO4*, *ACO6*, *CHI3*, *CHI9*, *ICS*, *LOX1.1*, *LOXB*, and *LOXC* at 5 dai, *CHI3* and *PAL* at 6 dai, *ACO6* and *PAL* at 7 dai as well as *ACO6*, *LOXB*, *LOX*, and *PR1b1* at 8 dai were significantly up-regulated for I plants compared to NI plants for control treatment (Fig. 13a and c).

3.12.2. IR stimulus treatment

Expressions of *LOX1.1* at 6 dai, *ACO6* at 7 dai, and *PPOF* and *PR1b1* at 8 dai were significantly up-regulated for NI plants compared to I plants for IR stimulus treatment. Expressions of *ACO1*, *ACO3*, *ACO4*, *ACO5*, *ACO6*, *CHI9*, *GLU*, and *PAL* at 5 dai, *ACO2*, *PDF1.2*, *POX3*, and *PPOB* at 6 dai, and *ACO4*, *CHI3*, *CHI9*, *GLU*, *PAL*, *POX3*, and *PPOF* at 8 dai were significantly up-regulated for I plants compared to NI plants for IR stimulus treatment (Fig. 13b and d).

3.12.3. Comparing control vs. IR stimulus treatments for NI and I plants

Non-inoculated plants

Expressions of *CHI3* and *PAL* at 8 dai were significantly up-regulated for control treatment compared to IR stimulus treatment. Expressions of *ACO2*, *ACO3*, *CHI9*, *LOXC*, *POX3*, and *PPOB* at 5 dai, *ACO2*, *ACO6*, *CHI9*, *LOXB*, *PDF1.2*, *POX3*, *PPOB*, *PPOF*, and *PR1b1* at 6 dai, *ACO6*, *LOXB*, and *PPOB* at 7 dai as well as *ACO1*, *ACO2*, *ACO4*, *ACO6*, *CHI9*,

GLU, *LOXB*, *PAL*, *PDF1.2*, *POX3*, *PPOF*, and *PR1b1* at 8 dai were significantly up-regulated for IR stimulus treatment compared to control treatment (Fig. 13a-b).

3.12.4. Inoculated plants

Expressions of *ACO4* at 4 dai, *PR1b1* at 6 and 8 dai, *CHI3* and *LOXC* at 8 dai as well as *TEF-1α* from 6 to 8 dai were significantly up-regulated for control treatment compared to IR stimulus treatment. Expressions of *ACO2*, *ACO3*, *ACO5*, *CHI9*, *ICS*, and *LOX1.1* at 5 dai, *CHI9*, *LOX1.1*, *LOXB*, *LOXC*, *PDF1.2*, *POX3*, and *PPOB* at 6 dai, *ACO4* and *PAL* at 7 dai as well as *ACO2*, *ACO4*, *CHI3*, *CHI9*, *LOX1.1*, *LOXB*, *PAL*, *PDF1*.2, and *PPOF* at 8 dai were significantly up-regulated for IR stimulus treatment compared to control treatment (Fig. 13 c-d).

3.12.5. PCA analysis

According to cluster analysis with complete linkage and Pearson distance, three clusters (C) were generated: C1 (I plants from control treatment), C2 (NI plants from IR stimulus treatment), and C3 (NI and I plants from control and IR stimulus treatments, respectively) (Fig. 14a). One principal component (PC) explained most of data variation (PC1 = 67% and PC2 = 22%) (Fig. 14a-b). The first PC was characterized by negative scores for Ci, E, A/gs, Y(NPQ), Y(NO), ETR/A, MDA, H2O2, O2•-, CAT, TSP, ACO1, ACO2, ACO4, ACO6, CHI3, CHI9, GLU, LOX1.1, LOXB, PAL3, POX3, PPOB, and PPOF. Positive scores were obtained for A, gs, WUE, Fv/Fm, Y(II), Chl a+b, Car, glucose, fructose, sucrose, starch, LTGA derivatives, APX, SOD, GR, ACO3, ACO5, ICS, LOXC, PDF1.2, and PR1b1 (Fig. 14a-b).

4. Discussion

The use of different IR stimuli for managing plant diseases that drastically reduce the yield of profitable crops towards more sustainable agriculture is gaining the attention of the scientific community and growers worldwide. Interestingly, the ability of the IR stimulus to reduce SLS symptoms was confirmed at the histochemical, biochemical, and molecular levels. Different formulations of phosphite can directly inhibit the growth of some pathogens (*e.g.*, *Colletotrichum lindemuthianum*, *Sclerotinia sclerotiorum*, and different species of oomycetes) *in vitro* by limiting phosphorylation reactions, reducing adenylate synthase activity, lowering the pool of nucleotides and pentose phosphate metabolism as well as causing rupture in hyphae cell wall with corresponding intense electrolytes leakage (Chaves et al., 2021; Fagundes-

Nacarath et al., 2018; Novaes et al., 2019; Mohammadi et al., 2021). In contrast to the aforementioned, the IR stimulus did not affect mycelial growth of *S. lycopersici* or even conidia germination *in vitro* suggesting its possible impact on reducing SLS symptoms through a direct activation of tomato defense responses.

Photosynthesis is the major physiological process greatly impacted on crops infected by pathogens of different lifestyles; thus, the pool of assimilates that could be allocated to mount host defense responses can be seriously compromised as reported for different pathosystems (Aucique-Pérez et al., 2020; Dias et al., 2020; Silveira et al., 2015; Silveira et al., 2019). In the present study, diffusional limitations explained reductions in A in infected leaves of IR stimulus-sprayed plants at 8 dai. Reduction in g_s in necrotic leaf tissues of blueberry plants infected with *Septoria albopunctata* occurred due to loss of stomata functionality while impairment on A was due to diffusion of non-host selective toxins to leaf tissues surrounding the fungal infection sites (Roloff er al. 2004). Reduction in photosynthesis was not exclusively associated with stomatal limitations in wheat and soybean leaves infected by *Pyricularia oryzae* and *Phakopsora pachyrhizi*, respectively (Aucique-Pérez et al., 2014; Rios et al., 2018). Interestingly, E was higher in infected leaves of tomato plants from control treatment at 8 dai. Reduced white mold symptoms were noticed in soybean leaves sprayed with manganese (Mn) phosphite, associated with higher A, g_s, and E values than not sprayed leaves, suggesting that the damage caused by *S. sclerotiorum* infection was attenuated by this phosphite. It can be assumed that great leaf tissues necrose and loss of cuticle integrity caused by SLS resulted in an increase in transpiration rate. By contrast, the photosynthetic apparatus in infected leaves of IR stimulus-sprayed plants was less impaired and associated with no biochemical limitations or an abrupt increase in transpiration. Great ETR/A ratio for infected leaves of plants from control treatment indicated an imbalance between electron flow and CO_2 assimilation during photosynthesis. This finding most likely contributed to the occurrence of alternative electron sinks (*e.g.*, photorespiration and Mehler reaction) that indicate a stressful condition and photoinhibition (Marçal et al., 2021). Infected leaves of IR stimulus-sprayed plants showed improved physiological performance than infected leaves from plants from control treatment based on great values of A, F_v/F_m, and Y(NPQ) and lower Y(NO) and ETR/A values. Based on imaging of Chl *a* fluorescence parameters, early and imperceptible damage imposed by pathogens on photosynthesis at the beginning of their infection process can be detected not invasively (Aucique-Pérez et al., 2014; Dias et al., 2020; Silveira et al., 2015; Silveira et al., 2019; Tatagiba 2015). The F_v/F_m parameter pictures any level of physiological stress imposed

on plant tissues and sharp decreases on its values indicate the magnitude of photoinhibition occurring at the PSII level (Pérez-Bueno et al., 2019). In the present study, lower F_v/F_m and Y(II) values linked to increases in both Y(NPQ) and Y(NO) occurred for infected leaves of plants from control treatment. Interestingly, infected leaves of IR stimulus-sprayed plants suffered less photodamage (*e.g.*, higher F_v/F_m and Y(II) values, concomitantly with reductions on Y(NPQ) and Y(NO)) indicating preservation of the photosynthetic apparatus. Leaves of tomato plants sprayed with Mn phosphite and of common bean plants sprayed with zinc (Zn) phosphite or copper (Cu) phosphite showed higher F_v/F_m, Y(II), and ETR values associated with lower values of Y(NPQ) and Y(NO) during the infection process of *S. sclerotiorum*, thus evidencing the potential of these phosphites to alleviate the stress imposed by pathogen infection on the photosynthetic apparatus (Chaves et al., 2021; Fagundes-Nacarath et al., 2021). Reductions in F_v/F_m and ETR values in soybean leaves infected by *P. pachyrhizi* were linked to an increase in Y(NPQ) and that heat dissipation may be used to alleviate the damage imposed on PSII (Einhardt et al., 2019). Many studies highlight lower concentration of photosynthetic pigments as one key physiological change occurring in leaf tissues of plants infected by hemibiotrophic and necrotrophic pathogens due to deleterious action of hydrolytic enzymes and non-host selective toxins targeting chloroplasts and their associated proteins (Aucique-Pérez et al., 2020; Dias et al., 2020; Silveira et al., 2015; Silveira et al., 2019; Tatagiba et al. 2015)The reduced symptoms caused by *S. lycopersici* infection in leaves of IR stimulus-sprayed plants was associated with higher pools of photosynthetic pigments denoting preservation of the photosynthetic apparatus functionality and more efficient use of light to optimize carbon fixation. Necrotic lesions resulting from *Phytophthora infestans* infection on potato leaves sprayed with potassium (K) phosphite were smaller, and chlorophylls and carotenoids concentrations were higher (Mohammadi et al., 2021). In the leaves of common bean, soybean, and tomato plants infected by *S. sclerotiorum* and common beans plants infected by *Xanthomonas axonopodis* pv. *phaseoli* sprayed with phosphites containing Cu, Mn, or Zn, the concentrations of Chl *a+b* and carotenoids were higher due to reduced symptoms caused by these pathogens (Chaves 2021; Fagundes-Nacarath et al., 2019; Novaes et al., 2019).

In the present study, discrete deposition of H_2O_2 and $O_2^{\bullet-}$ and their lower concentrations were noticed in infected leaves of IR stimulus-sprayed plants due to reduced SLS symptoms. In general, higher APX, CAT, and SOD activities and lower oxidative pressure (based on ETR/*A*) for IR stimulus-sprayed plants helped alleviate the harmful effect exerted by H_2O_2 and $O_2^{\bullet-}$ on leaf tissues infected by *S. lycopersici*. Other IR stimuli are able to promote greater

robustness of the antioxidant system. Common beans, soybean, tomato plants sprayed with different phosphites showed increased response of the antioxidative metabolism (greater APX, CAT, POX, and SOD) in response to pathogens infection (Chaves et al., 2021; Fagundes-Nacarath et al., 2019; Novaes et al., 2019). High GR activity was directly linked to redox homeostasis in tomato plants infected by *B. cinerea* (Zhang et al., 2020). A robust antioxidative metabolism depicted by great APX, CAT, GR, and SOD activities on leaves of tomato plants was closely linked to their resistance against *Alternaria alternata* infection (Meena et al., 2016).

Fine adjustments on the metabolic fluxes of soluble sugars in plant tissues can be decisive for the rapid activation of defense responses at the pathogen infection sites (Seifi et al., 2013). In the present study, perturbations on photosynthesis most likely contributed to reducing the pool of sugars and starch in leaves of plants from control treatment due to great SLS symptoms. The down-regulation of photosynthesis-related genes was observed in wheat plants during the necrotrophic phase of *Zymoseptoria tritici* infection (Yang et al., 2013). The sucrose and fructose concentrations in infected leaves of IR stimulus-sprayed plants were kept higher and accompanied by a great starch concentration during the *S. lycopersici* infection process possibly due to great *A* values and an increasing pool of sugars that could be allocated for host defense. This finding most likely explained the increased resistance of tomato plants against SLS instead of benefiting the infection process of *S. lycopersici*. Changes in leaf cell wall composition of Arabidopsis plants caused by high starch availability favored penetration by *Colletotrichum higginsianum* (Engelsdorf et al., 2013). Perturbations in the photosynthetic apparatus caused by *Phakopsora euvitis* infection on grape-fox leaves were linked to great sugars accumulation (Nogueira Júnior et al., 2017) Interestingly, fructose concentration was great in infected leaves of IR stimulus-sprayed plants. An increase in relative fructose concentration (amount of fructose in total soluble sugars) under limited glucose was closely linked to stem resistance of tomato plants against *B. cinerea* infection (Lacompte et al., 2017). Moreover, early activation of genes encoding for sucrose synthases (*Sl-SUS1* and *Sl-SUS3*), cell wall invertases (*Sl-LIN5* and *Sl-LIN9*), fructokinase (*FRK3*), and phosphofructokinase (*PFK2*) in the stem of tomato plants grown under sufficient or high nitrogen availability was linked to their increased resistance against *B. cinerea* infection (Lacrampe et al., 2021). Increased susceptibility of tomato plants against *B. cinerea* infection was linked to lower concentration of soluble sugars, possibly due to down-regulation of photosynthesis-related genes and lower photosynthetic rates (Berger et al., 2004). Therefore, the level of fructose in tissues of tomato plants appears to be a determinant factor for their prompt defense response against pathogens infection.

In the present study, the IR stimulus was able to elicit biochemical and physiological responses, in distinct ways, in tomato plants not challenged with *S. lycopersici* considering that most of the genes studied (except *ACO5*, *CHI3*, *ICS*, *LOX1.1*, and *PAL3* regardless of evaluation time) were up-regulated. Moreover, *CHI3*, *CHI9*, *GLU*, *PAL3*, *POX3*, *PPOB*, and *PPOF* were strongly up-regulated for IR stimulus-sprayed plants and, therefore, closely linked to their increased resistance against *S. lycopersici* infection. Massive colonization of plant tissues by fungi is hampered when CHI and GLU intensively hydrolyze chitin and *β*-1,3-glucan in their cell wall, respectively, besides the fact that host defense responses are boosted by chitin oligomers released and recognized by unspecific receptors (Sanchez-Vallet et al., 2015). In tomato leaves infected by *A. alternata*, higher CHI and GLU were important to decrease early blight symptoms (Moghaddam et al., 2019). Transgenic tomato plants expressing the *CHI* gene from rice showed increased resistance against *B. cinerea* infection (Chen et al., 2009). Plants raise PPO and POX activities in their tissues toward an efficient phenolics oxidation that results in quinone production as well as lignification of cell wall linked to cross-linking of cell wall components to reduce the extent of pathogen colonization (Chittoor et al., 1999). Transgenic tomato plants overexpressing the *PPO* gene from potato exhibited increased resistance to bacterial speck caused by *Pseudomonas syringae* pv. *tomato* (Li and Steffens 2002). Production of an array of phenolics from the deamination of the amino acid *L*-phenylalanine in the phenylpropanoid pathway depends on high PAL activity (Ojaghian et al., 2014). In infected leaves of IR stimulus-sprayed plants, great production of LTGA derivatives from the abundant pool of TSP can be linked to up-regulation of *PAL3*, *POX3*, *PPOB*, and *PPOF* during *S. lycopersici* infection ending up in reduced SLS symptoms. Higher ROS production and great CAT, SOD, and POD activities were associated with increased resistance of tomato plants sprayed with SA to control SLS (Chu et al., 2020). For many foliar diseases on different crops, reduced symptoms after spray of phosphites formulated with different nutrients (*e.g.*, Cu, K, Mn, and Zn) have been associated with an increase in the production of phenolics, phytoalexins, and lignin as well as higher CHI, GLU, PAL, PPO, and POX activities (Chaves et al., 2021; Fagundes-Nacarath et al., 2018; Mohammadi et al., 2021; Novaes et al., 2019). Azoxystrobin and *Pseudomonas fluorescens* were reported to induce resistance in tomato plants against SLS due to increased CHI, GLU, PAL, PPO, POX, and CAT activities and higher phenolics concentration (Anand et al., 2007). Increased resistance of tomato plants pretreated with some plant growth-promoting rhizobacteria against early blight was linked to enhanced PPO and POX activities (Babu et al., 2015).

For IR stimulus-sprayed plants, it turned out that both phenylpropanoid and isochorismate pathways were important for SA production considering the up-regulation of *PAL3* and *ICS* at 5 and 8 dai and the increased resistance of plants against SLS. The expression of *PR1b1* was up-regulated at 6 and 8 dai only for infected leaves of plants from control treatment. Interestingly, this finding suggests that the IR stimulus elicited (control *vs.* IR stimulus for non-inoculated plants) but did not prime *PR1b1* expression in tomato leaves infected by *S. lycopersici*. Moreover, the IR phenotype of inoculated and IR stimulus-sprayed plants cannot rely exclusively on *PR1*, but taking into consideration a holistic role played by other genes (*e.g.*, *PAL* and *ICS*) studied. In plant tissues infected by pathogens, especially the necrotrophic, LOX enzymes, classified into two major subfamilies known as 9-LOXs and 13-LOXs according to the position at which oxygen is incorporated into linoleic acid or linolenic acid, initiates hydroperoxidation of polyunsaturated fatty acids containing cis and cis-1,4-pentadiene moieties to produce oxylipins which are further enzymatically metabolized into traumatin, JA, and methyl jasmonate (Feussner and Wastrnack 2002). The *ACO* gene codes for the enzyme 1-aminocyclopropane-1-carboxylic acid (ACC) oxidase, which converts ACC into ET (Yim et al., 2014) and, along with JA, modulates plant response against necrotrophic pathogens through ISR (Aerts et al., 2021). In the present study, the IR stimulus induced tomato plants toward a more efficient defense response against *S. lycopersici* infection that involved the JA/ET-dependent signaling pathway taking into account the up-regulation of *ACO2*, *ACO3*, *ACO4*, *ACO5*, *LOX1.1*, *LOXB*, *LOXC*, and *PDF1.2*. Different IR stimuli have been shown to induce tomato resistance against soilborne and foliar diseases caused by pathogens of different lifestyles either through SAR or ISR. Tomato plants sprayed with κ-carrageenan from a marine red seaweed (*Kappaphycus alvarezii*) showed lower SLS severity and up-regulation of nine genes encoding for ET responsive transcription factors (Mauch-Mani et al., 2017). In tomato, similar SLS severity between JA-deficient mutants (*def1*) and wild-type plants indicated the involvement of the JA pathway in host resistance (Thaler et al., 2012). Tomato plants sprayed with SA (0.2 mM) showed reduced SLS symptoms and increased expression of some defense-related genes such as members of WRKY65, PR-proteins, MAPK, and abscisic acid receptor PYR/PYL families (Chu et al., 2020.

In the present study, the IR stimulus showed potential to induce both JA/ET and SA signaling pathways, but especially the former, resulting in reduction on SLS symptoms. Interestingly, synergism or even antagonism in the crosstalk between SA and JA/ET signaling pathways can occur in some plant species infected by pathogens (Pierterse et al., 2012. For

example, induced resistance of tomato plants by benzothiadiazole against gray mold occurred independently of SA and was linked to stronger priming of two genes (*Pti5* and *PI2*) involved in defense against *B. cinerea* (Król et al., 2015). Tomato seedlings originated from seeds soaked with MeJA solution (0.1 mM) showed increased resistance against *Fusarium oxysporum* f. sp. *lycopersici* infection, which was associated with high levels of phenolics (SA, kaempferol, and quercetin), up-regulation of *PAL5* and benzoic acid/SA carboxyl methyltransferase (*BSMT*) genes and down-regulation of *ICS* gene (Król et al., 2015). Indeed, the increased concentration of flavonols quercetin and kaempferol appeared to be closely related to the increased expressions of *PAL5*, chalcone synthase (*CHS*), and flavonol synthase/flavanone 3-hydroxylase-like (*FLS*) genes. Lower JA concentration (MeJA precursor) and an increase of 12-oxo-phytodienoic acid (JA precursor) were correlated with higher levels of SA in seedlings originated from MeJA-soaked seeds (Takshita et al., 2018). The severity of bacterial canker (*Clavibacter michiganensis* subsp. *michiganensis*) in tomato plants treated with *Pseudomonas* sp. 23S was reduced due to an increase in *PR1a* and *ACO* expressions indicating the involvement of both SA and ET in ISR rather than defense responses originated from JA signaling pathway (Takshita et al., 2018).

In conclusion, the present study brings robust physiological, biochemical, and molecular evidences regarding the potential of the IR stimulus to efficiently reduce the SLS symptoms in leaves of tomato plants. It is noteworthy in this context that the IR stimulus boosted tomato resistance against *S. lycopersici* infection through a well-tuned defensive strategy pictured as great lignin production, modulating genes expression involved in basal host defense as well as in SA and JA/ET signaling pathways, a more operant antioxidative metabolism, and preservation of the photosynthetic apparatus. Based on the PCA analysis, the isolation of the cluster inoculated IR stimulus-sprayed plants from other clusters (inoculated and non-inoculated plants for control and IR stimulus treatments, respectively) highlights the peculiar effect of the IR stimulus on the outcome of variables and parameters investigated. It is tempting to assume that using this IR stimulus associated with well-known control strategies may become a promising alternative to slow SLS epidemic rate under field conditions and ensure less yield losses caused by this very destructive disease on tomato.

5. References

Aerts N, Mendes MP, Van Wees SC (2021) Multiple levels of crosstalk in hormone networks regulating plant defense. The Plant Journal 105:489-504.

Ahammed GJ, Li X, Zhang G, Zhang H, Shi J, Pan C, Shi K (2018) Tomato photorespiratory glycolate-oxidase-derived H_2O_2 production contributes to basal defence against *Pseudomonas syringae*. Plant, Cell & Environment 41:1126-1138.

Aktar W, Sengupta D, Chowdhury A (2009) Impact of pesticides use in agriculture: their benefits and hazards. Interdisciplinary Toxicology 2:1-12.

Anand T, Chandrasekaran A, Kuttalam S, Raguchander T, Prakasam V, Samiyappan R (2007) Association of some plant defense enzyme activities with systemic resistance to early leaf blight and leaf spot induced in tomato plants by azoxystrobin and *Pseudomonas fluorescens*. Journal of Plant Interactions 2:233-244.

Aucique-Pérez CE, Rios VS, Neto LBC, Rios JA, Martins SCV, Rodrigues FA (2020) Photosynthetic changes in wheat cultivars with contrasting levels of resistance to blast. Journal of Phytopathology 168:721-729.

Aucique-Pérez CE, Rios VS, Neto LBC, Rios JA, Martins SCV, Rodrigues FA (2020) Photosynthetic changes in wheat cultivars with contrasting levels of resistance to blast. Journal of. Phytopathology. 168:721-729.

Awasthi JP, Saha B, Chowardhara B, Devi SS, Borgohain P, Panda SK (2018) Qualitative analysis of lipid peroxidation in plants under multiple stress through Schiff's reagent: a histochemical approach. Bio-protocol 8:e2807.

Babu AN, Jogaiah S, Ito SI, Nagaraj AK, Tran LSP (2015) Improvement of growth, fruit weight and early blight disease protection of tomato plants by rhizosphere bacteria is correlated with their beneficial traits and induced biosynthesis of antioxidant peroxidase and polyphenol oxidase. Plant Science 231:62-73.

Berger S, Papadopoulos M, Schreiber U, Kaiser W, Roitsch T (2004) Complex regulation of gene expression, photosynthesis and sugar levels by pathogen infection in tomato. Physiologia Plantarum 122:419-428.

Blancard D (2012) Tomato Diseases, 2nd Ed. CRC Press, United States.

Chaves JAA, Oliveira LM, Silva LC, Silva BN, Dias CS, Rios JA, Rodrigues FA (2021) Physiological and biochemical responses of tomato plants to white mold affected by manganese phosphite. Journal of Phytopathology 169:149-167.

Chen Z, Zheng Z, Huang J, Lai Z, Fan B (2009) Biosynthesis of salicylic acid in plants. Plant Signaling & Behavior 4:493-496.

Chittoor JM, Leach JE, White FF (1999) Induction of peroxidase during defense against pathogens. In: Datta SK, Muthukrishnan S (eds) Pathogenesis-related proteins in plants. CRC Press, Boca Raton, pp 171-193.

Chu N, Zhou JR, Fu HY, Huang MT, Zhang HL, Gao SJ (2020) Global gene responses of resistant and susceptible sugarcane cultivars to *Acidovorax avenae* subsp. *avenae* identified using comparative transcriptome analysis. Microorganisms 8:10.

Cohen Y, Vaknin M, Mauch-Mani B (2016) BABA-induced resistance: milestones along a 55-year journey. Phytoparasitica 44:513-538.

Daloso DM, Antunes WC, Pinheiro DP, Waquim JP, Araújo WL, Loureiro ME, Fernie ER, Williams TC (2015) Tobacco guard cells fix CO_2 by both Rubisco and PEPcase while sucrose acts as a substrate during light-induced stomatal opening. Plant, Cell & Environment 38:2353-2371.

Debona D, Rodrigues FA, Rios JA, Nascimento KJT (2012) Biochemical changes in the leaves of wheat plants infected by *Pyricularia oryzae*. Phytopathology 102, 1121-1129.

Dias CS, Rios JA, Einhardt AM, Chaves JA, Rodrigues FA (2020) Effect of glutamate on *Pyricularia oryzae* infection of rice monitored by changes in photosynthetic parameters and antioxidant metabolism. Physiologia Plantarum 169:179-193.

Einhardt AM, Ferreira S, Hawerroth C, Valadares SV, Rodrigues FA (2020) Nickel potentiates soybean resistance against infection by *Phakopsora pachyrhizi*. Plant Pathology 69:849-859.

Engelsdorf T, Horst RJ, Pröls R, Pröschel M, Dietz F, Hückelhoven R, Voll LM (2013) Reduced carbohydrate availability enhances the susceptibility of Arabidopsis toward *Colletotrichum higginsianum*. Plant Physiology 162:225-238.

Fagundes-Nacarath IR, Debona D, Rodrigues FA (2018) Oxalic acid-mediated biochemical and physiological changes in the common bean-*Sclerotinia sclerotiorum* interaction. Plant Physiology and Biochemistry 129:109-121.

Feussner I, Wasternack C (2002) The lipoxygenase pathway. Annual Review of Plant Biology 53:275-297.

Harel YM, Mehari ZH, Rav-David D, Elad Y (2014) Systemic resistance to gray mold induced in tomato by benzothiadiazole and *Trichoderma harzianum* T39. Phytopathology 104:150-157.

Jakab G, Cottier V, Toquin V, Rigoli G, Zimmerli L, Métraux JP, Mauch-Mani B (2001) β-Aminobutyric acid-induced resistance in plants. European Journal of Plant Pathology 107:29-37.

Kesel J, Conrath U, Flors V, Luna E, Mageroy MH, Mauch-Mani B, Pastor V, Pozo MJ, Pieterse CMJ, Ton J, Kyndt T (2021) The induced resistance lexicon: do's and don'ts. Trends in Plant Science 26:685-691.

Król P, Igielski R, Pollmann S, Kępczyńska E (2015) Priming of seeds with methyl jasmonate induced resistance to hemi-biotroph *Fusarium oxysporum* f. sp. *lycopersici* in tomato via 12-oxo-phytodienoic acid, salicylic acid, and flavonol accumulation. Journal of Plant Physiology 179:122-132.

Lacrampe N, Lopez-Lauri F, Lugan R, Colombié S, Olivares J, Nicot PC, Lecompte F (2021) Regulation of sugar metabolism genes in the nitrogen-dependent susceptibility of tomato stems to *Botrytis cinerea*. Annals of Botany 127:143-154.

Lecompte F, Nicot PC, Ripoll J, Abro MA, Raimbault AK, Lopez-Lauri F, Bertin N (2017) Reduced susceptibility of tomato stem to the necrotrophic fungus *Botrytis cinerea* is associated with a specific adjustment of fructose content in the host sugar pool. Annals of Botany 119:931-943.

Li L, Steffens JC (2002) Overexpression of polyphenol oxidase in transgenic tomato plants results in enhanced bacterial disease resistance. Planta 215:239-247.

Livak KJ, Schmittgen TD (2001) Analysis of relative gene expression data using real-time quantitative PCR and the $2^{-\Delta\Delta CT}$ method. Methods 25:402-408.

Marçal DM, Avila RT, Quiroga-Rojas LF, Souza RP, Junior CCG, Ponte LR, DaMatta FM (2021) Elevated [CO_2] benefits coffee growth and photosynthetic performance regardless of light availability. Plant Physiology and Biochemistry 158:524-535.

Mauch-Mani B, Baccelli I, Luna E, Flors V (2017) Defense priming: an adaptive part of induced resistance. Annual Review of Plant Biology 68:485-512.

Medeiros DB, Barros KA, Barros JAS, Omena-Garcia RP, Arrivault S, Sanglard LM, Detmann KC, Silva WB, Daloso DM, DaMatta FM, Nunes-Nesi A, Fernie AR, Araújo WL (2017). Impaired malate and fumarate accumulation due to the mutation of the tonoplast dicarboxylate transporter has little effects on stomatal behavior. Plant Physiology 175:1068-1081.

Meena M, Zehra A, Dubey MK, Aamir M, Gupta VK, Upadhyay RS (2016) Comparative evaluation of biochemical changes in tomato (*Lycopersicon esculentum* Mill.) infected by

Alternaria alternata and its toxic metabolites (TeA, AOH, and AME). Frontiers in Plant Science 7:1408.

Moghaddam GA, Rezayatmand Z, Esfahani MN, Khozaei M (2019) Genetic defense analysis of tomatoes in response to early blight disease, *Alternaria alternata*. Plant Physiology and Biochemistry 142:500-509.

Mohammadi MA, Cheng Y, Aslam M, Jakada BH, Wai MH, Ye K, He X, Luo T, Dong C, Hu B, Priyadarshani SVGN, Wang-Pruski G, Qin Y (2021) ROS and oxidative response systems in plants under biotic and abiotic stresses: revisiting the crucial role of phosphite triggered plants defense response. Frontiers in Microbiology 12:631318.

Monteiro ACA, Resende MLV, Valente TCT, Ribeiro Junior PM, Pereira VF, Costa JR, Silva JAG (2016) Manganese phosphite in coffee defence against *Hemileia vastatrix*, the coffee rust fungus: biochemical and molecular analyses. Journal of Phytopathology 164:1043-1053.

Moore KJ, Dixon PM (2015) Analysis of combined experiments revisited. Agronomy Journal 107:763-771.

Nayyer M, Ahmad MF, Shamim M, Lal D, Srivastava D, Tripathi VK (2022) Molecular approaches for the control of septoria leaf spot in tomato. In: Solankey SS, Shamim MD. (Eds.). Biotic Stress Management in Tomato: Biotechnological Approaches, Apple Academic Press, pp. 91-106.

Nogueira Júnior AF, Ribeiro RV, Appezzato-da-Glória B, Soares MK, Rasera JB, Amorim L (2017) *Phakopsora euvitis* causes unusual damage to leaves and modifies carbohydrate metabolism in grapevine. Frontiers in Plant Science 8:1675.

Novaes MIC, Debona D, Fagundes-Nacarath IRF, Brás VV, Rodrigues FA (2019) Physiological and biochemical responses of soybean to white mold affected by manganese phosphite and fluazinam. Acta Physiologiae Plantarum 41:186.

Odintsova TI, Slezina MP, Istomina EA, Korostyleva TV, Kasianov AS, Kovtun AS, Kudryavtsev AM (2019) Defensin-like peptides in wheat analyzed by whole-transcriptome sequencing: A focus on structural diversity and role in induced resistance. PeerJ 7:e6125.

Ojaghian MR, Chen Y, Chen S, Cui ZQ, Xie GL, Zhang JZ (2014) Antifungal and enzymatic evaluation of plant crude extracts derived from cinnamon and rosemary against *Sclerotinia* carrot rot. Annals of Applied Biology 164:415-429.

Pérez-Bueno ML, Pineda M, Barón M (2019) Phenotyping plant responses to biotic stress by chlorophyll fluorescence imaging. Frontiers in Plant Science 10:1135.

Pieterse CM, Van der Does D, Zamioudis C, Leon-Reyes A, Van Wees SC (2012) Hormonal modulation of plant immunity. Annual Review of Cell and Developmental Biology 28:489-521.

Rios VS, Rios JA, Aucique-Pérez CE, Silveira PR, Barros AV, Rodrigues FA (2018) Leaf gas exchange and chlorophyll *a* fluorescence in soybean leaves infected by *Phakopsora pachyrhizi*. Journal of Phytopathology 166:75-85.

Rodrigues FA, Jurick WM, Datnoff LE, Jones JB, Rollins JA (2005) Silicon influences cytological and molecular events incompatible rice-*Magnaporthe grisea* interactions. Physiological and Molecular Plant Pathology 66:144-159.

Roloff I, Scherm H, Van Iersel MW (2004) Photosynthesis of blueberry leaves as affected by Septoria leaf spot and abiotic leaf damage. Plant Disease 88:397-401.

Sanchez-Vallet A, Mesters JR, Thomma BP (2015) The battle for chitin recognition in plant-microbe interactions. FEMS Microbiology Reviews 39:171-183.

Seifi HS, Van Bockhaven J, Angenon G, Höfte M (2013) Glutamate metabolism in plant disease and defense: friend or foe?. Molecular Plant-Microbe Interactions 26:475-485.

Silveira PR, Milagres PO, Corrêa EF, Aucique-Pérez CE, Wordell Filho JA, Rodrigues FA (2019) Changes in leaf gas exchange, chlorophyll *a* fluorescence, and antioxidants in maize leaves infected by *Exserohilum turcicum*. Biologia Plantarum 63:643-653.

Silveira PR, Nascimento KJT, Andrade CCL, Bispo WMS, Oliveira JR, Rodrigues FA (2015) Physiological changes in tomato leaves arising from *Xanthomonas gardneri* infection. Physiological and Molecular Plant Pathology 92:130-138.

Stevenson WR (2014) Septoria leaf spot. In: Jones JB, Zitter TA, Momol TM, Miller SA (Eds.). Compendium of Tomato Diseases and Pests. APS PRESS, St. Paul, pp. 42-43.

Takishita Y, Charron JB, Smith DL (2018) Biocontrol rhizobacterium *Pseudomonas* sp. 23S induces systemic resistance in tomato (*Solanum lycopersicum* L.) against bacterial canker *Clavibacter michiganensis* subsp. *michiganensis*. Frontiers in Microbiology 9:2119.

Tarkowski ŁP, Signorelli S, Höfte M (2020) γ-Aminobutyric acid and related amino acids in plant immune responses: emerging mechanisms of action. Plant, Cell & Environment 43:1103-1116.

Tatagiba DS, DaMatta FM, Rodrigues FA (2015) Leaf gas exchange and chlorophyll *a* fluorescence imaging of rice leaves infected with *Monographella albescens*. Phytopathology 105:181-188.

Thaler JS, Humphrey PT, Whiteman NK (2012) Evolution of jasmonate and salicylate signal crosstalk. Trends in Plant Science 17:260-270.

Ting HM, Cheah BH, Chen YC, Yeh PM, Cheng CP, Yeo FKS, Vie AK, Roloff J, Winge P, Bone AM, Kissen R (2020) The role of a glucosinolate-derived nitrile in plant immune responses. Frontiers in Plant Science 11:257.

Tistama R, Widyastuti U, Sopandie D, Yokota A, Akashi K (2012) Physiological and biochemical responses to aluminum stress in the root of a biodiesel plant *Jatropha curcas* L. HAYATI Journal of Biosciences 19:37-43.

Vinas M, Mendez JC, Jiménez VM (2020) Effect of foliar applications of phosphites on growth, nutritional status and defense responses in tomato plants. Scientia Horticulturae 265:109200.

Vlot AC, Sales JH, Lenk M, Bauer K, Brambilla A, Sommer A, Chen Y, Wenig M, Nayem S (2021) Systemic propagation of immunity in plants. New Phytologist 229:1234-1250.

Yang F, Li W, Jørgensen HJ (2013) Transcriptional reprogramming of wheat and the hemibiotrophic pathogen *Septoria tritici* during two phases of the compatible interaction. PLoS One 8:e81606.

Yim WJ, Kim KY, Lee YW, Sundaram SP, Lee Y, Sa TM (2014) Real time expression of ACC oxidase and PR-protein genes mediated by *Methylobacterium* spp. in tomato plants challenged with *Xanthomonas campestris* pv. *vesicatoria*. Journal of Plant Physiology 171:1064-1075.

Zeier J (2021) Metabolic regulation of systemic acquired resistance. Current Opinion in Plant Biology 62:102050.

Zhang X, Ren A, Zhang P, Yang H, Zhao T, Xu X, Jiang J, Li J (2020) Identification of salicylic acid conferred resistance genes against gray leaf spot disease in tomato. International Journal of Agriculture and Biology 23:109-116.

List of Tables and Figures

Table 1. Genes and their primer sequences analyzed in the leaves of tomato plants sprayed with water (control) or with the induced resistance stimulus and non-inoculated or inoculated with *Septoria lycopersici* by using reverse transcription quantitative real-time PCR (RT-PCR).

Genes	GenBank Identifications	Primer Sense 5'-3'	Primer Antisense 5'-3'
ACO1	544052	TTGCGCCATCTTCCTACTTC	ACACACACACTTAGTGAATCTTG
ACO2	101251255	TCAATCAAGGCTGGCAAAGT	TGATTCGACCCCTGGTCTTA
ACO3	101268031	TTGTCTGAAGGTCTCGGTCT	TGTGTTGCGCGATAAACTTTG
ACO4	543506	TGTTGTAGCAGGTAATCGCC	ACAGTAGTCTCCACAGCCTT
ACO5	543800	TCTTTGTTTGGCATCGTCCA	GCTTTGCTGCACACAACATA
ACO6	100125909	CACTACTTCGGATACCTTGCT	CGGATTGTAGAACGAAGCCA
CHI3	544149	GGTTTTGGTACTGCTGGTGA	TATTCGGACCCATCCCACAT
CHI9	544148	TAGTCAATGGCCTTGTGCTC	TTGTAGTTGCTGTGTTCAAATGT
GLU	543986	AGATCTTGAAGCCCTAGCCA	AATATGTCGCGGTTGAGACC
ICS	778225	ACCTTCTTGTTCCTAATGTGTGA	TGTGGAAGAATTGGGTGTGG
LOX1.1	543994	AATTTCTGACTTCGCCACCG	AGCTCTGGTGTTTCACTTGG
LOXB	543997	ACGAGGATACGGGTACTCAG	CCTTAACTTTGTTTTGTTGCGG
LOXC	544008	TTGGCCAAAATAACATACGCAG	TCGGAGAGCGTAGAAGTCAA
PAL3	101243922	ATGTGGGGTTTGGGAAAAGTT	TGACAAGAGATGGCACATGG
PDF1.2	*	CACTTCACAAATGTCGATCCG	AGCCAAATCCAATGCAGTCTC
POX3	101250523	GCTTTGTCAGGGGTTGTGAT	TGCATCTCTAGCAACCAACG
PPOB	101258774	TGGCAAGTGTAGTGTGCAAT	GGTGTCAAAGTTAGTCGGCA
PPOF	101259064	GATTCGATTACGCGCCAATG	ACTAGCAAGGCAGTAATGAGC
PR1b1	*	TGATTCATTCTGGTGCTGGG	TTATAGCTTGGCCTCTCGGA
TEF-1α	KF253411.1	CTCCAATTTCTGGTGGGGTG	ACTTTGGAGTCTCGAACTTCC
ACT	957571262	TGGTCGGAATGGGACAGAAG	CTCAGTCAGGAGAACAGGGT

* Primer sequences for *PDF1.2* and *PR1b1* genes were obtained from Moghaddam et al., (2019) and Ahammed et al., (2018), respectively.

Table 2. Analysis of variance for the effects of induced resistance (IR) stimulus, plant inoculation (PI), and IR stimulus × PI interaction for severity (Sev), leaf gas exchange (net carbon assimilation rate (*A*), stomatal conductance to water vapor (g_s), internal CO_2 concentration (C_i), transpiration rate (*E*), intrinsic water-use efficiency (A/g_s), and water-use efficiency (WUE)), and chlorophyll *a* (maximum PSII quantum efficiency (F_v/F_m), photochemical yield (Y(II)), yield for dissipation by down-regulation (Y(NPQ)), yield for non-regulated dissipation (Y(NO)) parameters, ratio of electron transport rate-to-net carbon assimilation rate (ETR/*A*), concentrations of chlorophyll *a*+*b* (Chl *a*+*b*), carotenoids (Car), carbohydrates (glucose, fructose, sucrose, and starch), malondialdehyde (MDA), hydrogen peroxide (H_2O_2), and superoxide anion radical ($O_2^{\bullet-}$), activities antioxidative enzymes (superoxide dismutase (SOD), ascorbate peroxidase (APX), catalase (CAT), glutathione reductase (GR)), concentrations of total soluble phenolics (TSP) and lignin-thioglycolic acid (LTGA) derivatives and expression of the genes 1-aminocyclopropane-1-carboxylic acid oxidase (*ACO1*, *ACO2*, *ACO3*, *ACO4*, *ACO5*, and *ACO6*), chitinase (*CHI3* and *CHI9*), glucanase (*GLU*), isochorismate synthase (*ICS*), lipoxygenase (*LOX1.1*, *LOXB*, and *LOXC*), phenylalanine ammonia-lyase (*PAL3*), plant defensin 1.2 (*PDF1.2*), peroxidase (*POX3*), polyphenoloxidase (*PPOB* and *PPOF*), pathogenesis-related protein 1 (*PR1b1*), and translation elongation factor 1-alfa (*TEF-1α*).

Variables/Parameters	IR stimulus	PI	IR stimulus × PI
Sev	**<0.001**	**-**	-
A	**0.015**	**<0.001**	0.065
g_s	0.481	**0.021**	0.403
C_i	**0.001**	**0.005**	**0.008**
E	0.399	0.857	0.767
A/g_s	**0.022**	**0.008**	**0.035**
A/C_i	**0.009**	**<0.001**	**0.006**
WUE	**0.018**	**0.007**	**0.043**
F_v/F_m	**0.002**	**<0.001**	**0.001**
Y(II)	**0.025**	**<0.001**	**0.003**
Y(NPQ)	0.072	0.431	0.146
Y(NO)	**0.005**	**< 0.001**	**0.003**
ETR/*A*	**0.001**	**<0.001**	**0.002**
Chl *a*+*b*	**0.001**	**0.001**	**0.007**
Car	0.069	**0.016**	**0.024**
Glucose	**0.005**	0.077	0.108
Fructose	**<0.001**	0.292	**<0.001**
Sucrose	**<0.001**	0.106	**0.009**
Starch	**<0.001**	**<0.001**	**0.027**

MDA	**0.006**	**0.002**	**0.020**
H_2O_2	**0.004**	**<0.001**	**0.012**
$O_2^{\bullet-}$	**0.025**	**0.045**	**0.020**
SOD	0.071	0.119	0.310
APX	0.062	0.171	**0.044**
CAT	0.592	**0.013**	0.858
GR	0.493	0.681	0.887
TSP	**0.010**	0.077	0.154
LTGA derivatives	**<0.001**	**0.009**	0.092
ACO1	0.180	0.270	0.269
ACO2	**0.029**	0.055	0.058
ACO3	0.058	0.081	0.080
ACO4	0.580	0.374	**0.010**
ACO5	0.138	0.174	0.173
ACO6	0.134	0.135	0.136
CHIA	0.532	**0.004**	0.524
CHIB	**0.004**	0.532	0.524
GLU	0.252	0.094	0.212
ICS	**0.025**	0.191	0.352
LOX1.1	0.214	0.214	0.214
LOXB	0.360	**0.001**	0.822
LOXC	0.130	0.119	0.130
PAL3	0.086	0.085	0.086
PDF1.2	**0.017**	**0.017**	**0.017**
POX	0.079	0.079	0.079
PPOB	0.149	0.149	0.149
PPOF	0.201	0.201	0.201
PR1	**0.049**	**0.049**	**0.049**
TEF-1α	**<0.001**	-	-

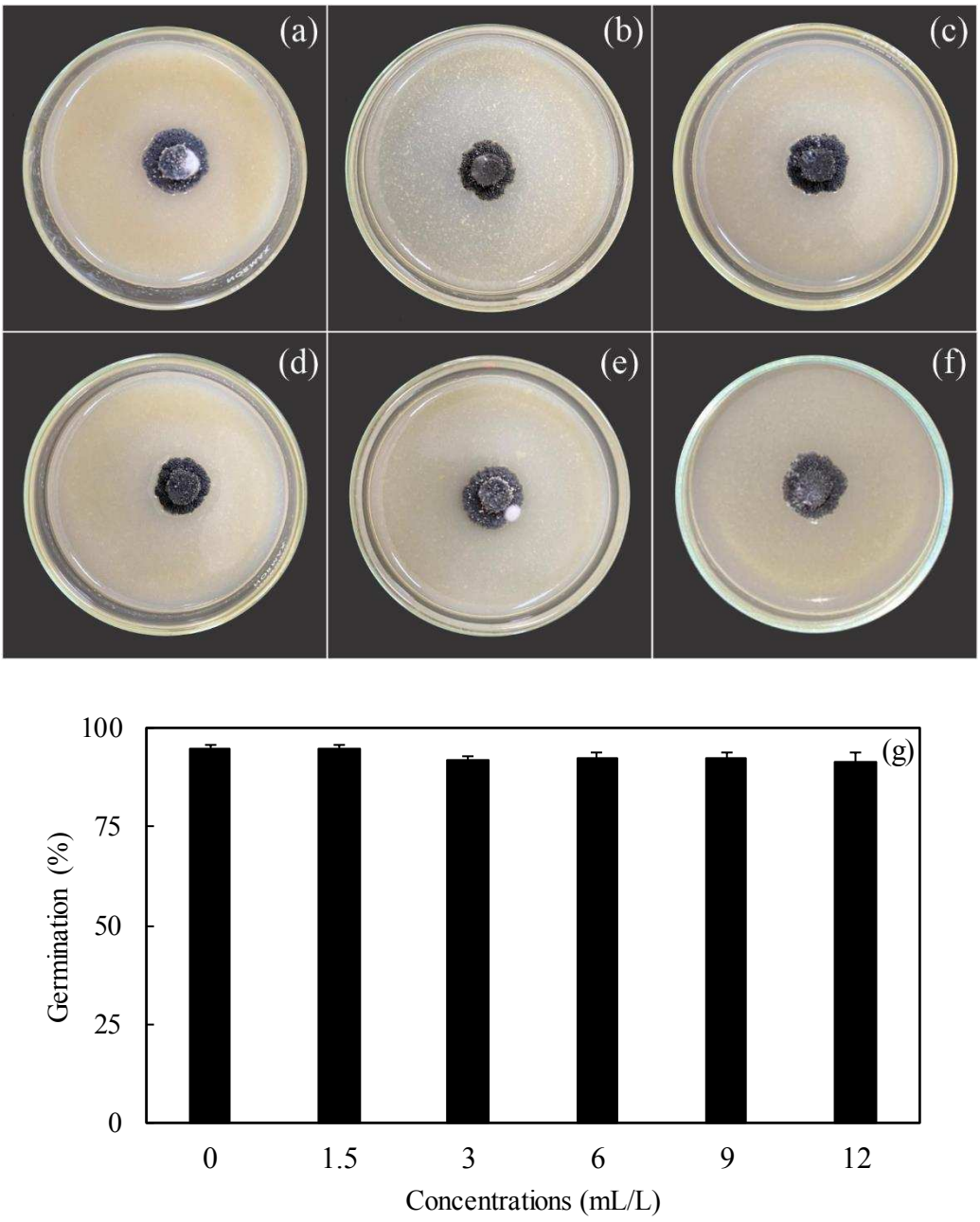

Figure 1. Visual aspect of mycelial growth of *Septoria lycopersici* in Petri dishes containing V8 medium amended with 0 (a), 1.5 (b), 3 (c), 6 (d), 9 (e), and 12 (f) mL of induced resistance (IR) stimulus per liter. Conidia germination of *S. lycopersici* (g) previously exposed to different IR stimulus concentrations.

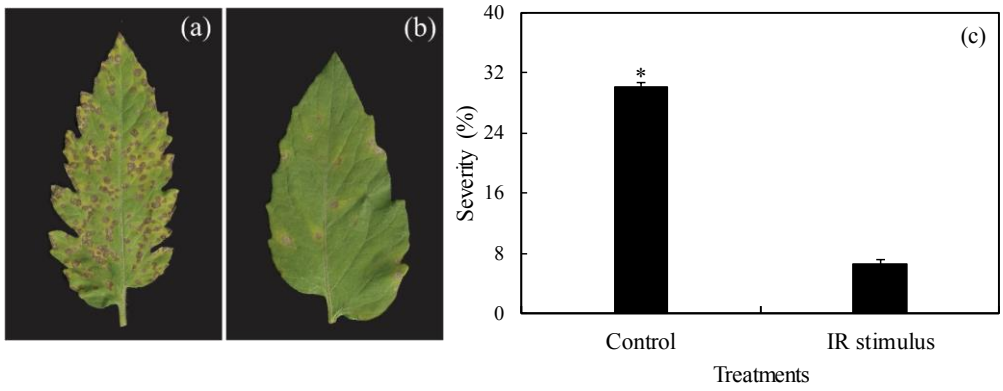

Figure 2. Symptoms of Septoria leaf spot (a and b) and severity (c) at 8 days after inoculation with *Septoria lycopersici* on leaves of tomato plants sprayed with water (control) or with the induced resistance (IR) stimulus. The asterisk (*) indicates differences between the treatments control and IR stimulus (C) according to *F* test. Bars represent the standard error of the means.

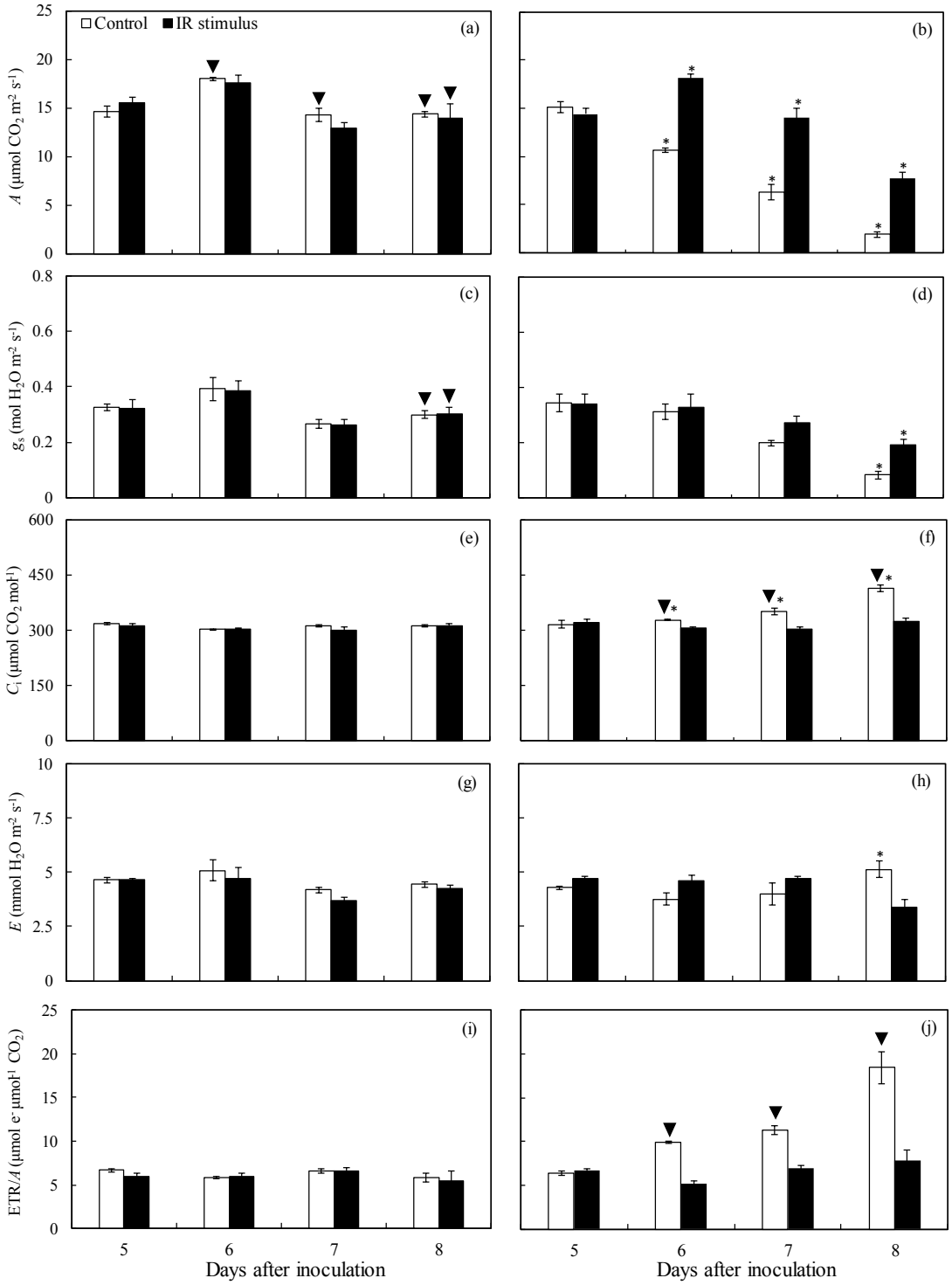

Figure 3. Leaf gas exchange parameters: net carbon assimilation rate (*A*) (a and b), stomatal conductance to water vapor (g_s) (c and d), internal CO_2 concentration (C_i) (e and f), transpiration rate (*E*) (g and h), and ratio of electron transport rate-to-net carbon assimilation rate (ETR/*A*) (i and j) determined on leaves of tomato plants non-inoculated (a, c, e, g, and i) or inoculated (b, d, f, h, and j) with *Septoria lycopersici* and sprayed with water (control) or with the induced

resistance (IR) stimulus. Means for non-inoculated and inoculated plants followed by an inverted triangle (▼) and for control and IR stimulus treatments followed by an asterisk (*), at each evaluation time, are significantly different according to *F* test ($P \leq 0.05$). Bars represent the standard deviation of the means.

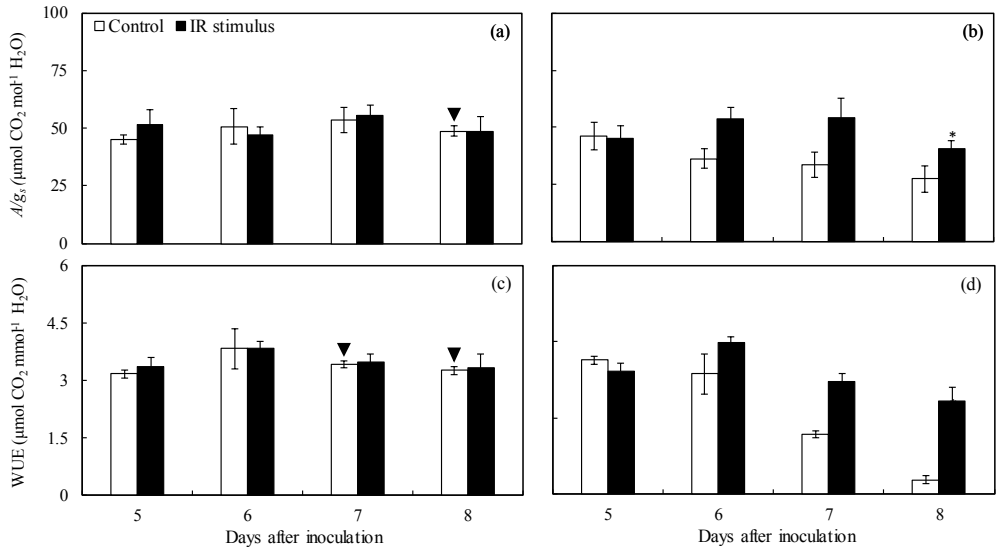

Figure 4. Intrinsic water use efficiency (A/g_s) (a and b) and water-use efficiency (WUE) (c and d) determined on leaves of tomato plants non-inoculated (a and c) or inoculated (b and d) with *Septoria lycopersici* and sprayed with water (control) or with the induced resistance (IR) stimulus. Means for non-inoculated and inoculated plants followed by an inverted triangle (▼) and for control and IR stimulus treatments followed by an asterisk (*), at each evaluation time, are significantly different according to *F* test ($P \leq 0.05$). Bars represent the standard deviation of the means.

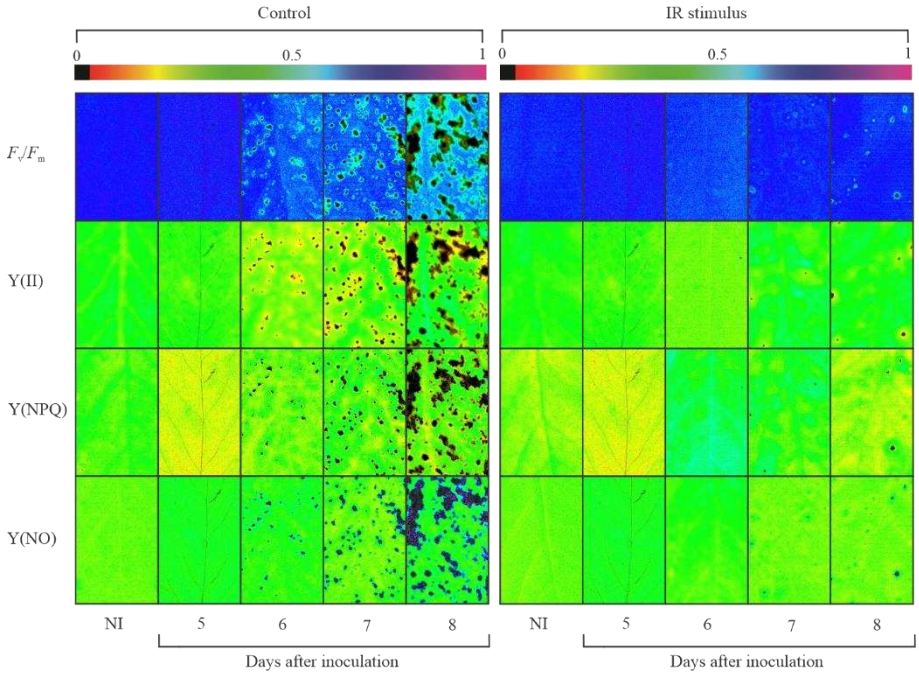

Figure 5. Images of chlorophyll *a* fluorescence parameters: maximum PSII quantum efficiency (F_v/F_m), photochemical yield (Y(II)), yield for dissipation by down-regulation (Y(NPQ)), and yield for non-regulated dissipation (Y(NO)) obtained from leaves of tomato plants sprayed with water (control) or with the induced resistance (IR) stimulus and non-inoculated (NI) or at different times after inoculation with *Septoria lycopersici*.

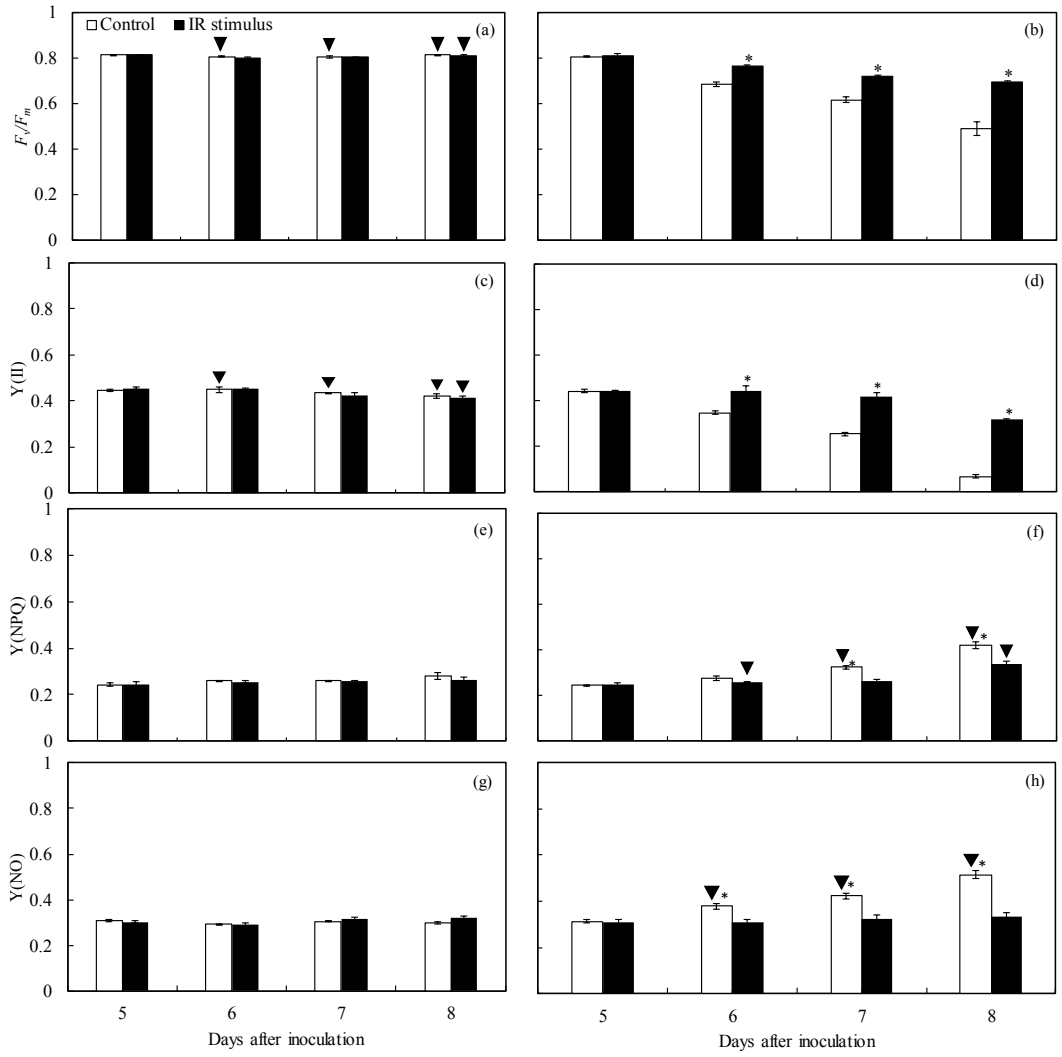

Figure 6. Chlorophyll *a* parameters: maximum PSII quantum efficiency (F_v/F_m) (a and b), photochemical yield (Y(II)) (c and d), yield for dissipation by down-regulation (Y(NPQ)) (e and f), and yield for other non-photochemical (non-regulated) losses (Y(NO)) (g and h) determined on leaves of tomato plants non-inoculated (a, c, e, and g) or inoculated (b, d, f, and h) with *Septoria lycopersici* and sprayed with water (control) or with the induced resistance (IR) stimulus. Means for non-inoculated and inoculated plants followed by an inverted triangle (▼) and for control and IR stimulus treatments followed by an asterisk (*), at each evaluation time, are significantly different according to *F* test ($P \leq 0.05$). Bars represent the standard deviation of the means.

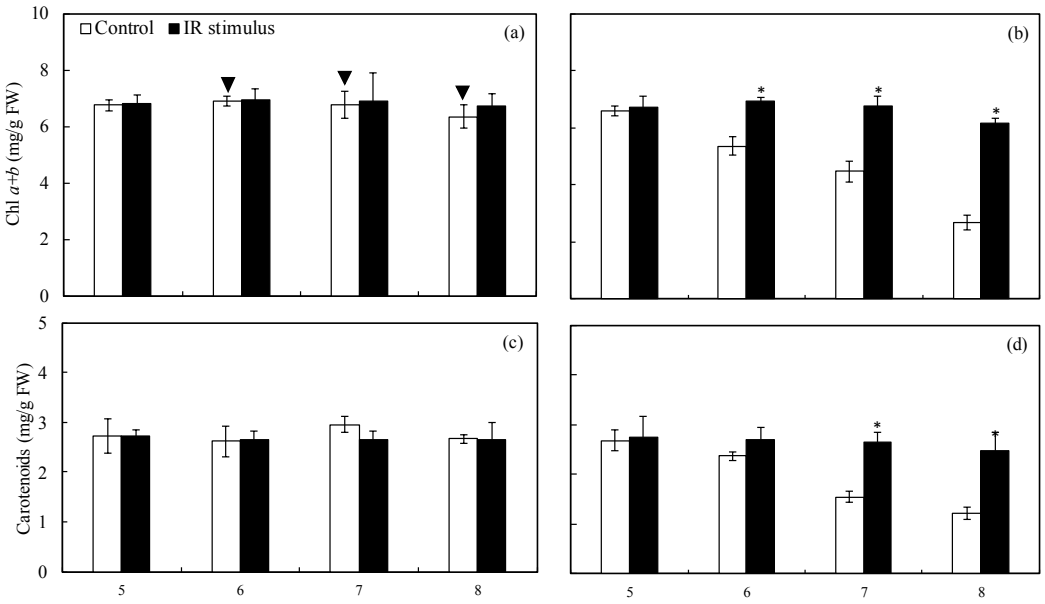

Figure 7. Concentrations of chlorophyll *a*+*b* (Chl *a*+*b*) (a and b) and carotenoids (c and d) determined on leaves of tomato plants non-inoculated (a and c) or inoculated (b and d) with *Septoria lycopersici* and sprayed with water (control) or with the induced resistance (IR) stimulus. Means for non-inoculated and inoculated plants followed by an inverted triangle (▼) and for control and IR stimulus treatments followed by an asterisk (*), at each evaluation time, are significantly different according to *F* test ($P \leq 0.05$). Bars represent the standard deviation of the means.

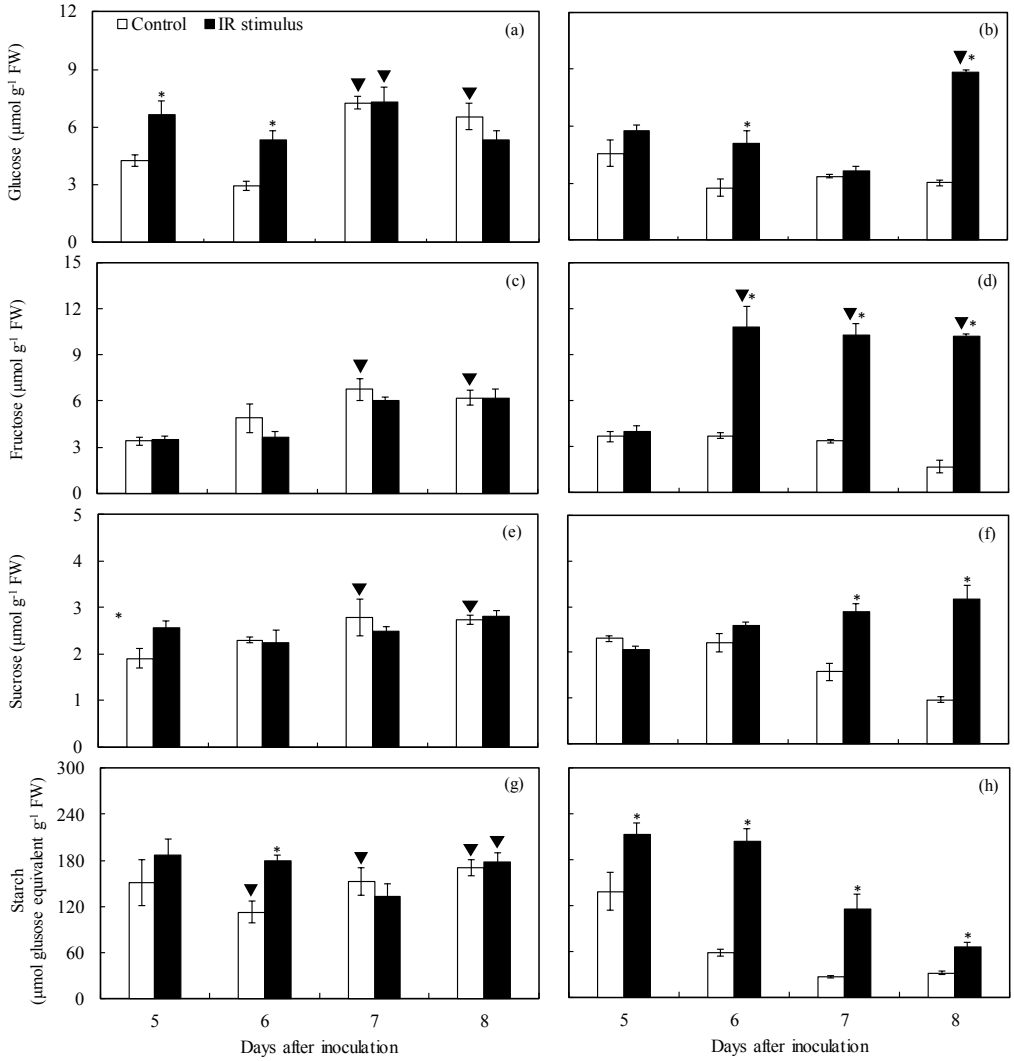

Figure 8. Glucose (a and b), fructose (c and d), sucrose (e and f), and starch concentrations (g and h) determined on leaves of tomato plants non-inoculated (a, c, e, and g) or inoculated (b, d, f, and h) with *Septoria lycopersici* and sprayed with water (control) or with the induced resistance (IR) stimulus. Means for non-inoculated and inoculated plants followed by an inverted triangle (▼) and for control and IR stimulus treatments followed by an asterisk (*), at each evaluation time, are significantly different according to *F* test ($P \leq 0.05$). Bars represent the standard deviation of the means. FW and DW = fresh weight and dry weight, respectively.

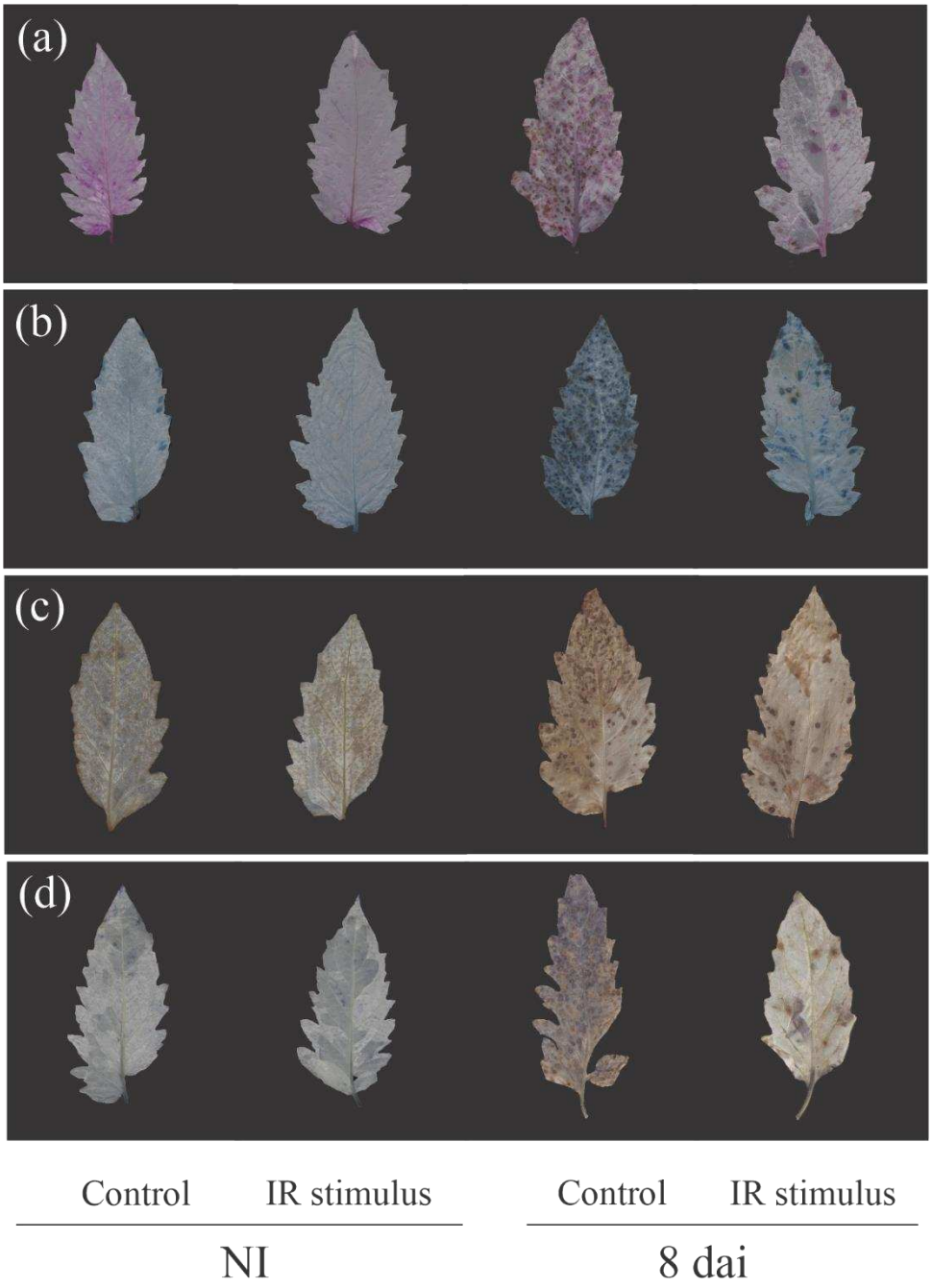

Figure 9. Histochemical detection of lipid peroxidation (a), membrane damage (b), hydrogen peroxide (c), and superoxide anion radical (d) on leaves of tomato plants non-inoculated (NI) or at 8 days after inoculation (dai) with *Septoria lycopersici* previously sprayed with water (control) or with the induced resistance (IR) stimulus.

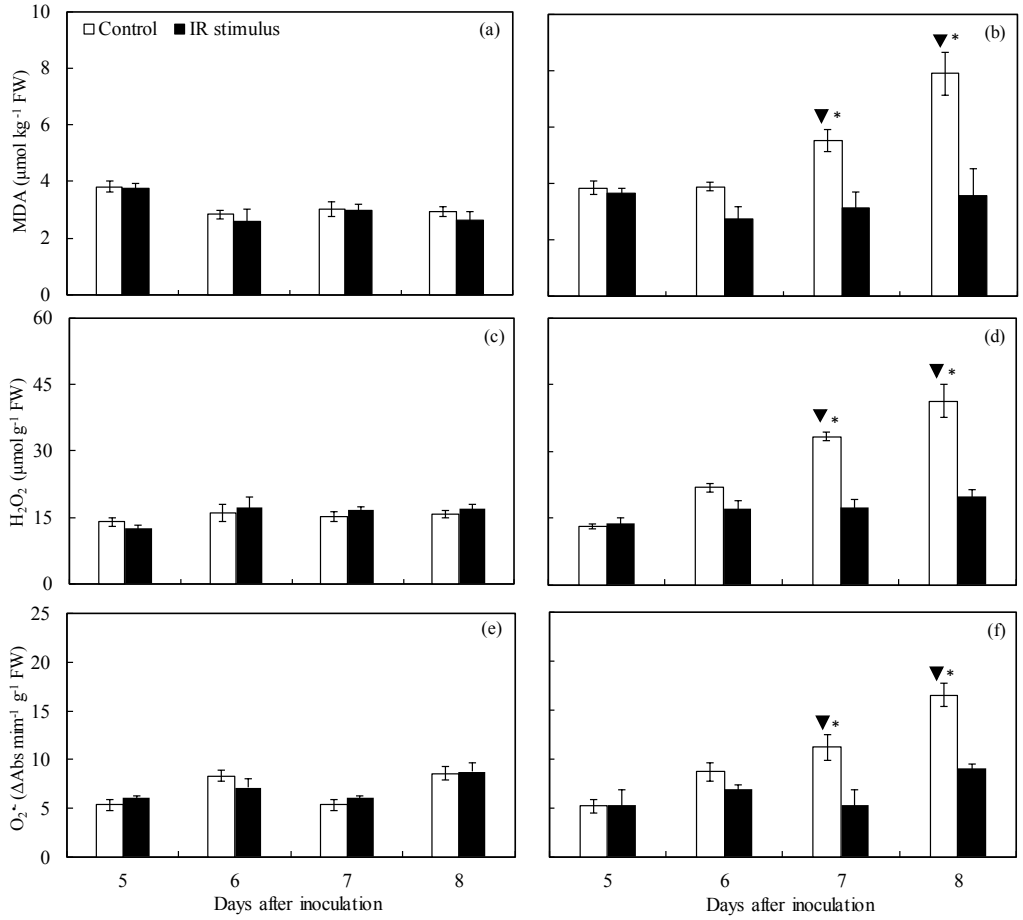

Figure 10. Concentrations of malondialdehyde (MDA) (a and b), hydrogen peroxide (H_2O_2) (c and d), and superoxide anion radical ($O_2^{\bullet-}$) (e and f) determined on leaves of tomato plants non-inoculated (a, c, and e) or inoculated (b, d, and f) with *Septoria lycopersici* and sprayed with water (control) or with the induced resistance (IR) stimulus. Means for non-inoculated and inoculated plants followed by an inverted triangle (▼) and for control and IR stimulus treatments followed by an asterisk (*), at each evaluation time, are significantly different according to *F* test ($P \leq 0.05$). Bars represent the standard deviation of the means. FW = fresh weight.

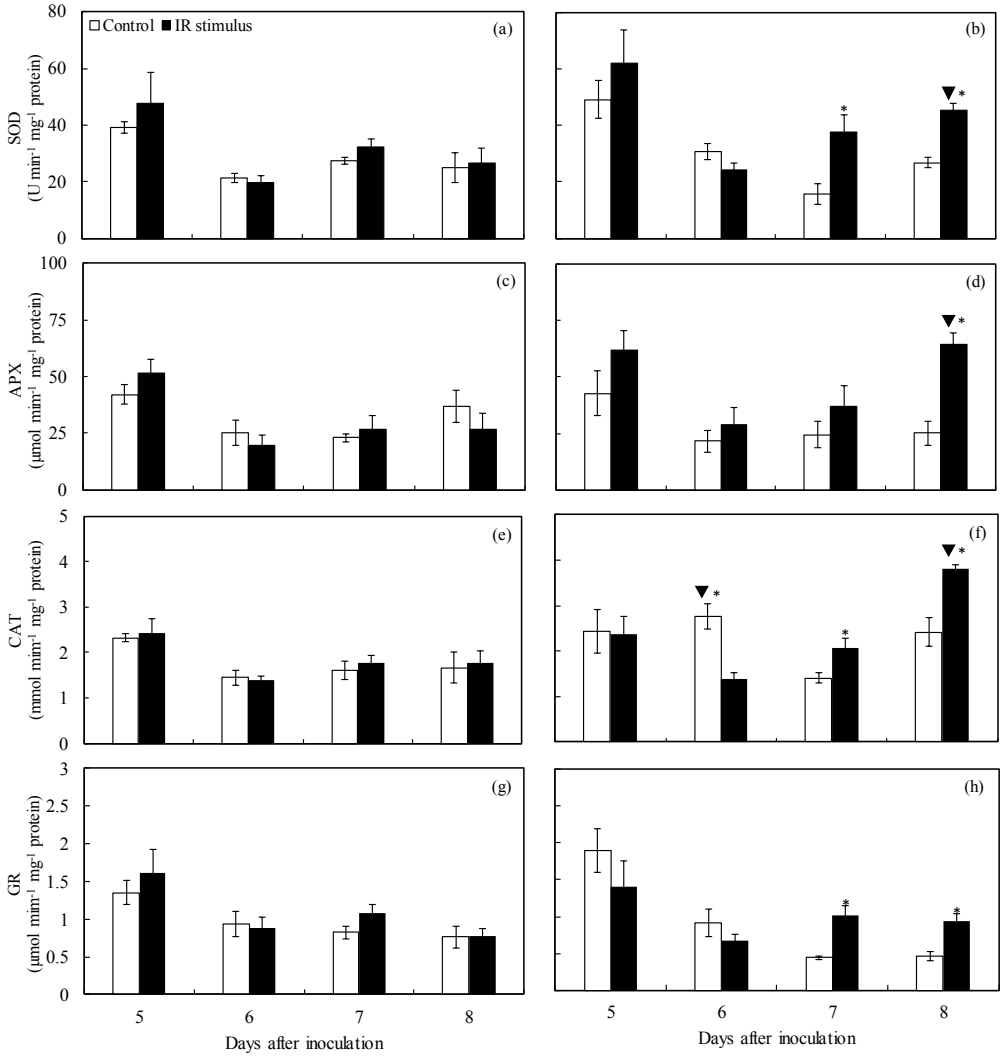

Figure 11. Activities of superoxide dismutase (SOD) (a and b), ascorbate peroxidase (APX) (c and d), catalase (CAT) (e and f), and glutathione reductase (GR) (g and h) determined on leaves of tomato plants non-inoculated (a, c, e, and g) or inoculated (b, d, f, and h) with *Septoria lycopersici* and sprayed with water (control) or with the induced resistance (IR) stimulus. Means for non-inoculated and inoculated plants followed by an inverted triangle (▼) and for control and IR stimulus treatments followed by an asterisk (*), at each evaluation time, are significantly different according to *F* test ($P \leq 0.05$). Bars represent the standard deviation of the means.

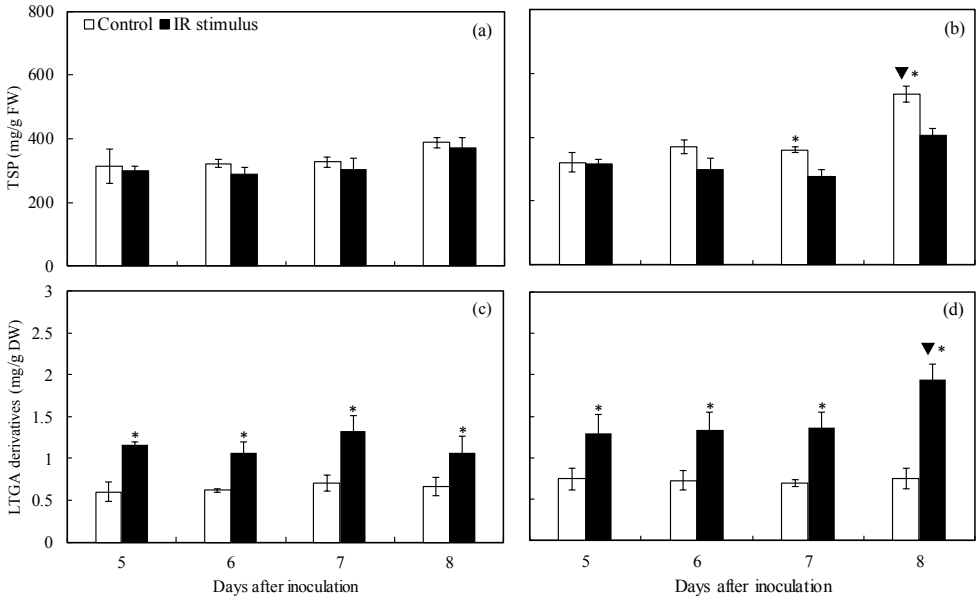

Figure 12. Concentrations of total soluble phenolics (TSP) (a and b) and lignin-thioglycolic acid (LTGA) derivatives (c and d) determined on leaves of tomato plants non-inoculated (a and c) or inoculated (b and d) with *Septoria lycopersici* and sprayed with water (control) or with the induced resistance (IR) stimulus. Means for non-inoculated and inoculated plants followed by an inverted triangle (▼) and for control and IR stimulus treatments followed by an asterisk (*), at each evaluation time, are significantly different according to *F* test ($P \leq 0.05$). Bars represent the standard deviation of the means. FW and DW = fresh weight and dry weight, respectively.

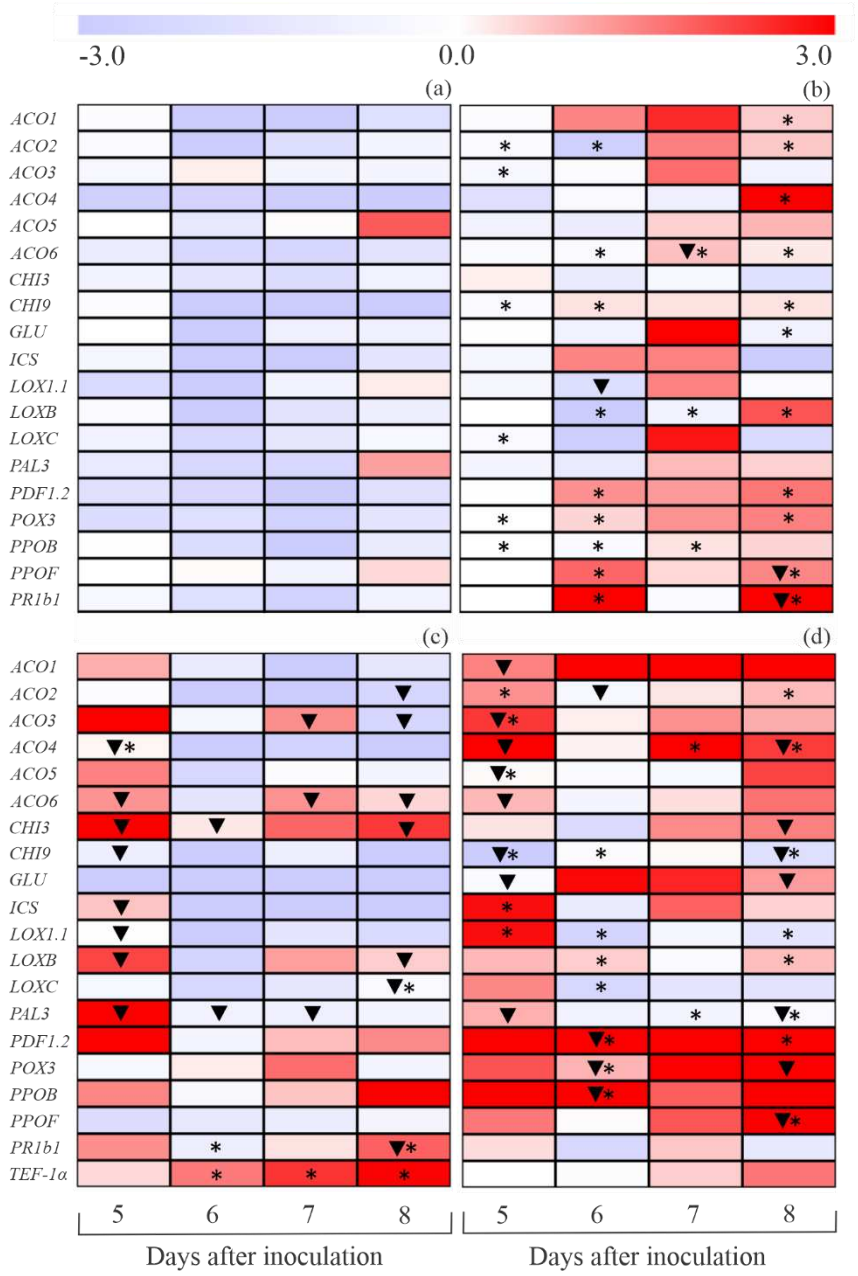

Figure 13. Expression profile of host defense-related genes determined on leaves of tomato plants non-inoculated (NI) (a and b) or inoculated (I) (c and d) with *Septoria lycopersici* and sprayed with water (control) (a and c) or with the induced resistance (IR) stimulus (b and d). Color cells represent the relative transcript levels ranging from blue (-3.0) to red (3.0). Amplification of actin gene (*ACT*) from tomato plants was used as an internal control for data normalization. Fold changes for each gene expression, except for *TEF-1α*, were calculated based on the transcript level obtained for leaves from NI plants of control treatment at 5 days after inoculation (dai). For *TEF-1α*, transcript level obtained for leaves from I plants of control treatment at 5 dai was used in the calculation. For each leaf, four biological replications were

used with three technical replicates each. Means for NI and I plants followed by an inverted triangle (▼) and for control and IR stimulus treatments followed by an asterisk (*), at each evaluation time, are significantly different according to *F* test ($P \leq 0.05$).

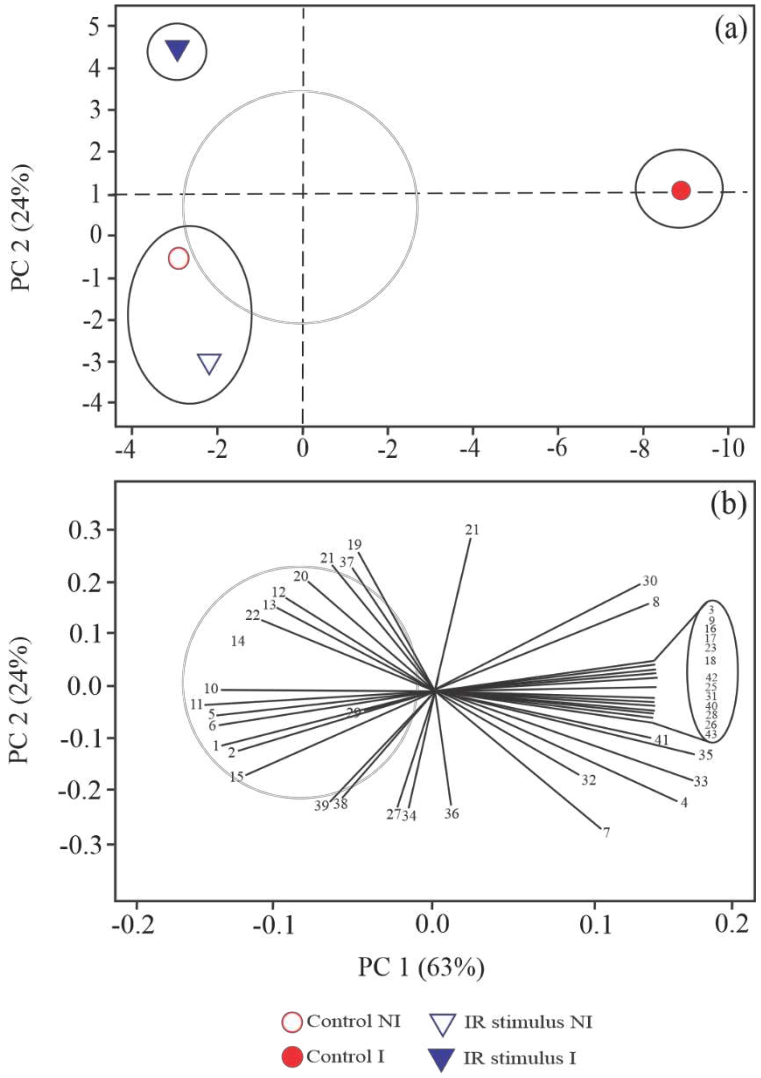

Figure 14. Score (a) and loading (b) plots of principal component analysis comparing different physiological variables and parameters, biochemical variables, and expression of genes determined on leaves of tomato plants non-inoculated (NI) or inoculated (I) with *Septoria lycopersici* and sprayed with water (control) or with the induced resistance (IR) stimulus. Numbers in the loading plot (b) are as follow: leaf gas exchange (1, 2, 3, and 4, respectively, to A, g_s, C_i, and E) and chlorophyll *a* fluorescence (5, 6, 7, 8, and 9, respectively, to F_v/F_m, Y(II), Y(NPQ), Y(NO), and ETR/A) parameters, concentrations of photosynthetic pigments (10 and 11, respectively, to Chl $a+b$ and Car), carbohydrates (12, 13, 14, and 15, respectively, to glucose, fructose, sucrose, and starch), and metabolites (16, 17, 18, 23, and 24, respectively, to MDA, H_2O_2, $O_2^{\bullet-}$, TSP, and LTGA derivatives), activities of antioxidant enzymes (19, 20, 21, and 22, respectively, to SOD, APX, CAT, and GR), and genes expression (25, 26, 27, 28, 29, 30, 31, 32, 33, 34, 35, 36, 37, 38, 39, 40, 41, 42, and 43, respectively, to *ACO1*, *ACO2*, *ACO3*,

ACO4, *ACO5*, *ACO6*, *CHI3*, *CHI9*, *GLU*, *ICS*, *LOX1.1*, *LOXB*, *LOXC*, *PAL3*, *PDF1.2*, *POX3*, *PPOB*, *PPOF*, and *PR1b1*). Groups were generated from cluster analysis with complete linkage and Pearson distance.